QCD Tests using LHC at CERN

Sudeep Chatterji
University Of Delhi, India

Postdoctoral Interview, FNAL, 23-24 January, 2007

Outline

- Silicon Microstrip Sensors for CMS PreShower
  - Metal Overhang as Junction Termination Technique
  - Radiation Damage Study
  - Noise Measurement and Interstrip Capacitance
- Gamma+Jet analysis for the CMS
  - Gamma+Jet Physics
  - Data Samples
  - Photon Isolation Studies
  - Analysis
  - Extraction of Gluon PDF (Future Plans)

Sudeep Chatterji, University of Delhi, India

Large Hadron Collider (LHC), CERN

- p-p Collider
- Centre of Mass Energy = 14 TeV
- Luminosity = 10^{34} /cm^2/s

- ***Physics at LHC***
  - Search for SM Higgs Boson
  - SUSY Physics
  - B-Physics
  - New Physics
  - Test of QCD
  - Quark Gluon Plasma

- ***Experiments at LHC***
  - **Compact Muon Solenoid (CMS)**
  - ATLAS
  - ALICE
  - LHC-B

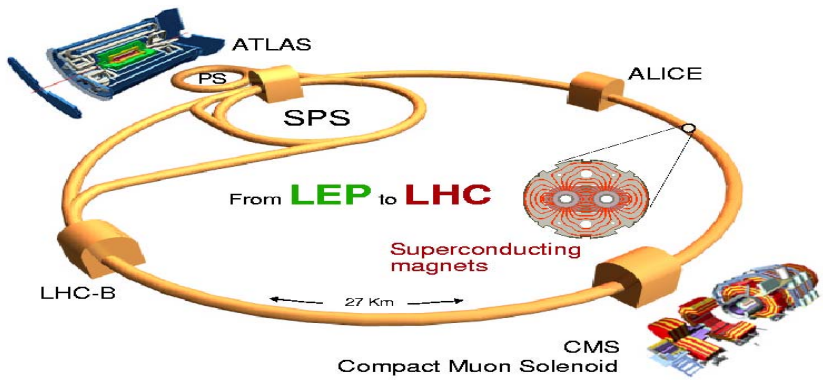

CMS Detector

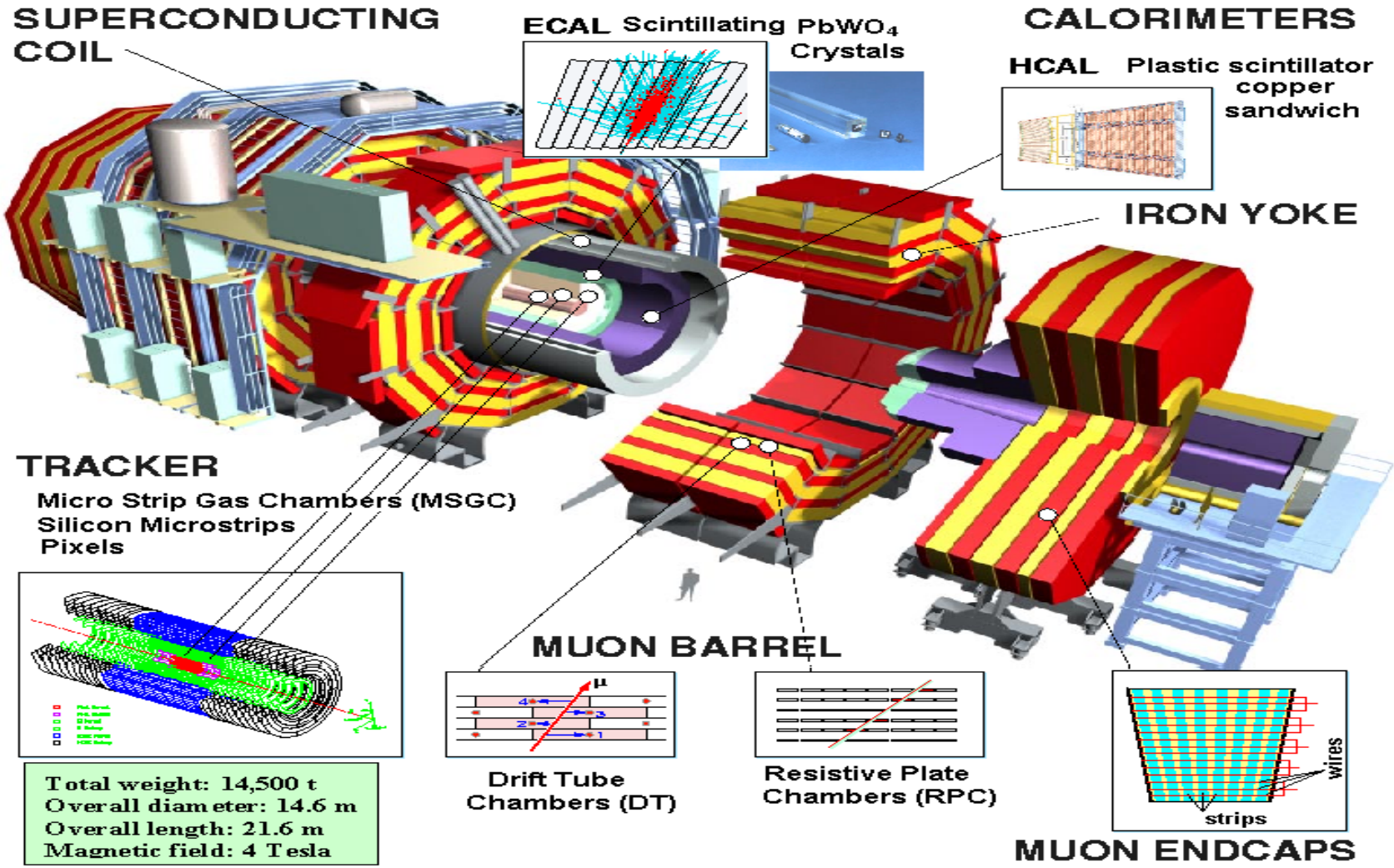

CMS Preshower

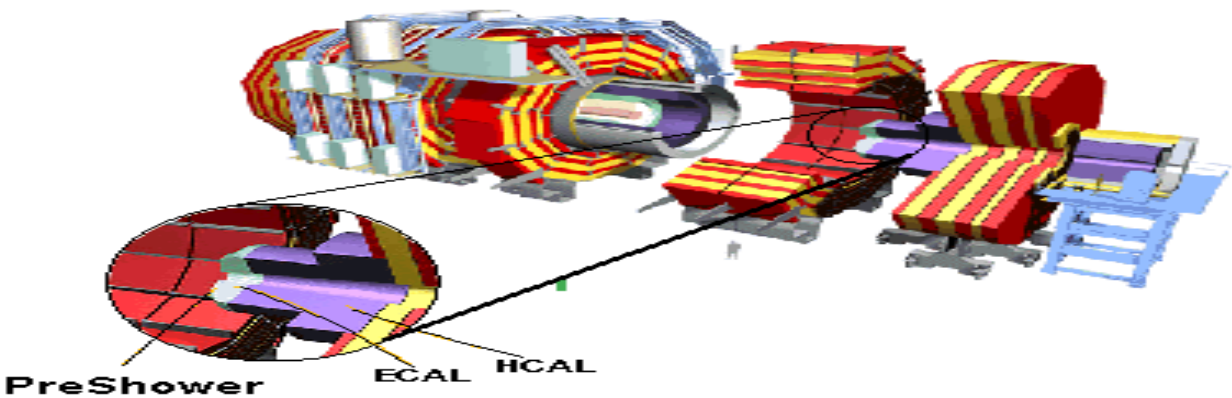

Light Higgs : $H \rightarrow \gamma\gamma$

Major Bgd. : $\pi^0 \rightarrow \gamma\gamma$

- The main function of the PSD is to provide γ/π^0 separation in Endcap.

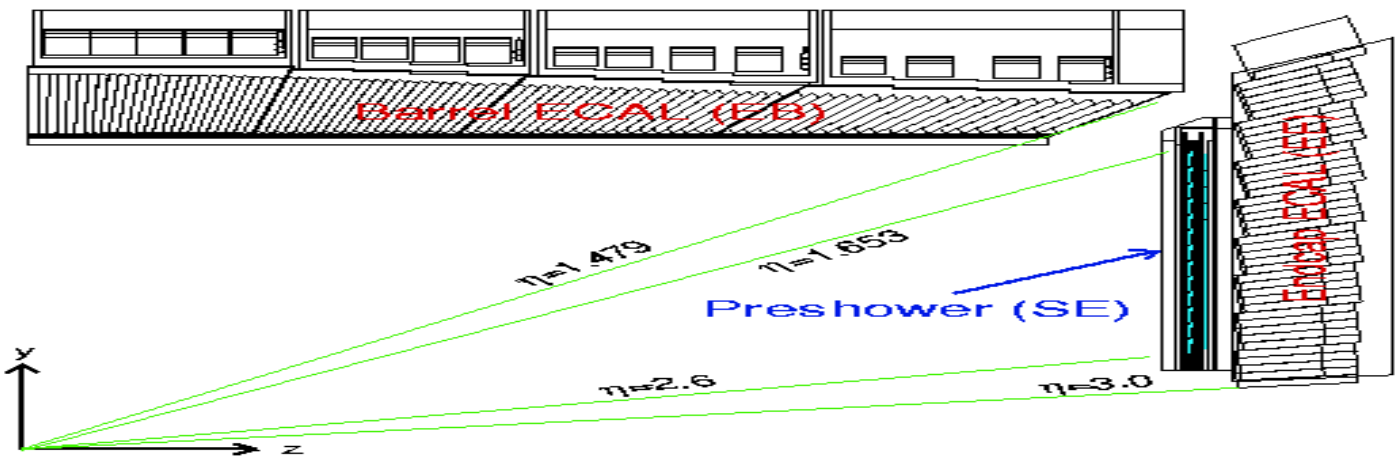

CMS Preshower

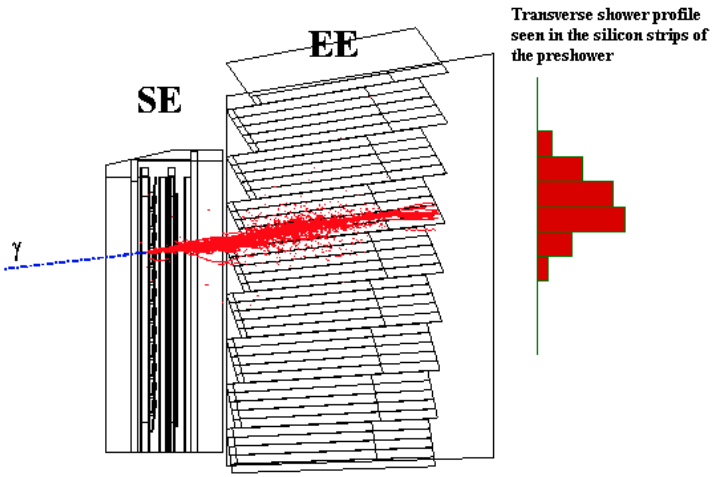

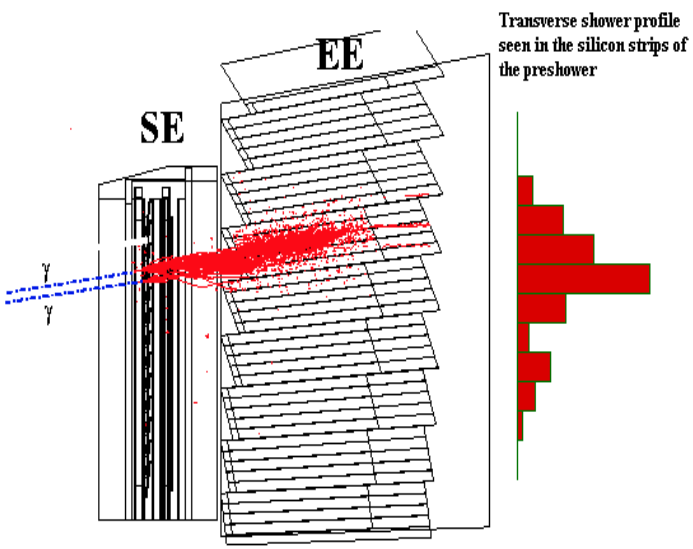

Why?

- In Endcap region ($1.65 < |\eta| < 2.6$), the important background to the "gold-plated" $H \rightarrow \gamma\gamma$ decay is $\pi^0 \rightarrow \gamma\gamma$ (closely spaced), faking as real photon.

- The main function of the PSD is to provide γ-π^0 separation

Components

- PSD contains two thin lead 'absorbers' followed by Si micro-strip detector planes

Si Strip Detector for PSD

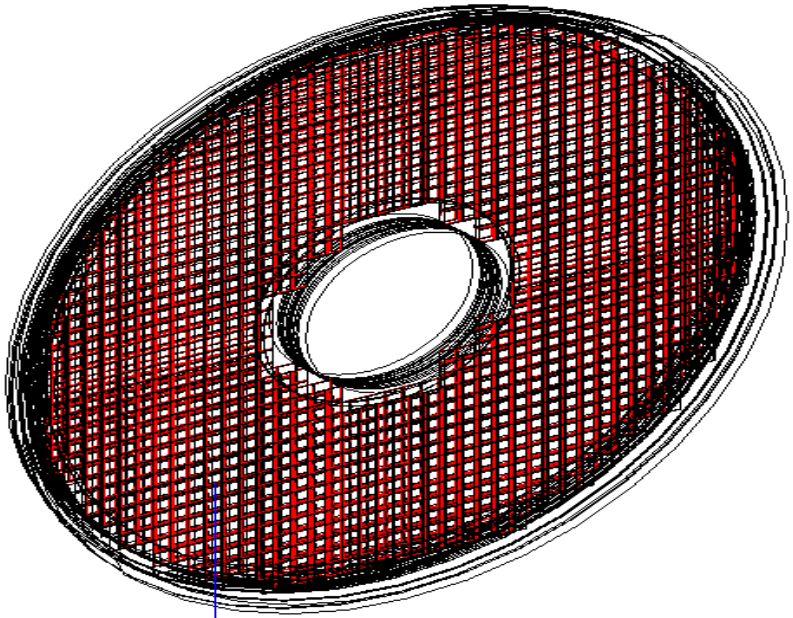

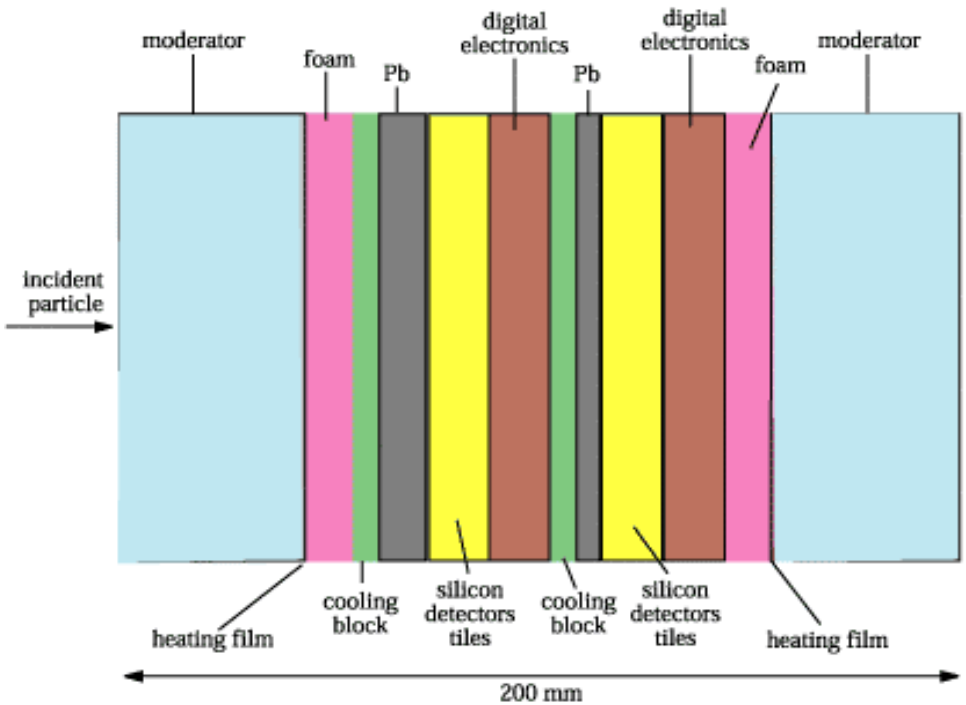

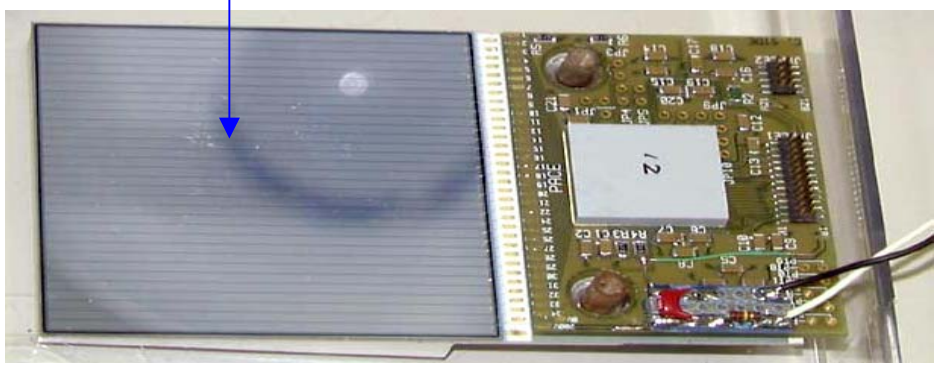

Si Strip Detector for PSD

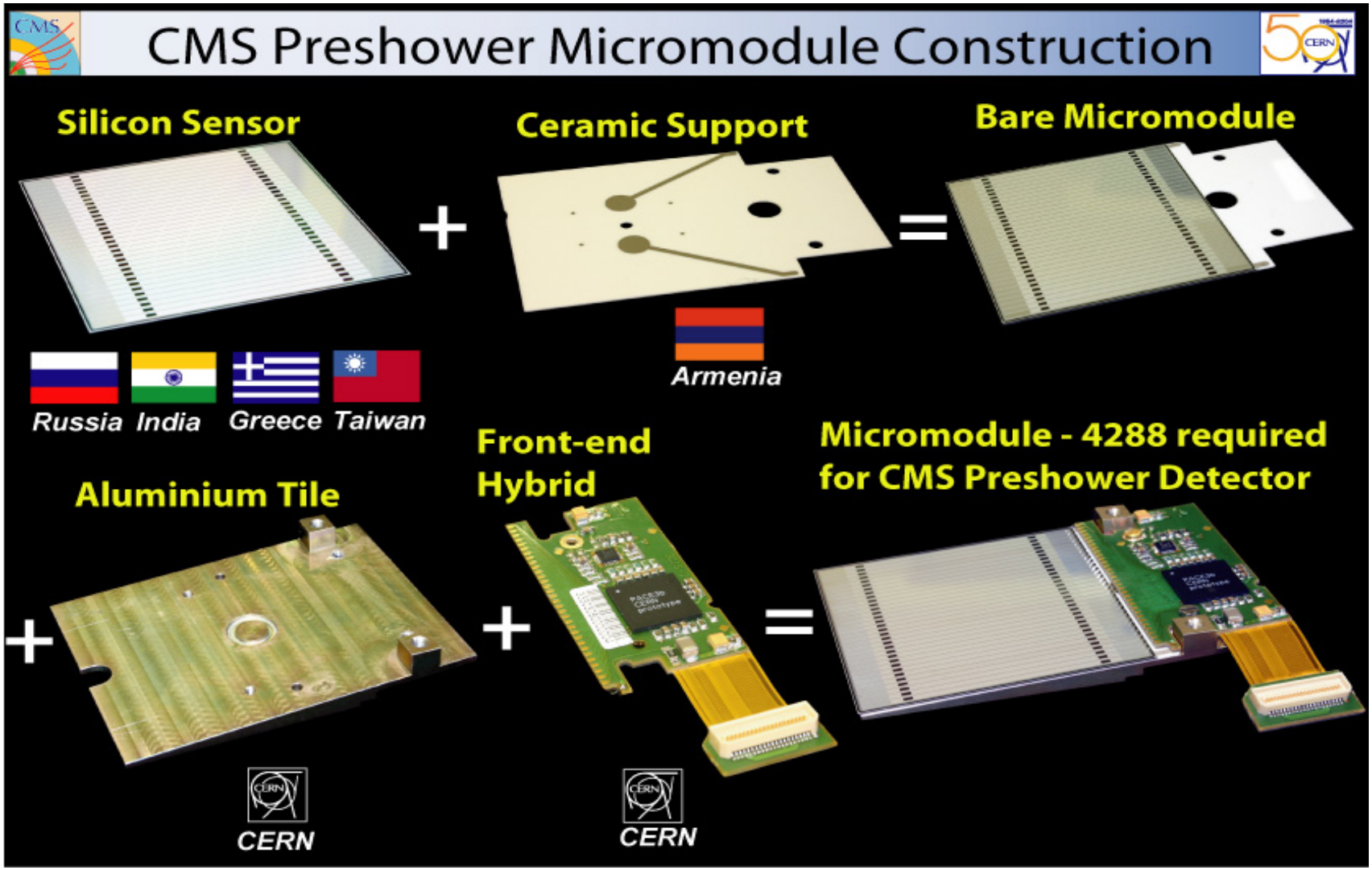

Principle of operation of Silicon Sensors

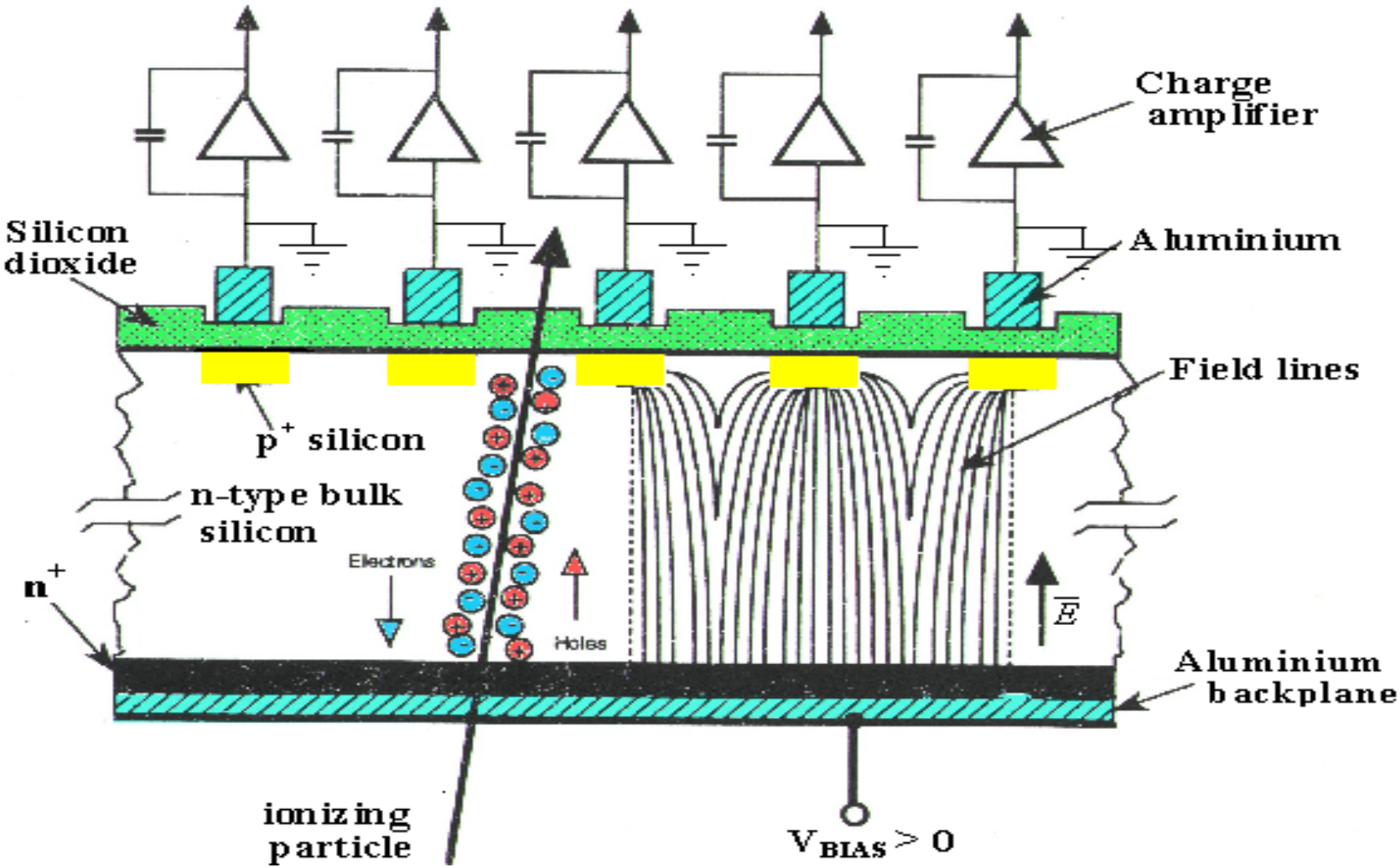

Preliminary Specifications of Si Sensors

Parameter	Value
Wafer size	4"
Thickness	320 ± 20 μm
Resistivity	2.5 KΩ cm – 4 KΩ cm
Polishing	Single-sided
n^+ layer thickness	> 2.5 μm
Total area	63 x 63 mm^2
Number of strips	32
Strip pitch	1.9 mm
p^+ strip width	1.78 mm
Al strip width	1.8 mm

Test	Criterion
Width (W)	W < 63 mm
Thickness (t)	300 μm < t < 340 μm
I-V (Global)	I < 5 μA at V_{FD} I < 10μA at 300 V **V_{BD} > 300 V for category 1** **V_{BD} > 500 V for category 2**
C-V (Global)	55 V < V_{FD} < 150 V
I (Strip-by-strip)	Max. 1 strip with I > 1 μA at V_{FD} Max. 1 strip with I > 5 μA at 300 V
C (Strip-by-strip)	No strips connected to the neighbour or guard ring

Test Set-up at BEL, Bangalore

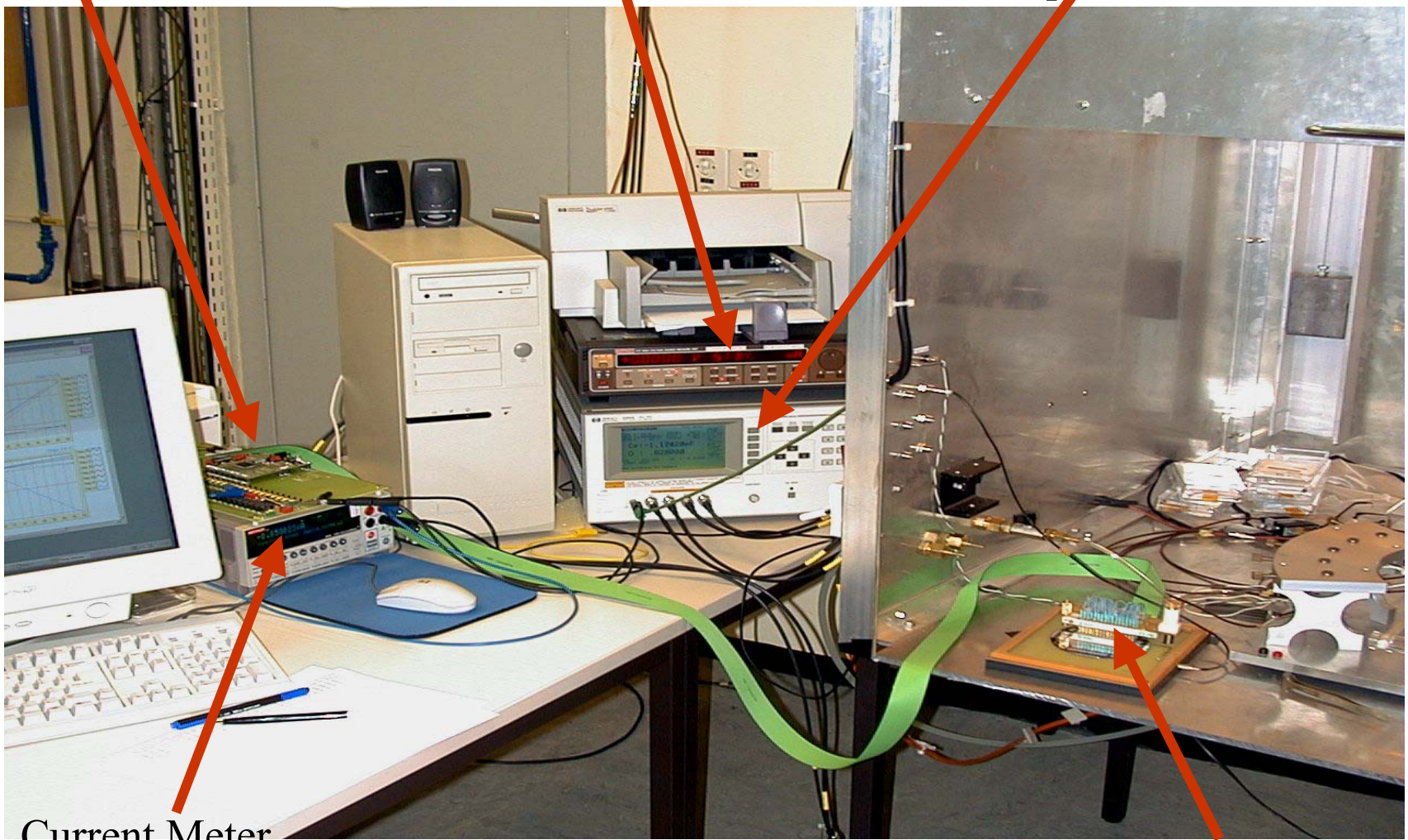

Motivation : High–Voltage Si Detectors

- Long term operation of Si detectors at LHC - ***Challenges***
  - Maintain functionality throughout for 10 years
  - Unprecedented Radiation Flux (~ $2x10^{14}$ particles/cm^2 for PSD)
  - Radiation hardness – Crucial issue
  - High voltage operation limited by V_{BD}

- Termination techniques to improve V_{BD} *(For Detector grade planar Si Technology)*
  - Metal – Overhang (MO) ***(Introduced in 1996)***
  - *Radiation Damage in MO equipped devices*
  - *Analysis of Interstrip capacitance*

Junction Curvature (Edge) Effect

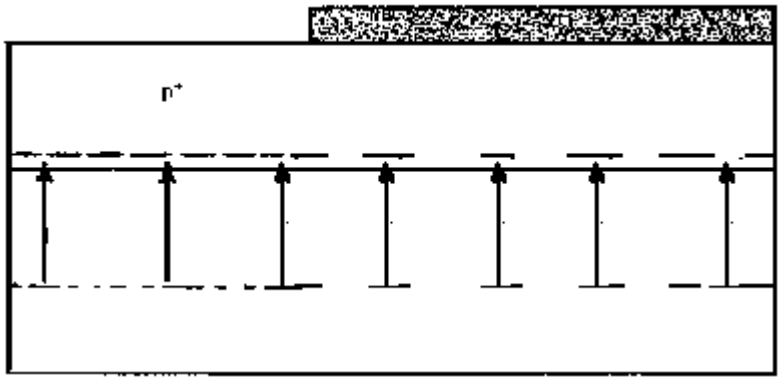

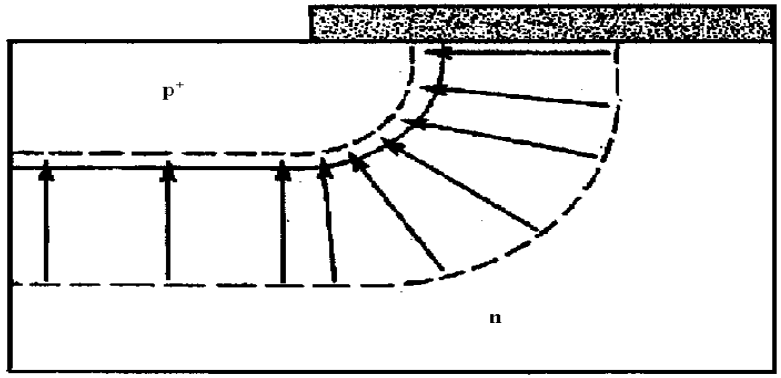

- Curved (Cylindrical and Spherical) junctions are formed at the corners of diffusion windows
- Electric field lines become crowded at the curved junctions resulting in a local increase in the electric field.
- ***Real devices with curved p-n junctions have significantly lower V_{BD} than the plane-parallel idealization.***

Metal-Overhang Analysis

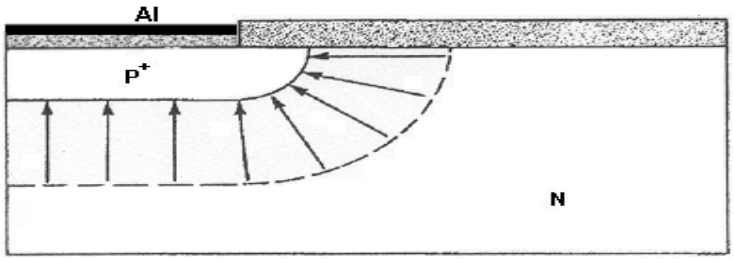

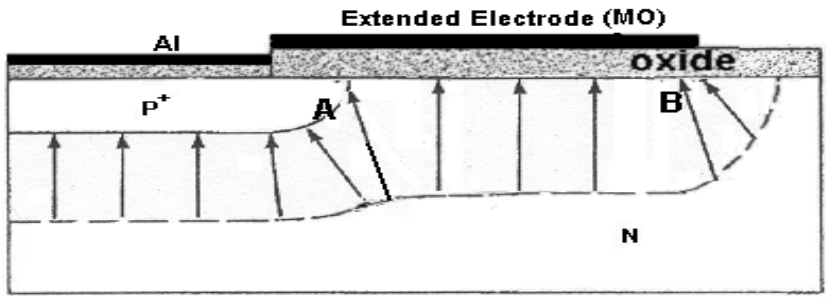

- **What is MO ?**
  - Extension of the metal layer over the oxide
- **How it Helps ?**
  - MO divides the applied bias between the main junction and the MO edge
  - Reduces the crowding of electric field by distributing it at two points:
    - Near the Junction Curvature (A)
    - Near the MO edge (B)
- **Need for Optimization ?**
  - Effect of MO becomes insignificant for ***too thin or too thick*** oxides

Device Structure for Simulation

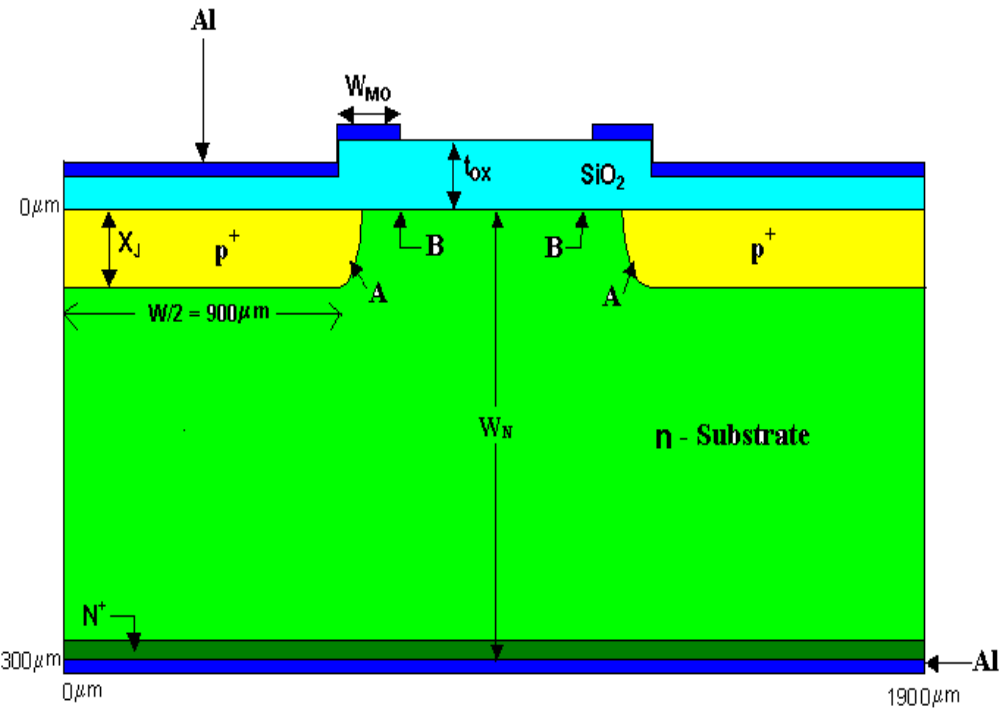

Detector dimension = 1900 μm X 300 μm

Strip-width (W) = 1800 μm

Strip-pitch (P) = 1900 μm

Doping Profile : GAUSSIAN

P^+ - Peak Doping Conc. = $5 \times 10^{19}/cm^3$

t_{ox} : thickness of oxide below metal overhang
X_J : radius of cylindrical junction
W_{MO} : width of metal-overhang
Q_F : density of surface charge
W_N : thickness of n-layer below the field oxide

Radiation Damage in Si Detectors

Radiation Damage

Bulk Damage | Surface Damage

- Bulk damage in Si is caused mainly by Non-Ionizing Energy Loss (NIEL) interaction of primary particle with a lattice displacing a Primary Knock-on Atom (PKA)
- The major effects expected from bulk damage are:
  - Increase in the leakage current
  - Deterioration of charge collection efficiency
  - Change in the effective carrier concentration (N_{eff}) which leads to Type Inversion
- The main obstacle to the operation of Si detectors is the change in N_{eff} which results in an increased value of full depletion voltage
  - The effective doping concentration is parameterized using Hamburg model:

$$\Delta N_{eff} = N_{eff,0} - N_{eff}(\varphi_{eq}, t) = N_A(\varphi_{eq}, t) + Nc(\varphi_{eq}) + N_Y(\varphi_{eq}, t)$$

- To incorporate the effect of increase in leakage current with fluence, we have changed the minority carrier lifetime Kraner's model

$$1/\tau = 1/\tau_0 + k\varphi_{eq}$$

Surface Damage in Si Detector

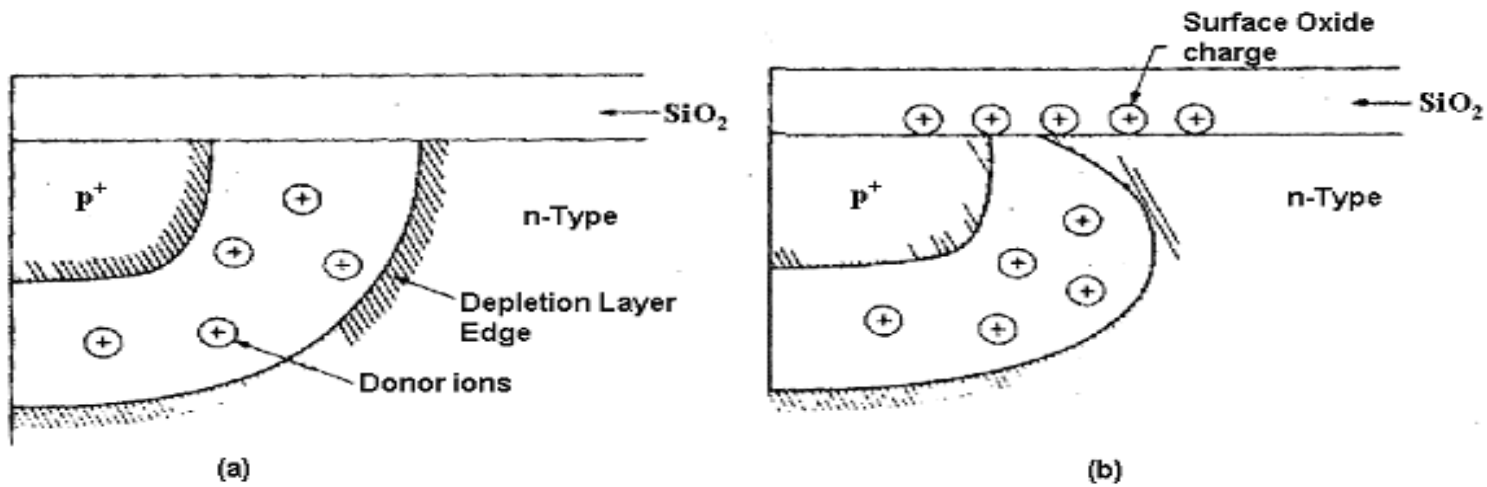

- Charge situated at the Si-SiO_2 interface

- For high quality SiO_2 grown on <111> oriented Si :
  - For non-irradiated detectors $Q_F \sim 3 \times 10^{11}$ cm^{-2}
  - Under ionizing radiation, Q_F saturates at about 1×10^{12} cm^{-2}

- Lead to dense accumulation layer beneath the surface → contraction of the depletion region → ***Premature Breakdown of the Device***.

Effect of Irradiation on the Breakdown Voltage

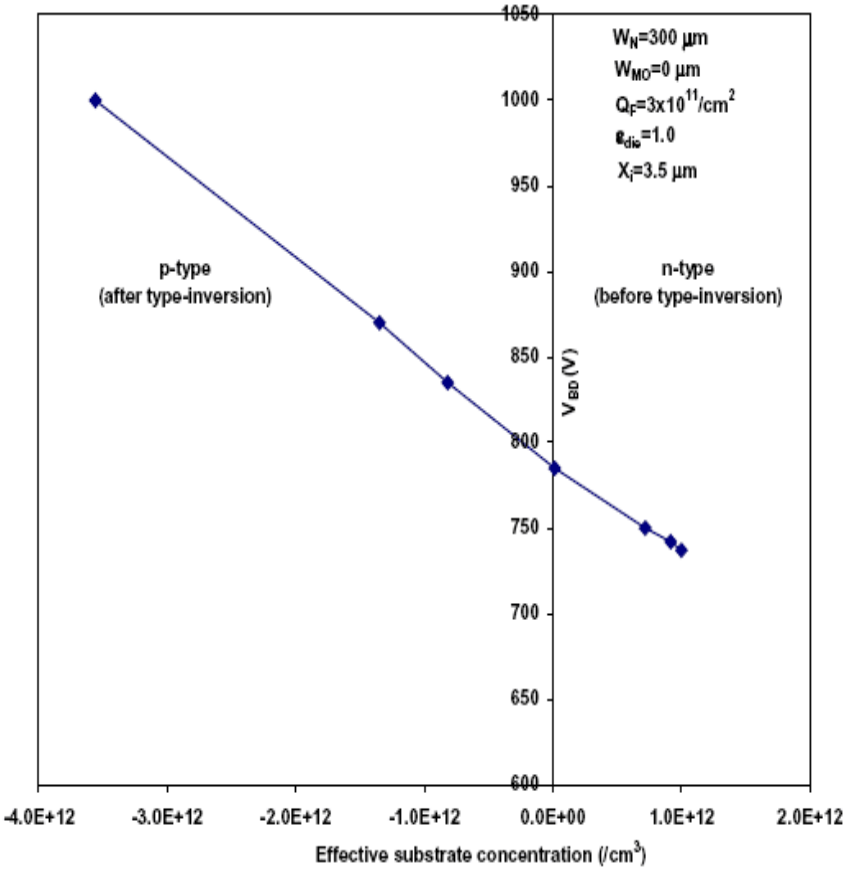

Year	Fluence (each year) x 10^{13} (n/cm^2)	Integrated fluence x 10^{13} (n/cm^2)	N_{eff}x10^{11} (/cm^3)	Minority carrier lifetime (ms)
1	0.2	0.2	9.16	0.01111
2	0.6	0.8	7.19	0.00303
3	1.2	2.0	3.68	0.00123
4	2.5	4.5	-2.62	0.00055
5	2.5	7.0	- 8.18	0.00036
6	2.5	9.5	- 13.5	0.00026
7	2.5	12.0	- 18.8	0.00021
8	2.5	14.5	- 24.3	0.00017
9	2.5	17.0	- 29.9	0.00014
10	2.5	19.5	- 35.6	0.00013

- Simulated radiation damage by varying N_{eff} and minority carrier life time (τ)
- Artificially located surface state fixed oxide charge at Si-SiO_2 interface
- V_{BD} increases with increase in Fluence

Does Radiation improve V_{BD}?

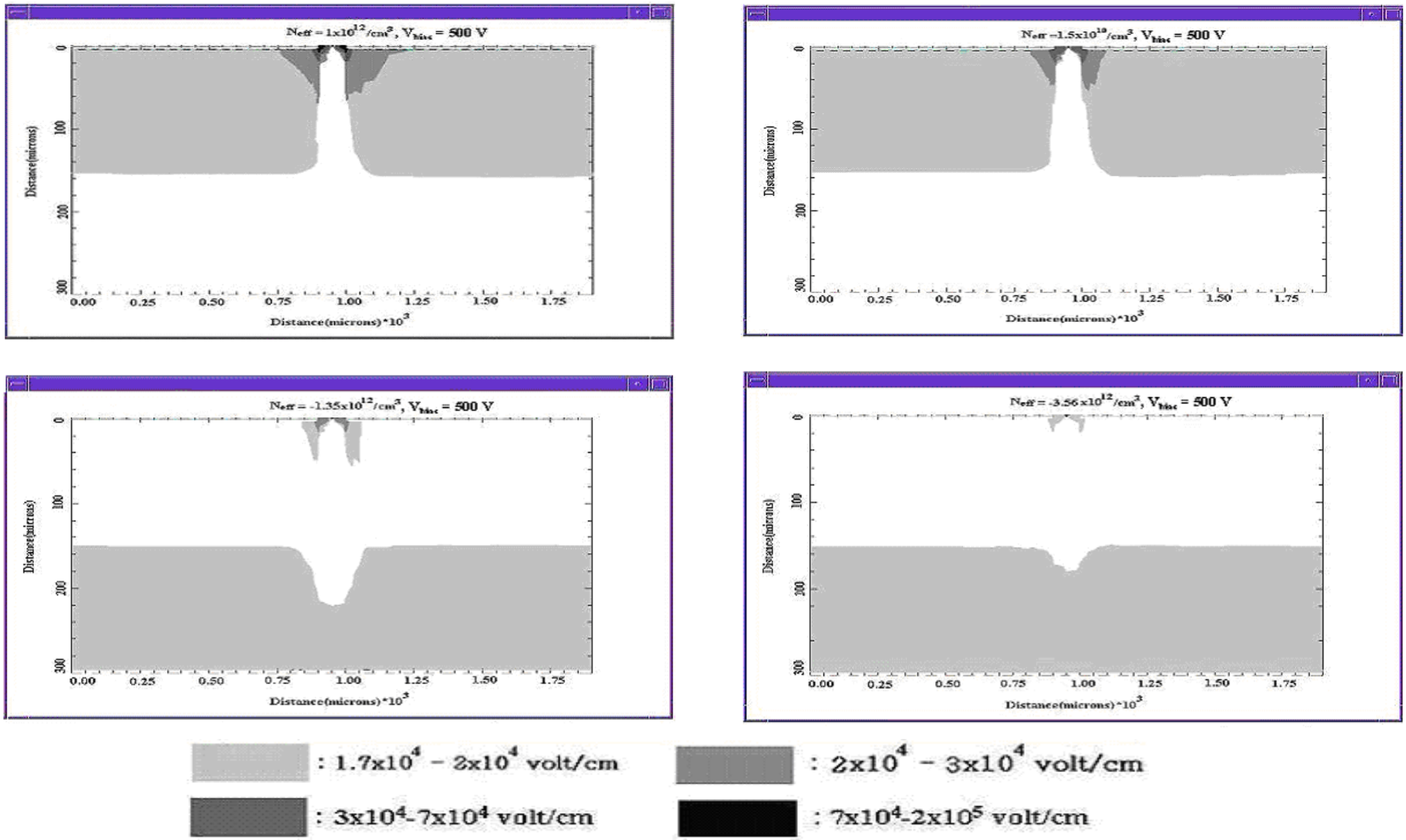

Annealing Studies on Irradiated Sensors

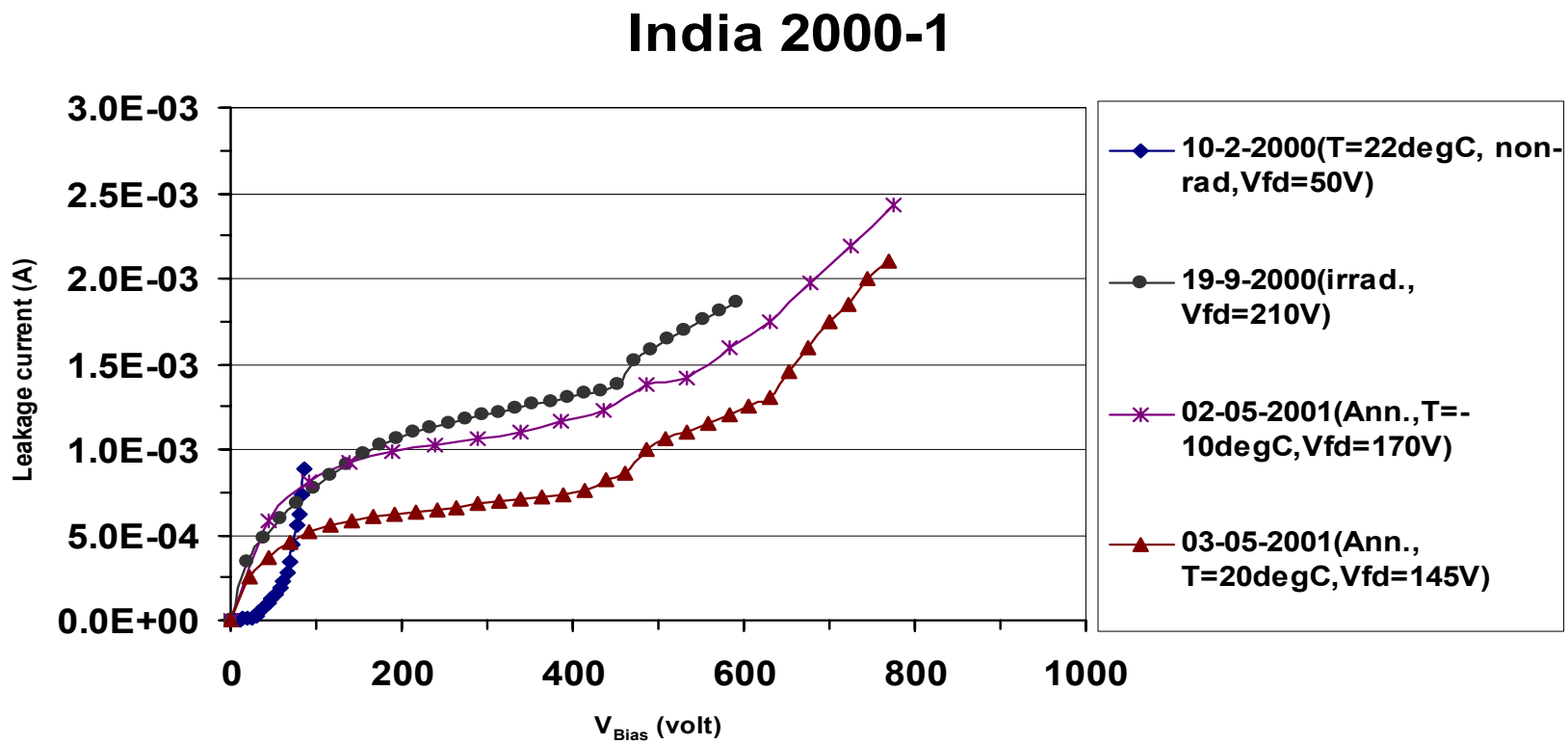

- The post-irradiation behaviour of all the detectors show an improvement in stability and breakdown Voltage.
- The V_{FD} and leakage current are decreasing with time.
- The detector is still in the beneficial annealing phase.

Effect of Passivation

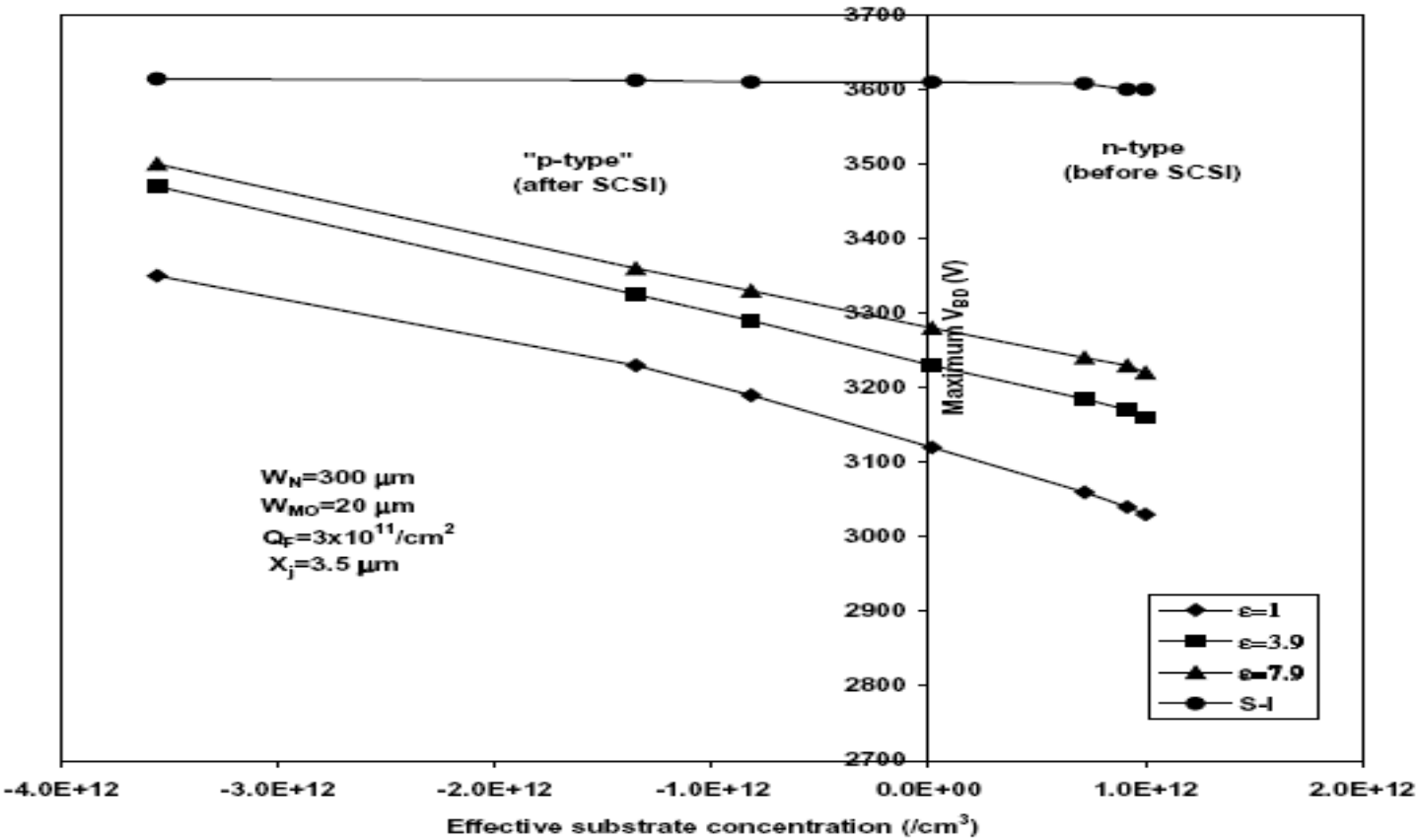

- V_{BD} of the device improves as the value of ε increases.
- S-I passivated device is insensitive to the variation in N_{eff}.

Potential distribution near the surface at breakdown

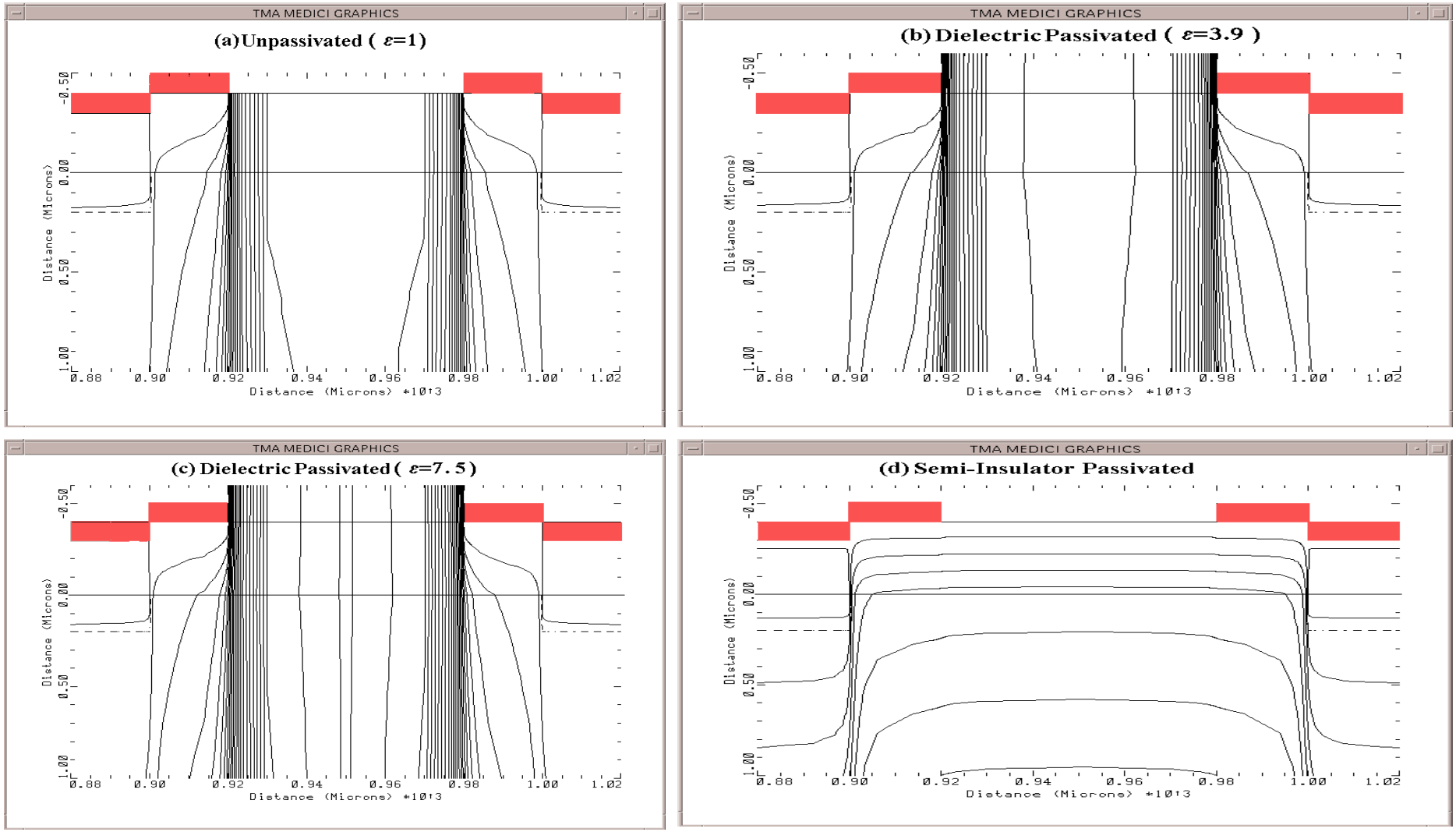

Effect of Field – Oxide Thickness (t_{OX})

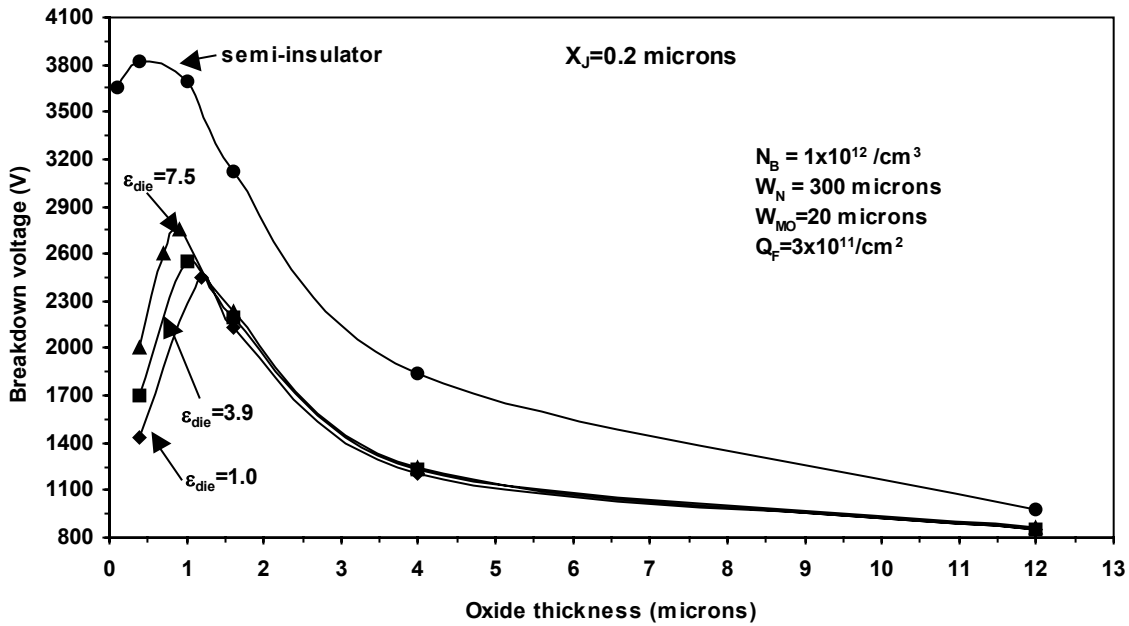

- V_{BD} initially ↑ with ↑ in t_{OX}, attains a maximum value corresponding to $t_{OX(OPT)}$ and then ↓ for further increase in t_{OX}.
- In the region t_{ox}>$t_{ox(OPT)}$, V_{BD} is insensitive to the variation in ε_{die}.
- The value of $t_{ox(OPT)}$ is lower if higher value of ε_{die} is used and it is even less if semi-insulated passivated device is used.

Optimal oxide thickness Vs. N_{eff}

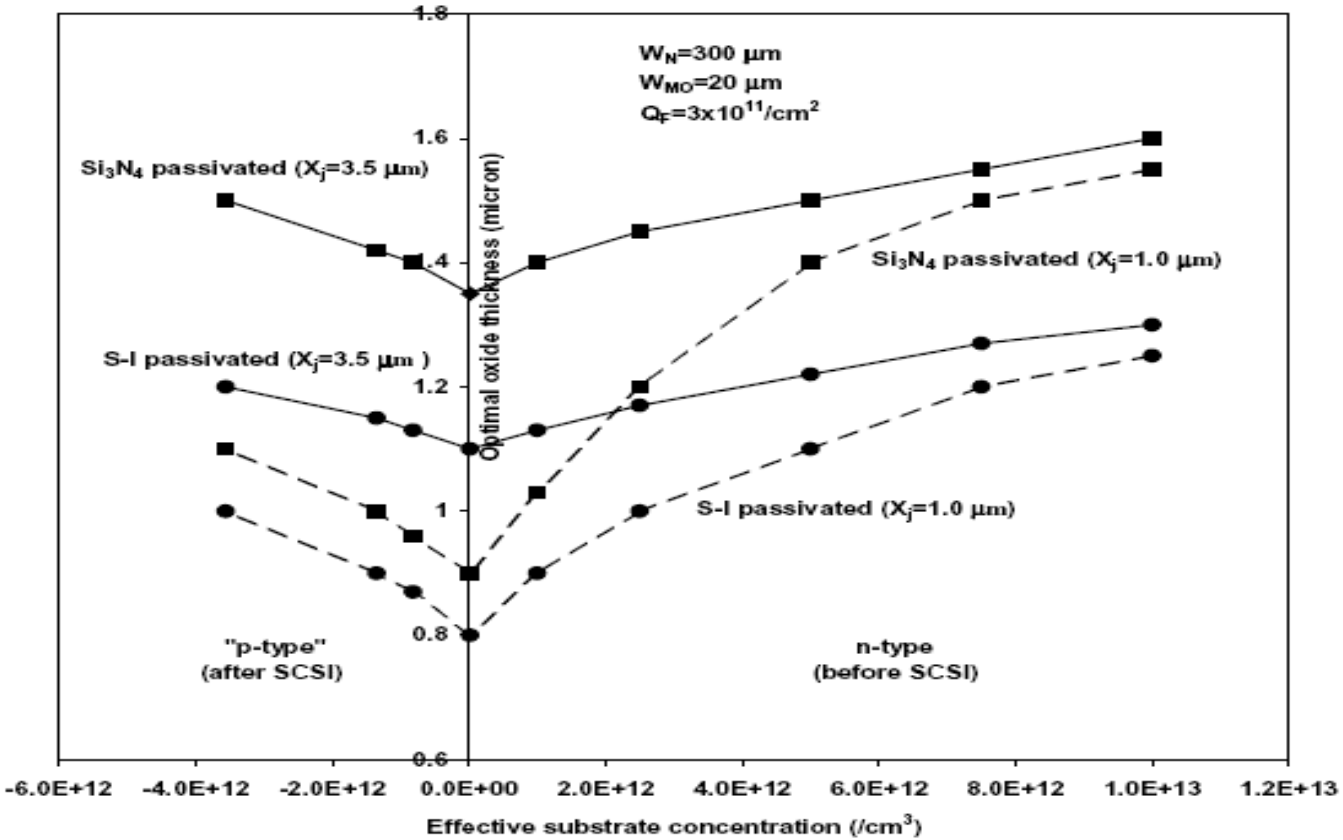

- Initially $t_{ox(opt)}$ decreases up to SCSI and then increases.
- S-I passivated devices are less sensitive to the variation of $t_{ox(opt)}$.

Utility of MO after irradiation

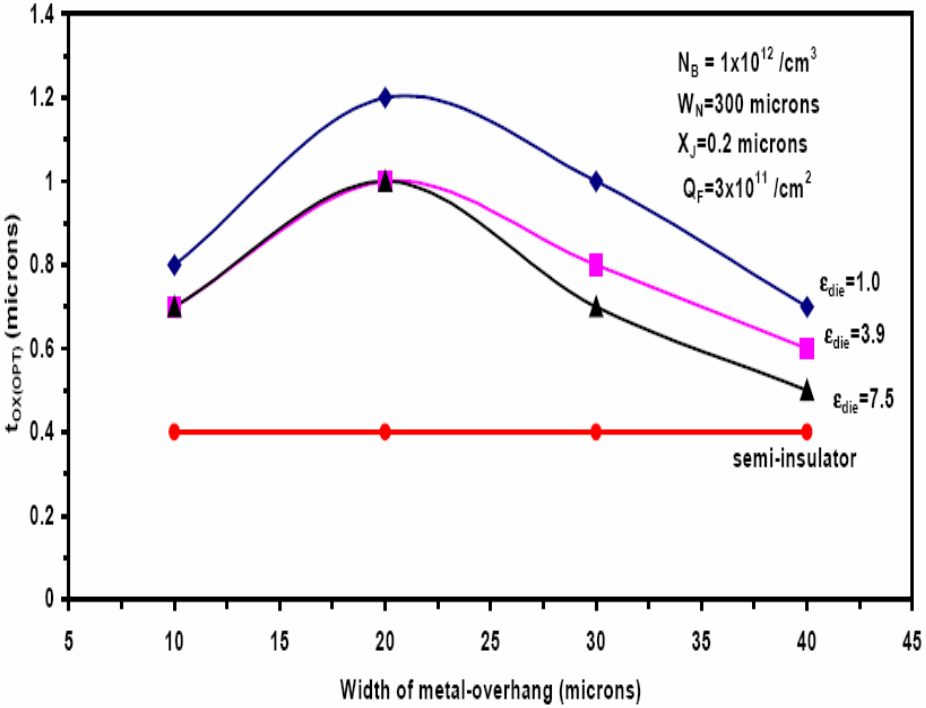

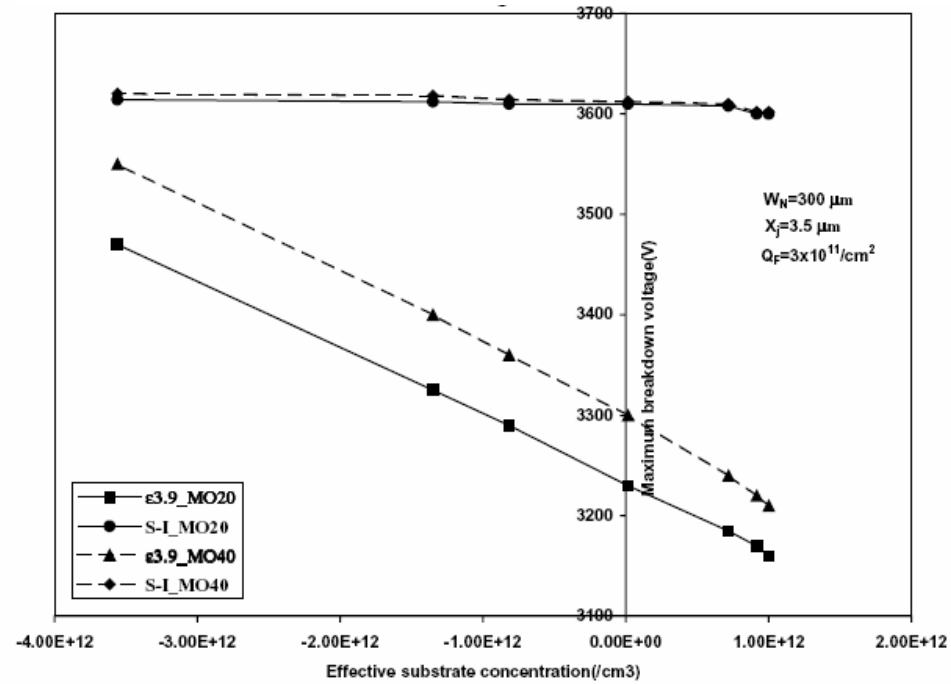

- For S-I passivated device, $t_{ox(opt)}$ does not change with W_{MO}.
- For dielectric passivated device, max. V_{BD} ↑ with ↑ W_{MO}.
- Strip pitch becomes a limiting factor for ↑ in W_{MO} and also the noise ↑ with ↑ in W_{MO}.

Impact of W_N on the V_{BD}

W_N (microns)	V_{BD} (N_{eff}=1x10^{12}/cm^3)	V_{BD} (N_{eff}= -3.56x10^{12}/cm^3)	ΔV_{BD} (V)
50	600	600	0
100	1050	1050	0
200	2050	2170	120
300	3220	3500	280
400	4150	4500	350

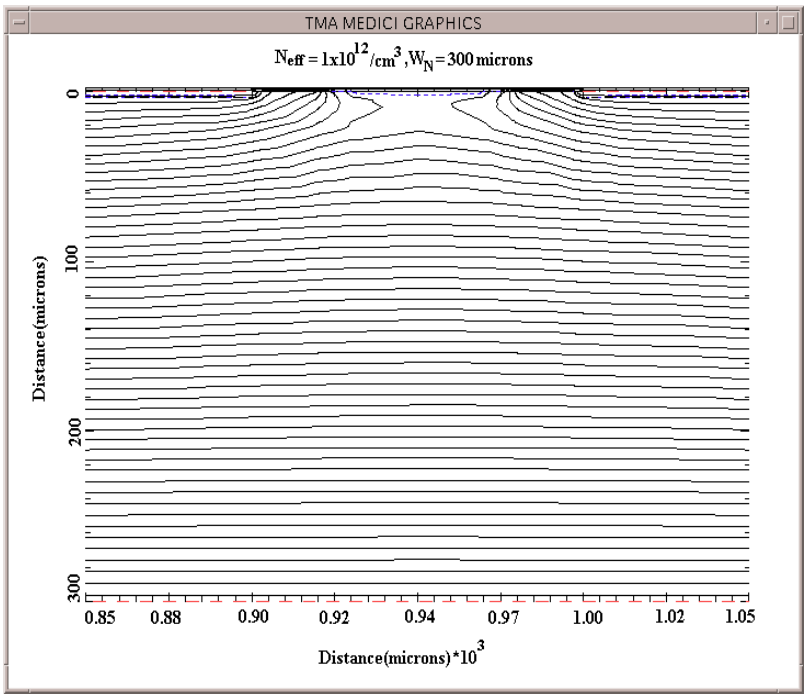

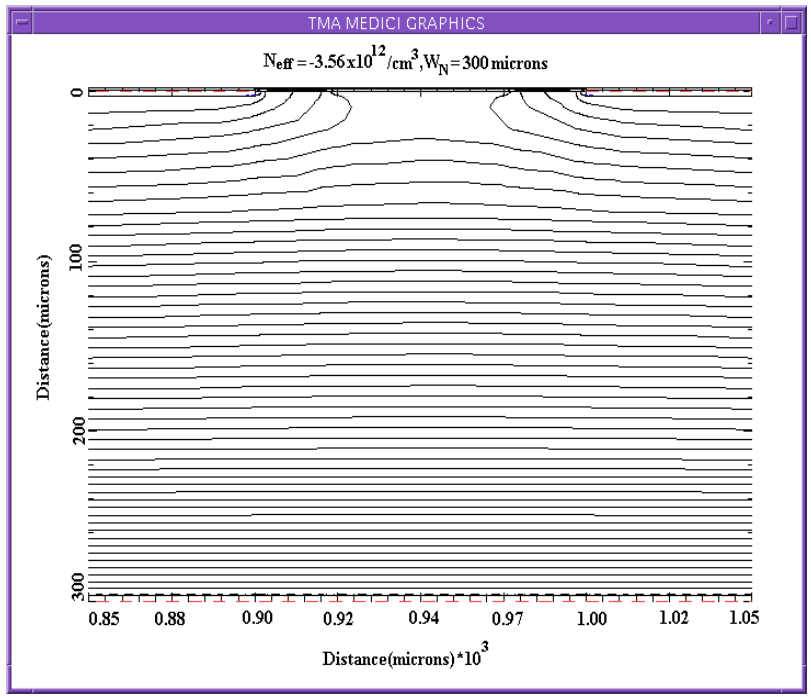

Impact of W_N on the V_{BD}

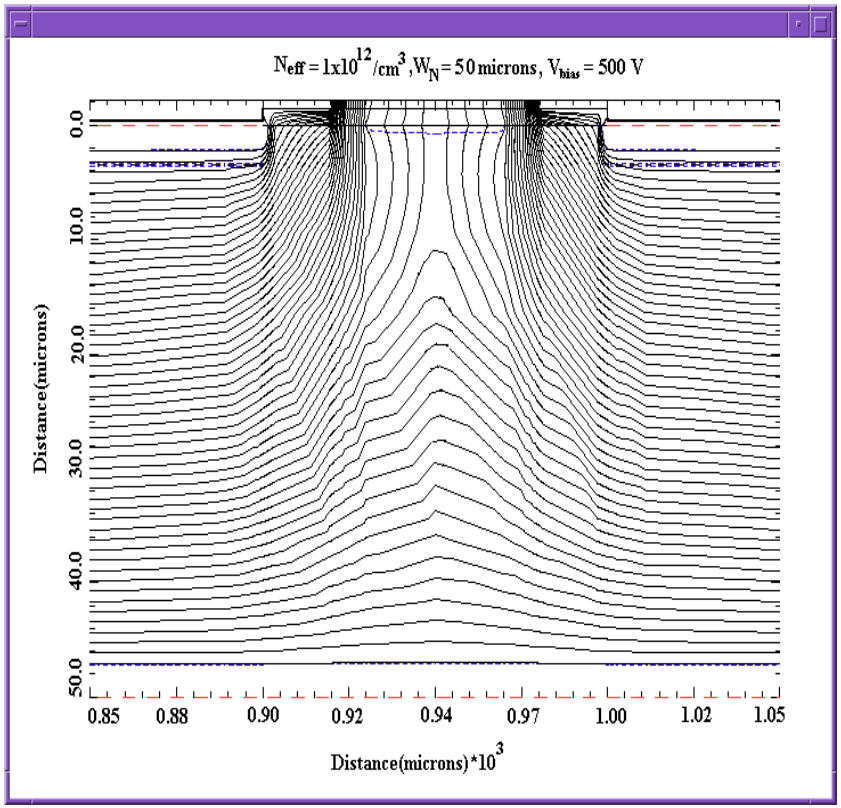

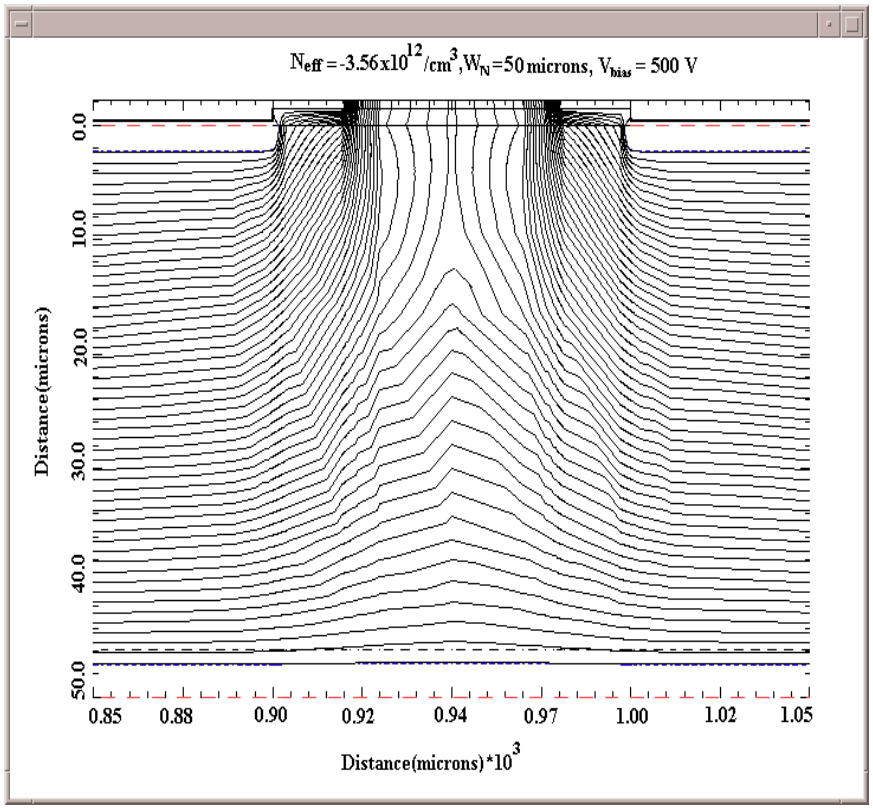

- The W_N is varied from 50 to 400 μm.
- There is no improvement in V_{BD} due to SCSI for W_N=50 and 100 μm.
- Thus, there is some minimum value of W_N for the beneficial effect of SCSI to occur.

Effect of Surface Charge Density (Q_F)

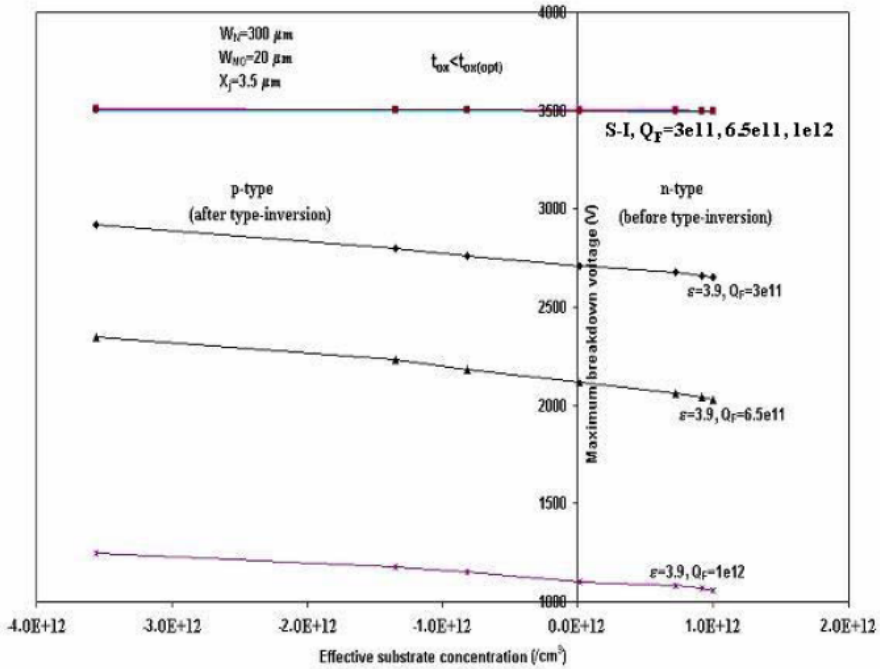

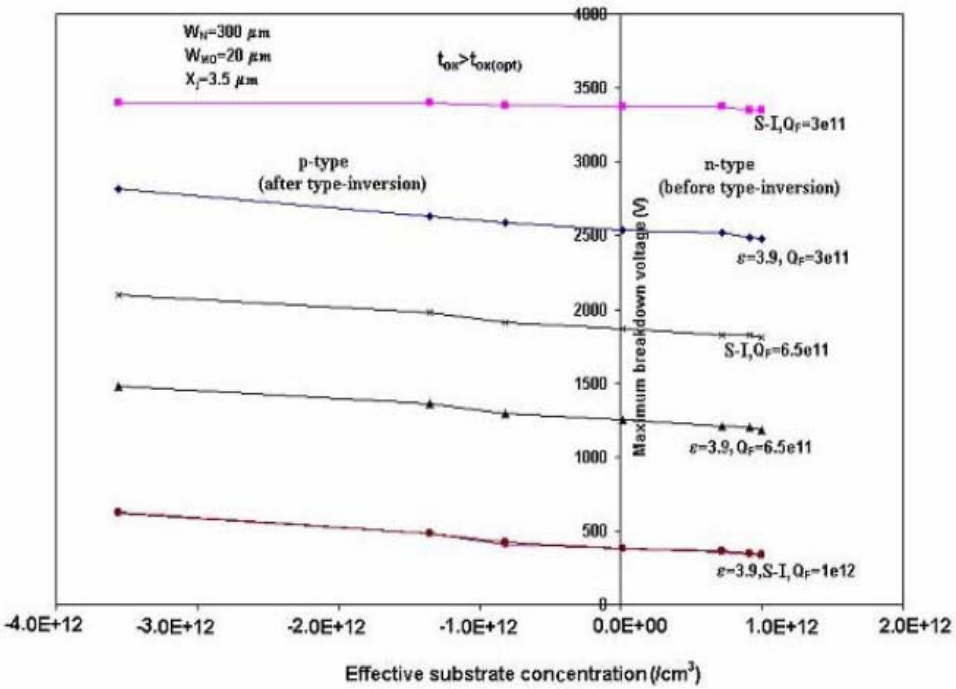

- For $t_{ox} \leq t_{ox(opt)}$, the S-I passivated device is insensitive to the variation in N_{eff} and Q_F.
- For $t_{ox} > t_{ox(opt)}$, the V_{BD} of S-I passivated device is decreasing with increase in Q_F.
- In order to make full use of S-I passivation, $t_{ox} \leq t_{ox(opt)}$.

Sudeep Chatterji, University of Delhi, India

Interstrip Capacitance and Noise Measurement of Si Sensors

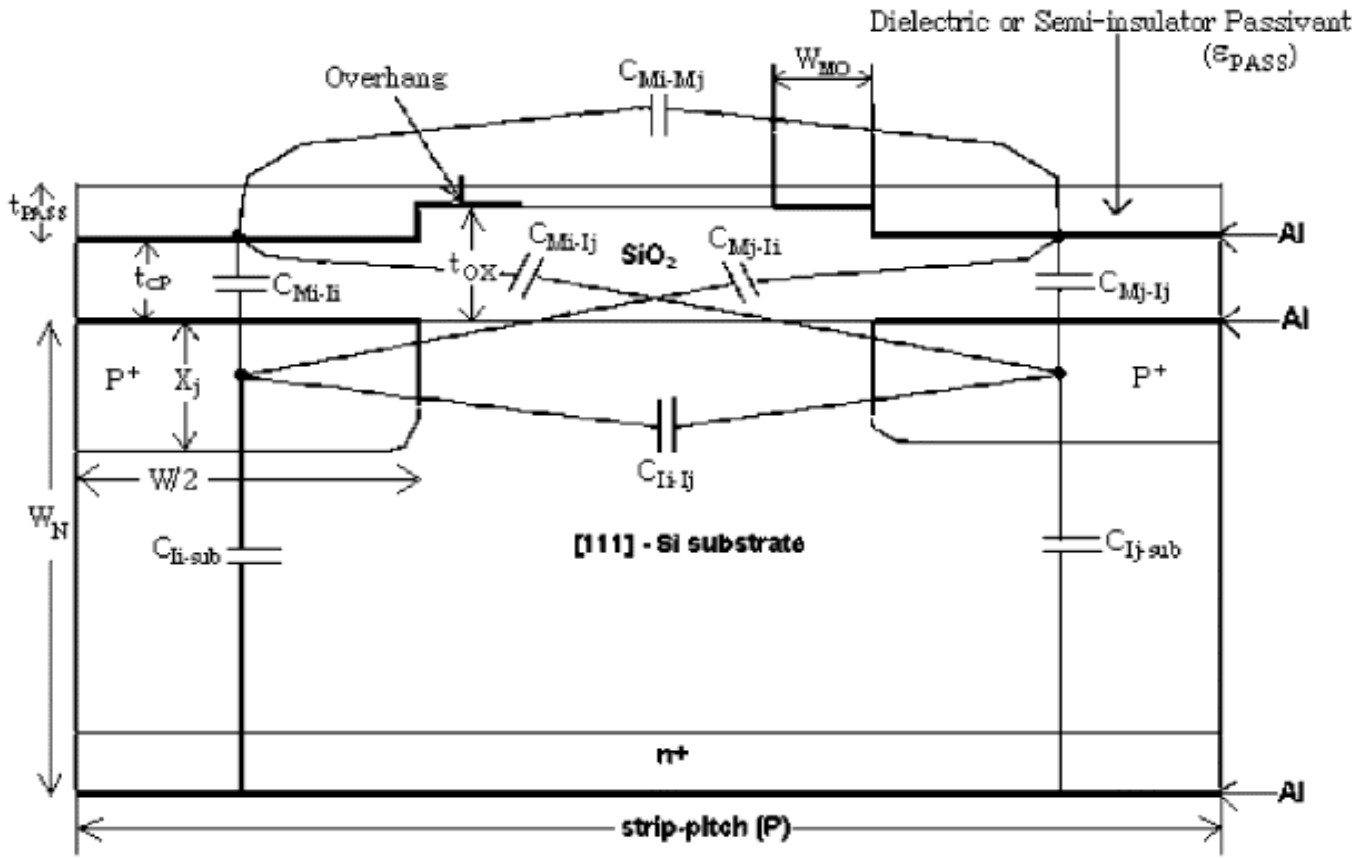

Significance of Interstrip capacitance (C_{int})

- Although helpful in improving the V_{BD}, metal-overhang is found to have detrimental effect on S/N ratio.
- Equivalent Noise Charge (ENC) α $24kT\ (C_D + C_{FET})^2 / (3g_m)$
  - C_D = backplane capacitance + interstrip capacitance
  - C_{FET} = Capacitance associated with input FET of the preamplifier
- The backplane capacitance ($C_{Ii\text{-}sub}$, $C_{Ij\text{-}sub}$) has not been analyzed.
- The total interstrip capacitance between two facing strips is given by:

$$C_{int} = C_{Mi\text{-}Mj} + C_{Ii\text{-}Ij} + C_{Mi\text{-}Ij}$$

  - Capacitance between metal of ith and j^{th} strips ($C_{Mi\text{-}Mj}$)
  - Capacitance between the implanted strips ($C_{Ii\text{-}Ij}$)
  - Capacitance between a metal and adjacent strip's implant ($C_{Mi\text{-}Ij}$, $C_{Mj\text{-}Ii}$)
- Dependence of C_{int} on metal-overhang extension has been explored.
- Also the effect of other geometrical and physical parameters like strip-width/pitch ratio and relative permittivity of the passivant on C_{int} has been performed.

Dependence of C_{int} on W_{MO}

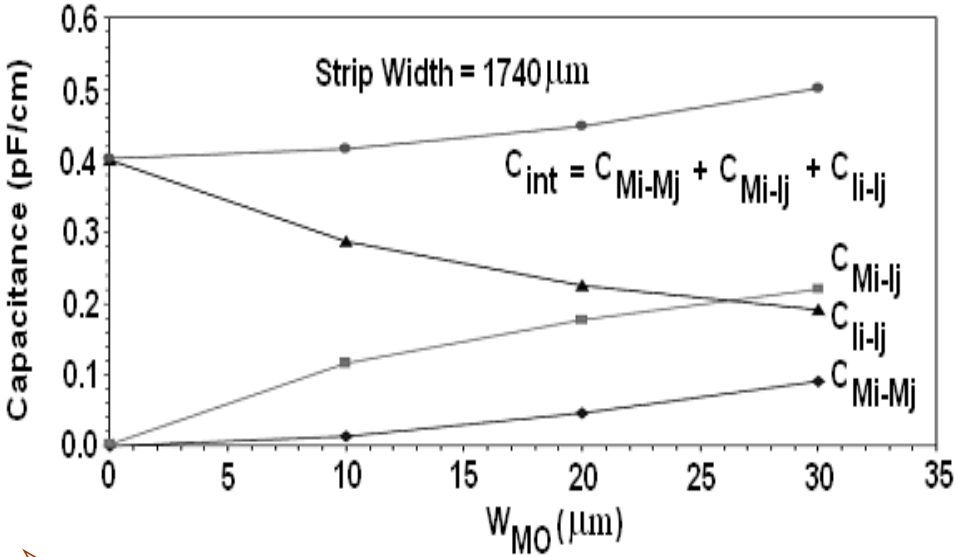

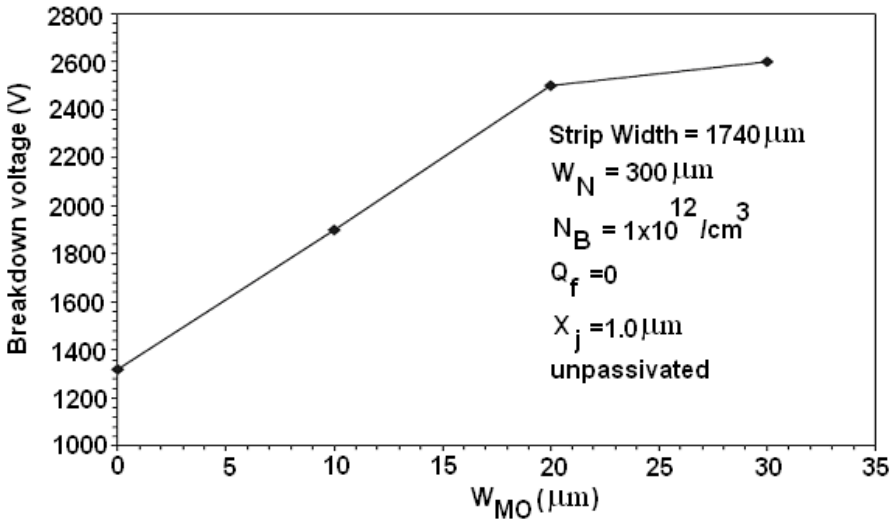

- When overhang is absent, C_{Ii-Ij} dominates and A decrease in C_{Ii-Ij} is also observed with increase in overhang
- On increasing W_{MO}, other two components C_{Mi-Mj} and C_{Mi-Ij} show an ↑ in their values
- The increase in the values of two components C_{Mi-Mj} and C_{Mi-Ij} is greater than the decrease in the value of C_{Ii-Ij}
- Thus C_{int} increases with increase in W_{MO}
- It can be seen that "short" overhang (10 μm) have no appreciable influence on C_{int}
- The capability of the overhang to suppress breakdown is loosely related to its actual size

Effect of Surface state fixed oxide charge (Q_f)

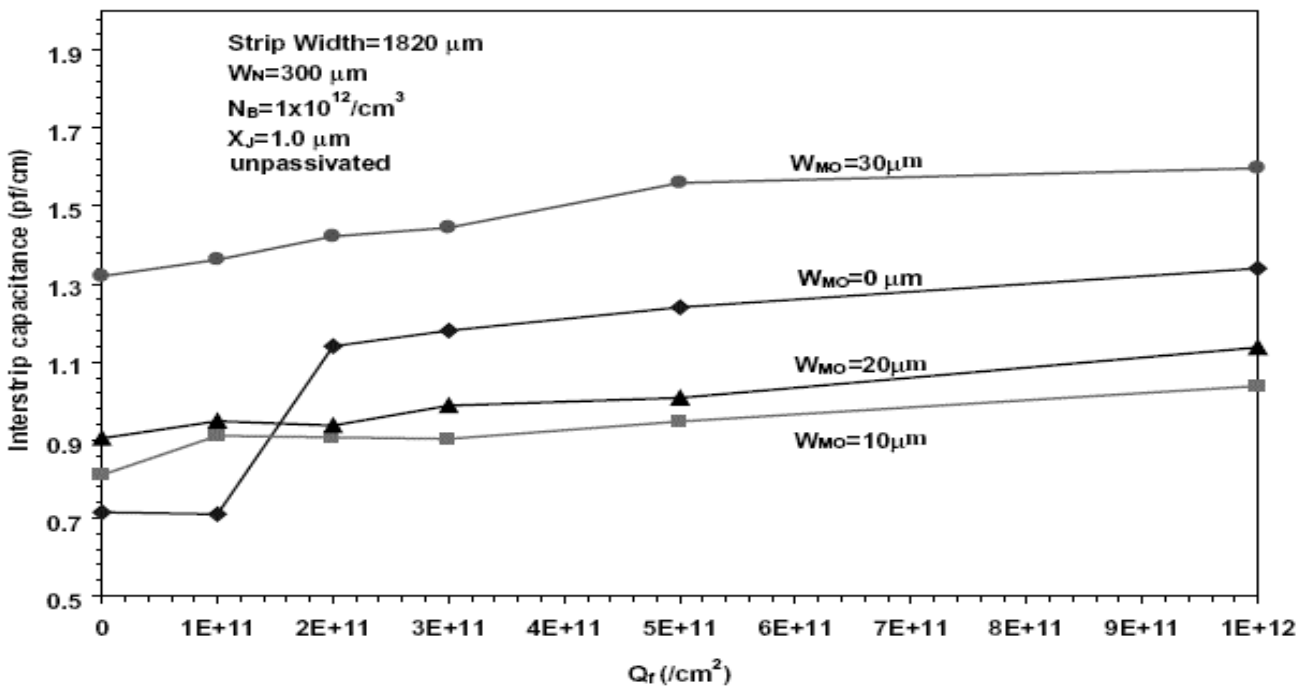

- For structures without MO, C_{int} shows a sharp increase at $Q_f = 2 \times 10^{11}$ /cm^2
- However, MO equipped devices are insensitive to variation with Q_f
- For Q_f exceeding 2×10^{11}/cm^2, the value of C_{int} for W_{MO}=0 exceeds that of W_{MO}=10 and 20 μm
- For Q_f=0, C_{int} increases with increase in W_{MO} whereas for $Q_f \geq 2\times 10^{11}$/cm^2 C_{int} first decreases up to W_{MO}=10 μm and then increases

Effect of Surface state fixed oxide charge (Q_f)

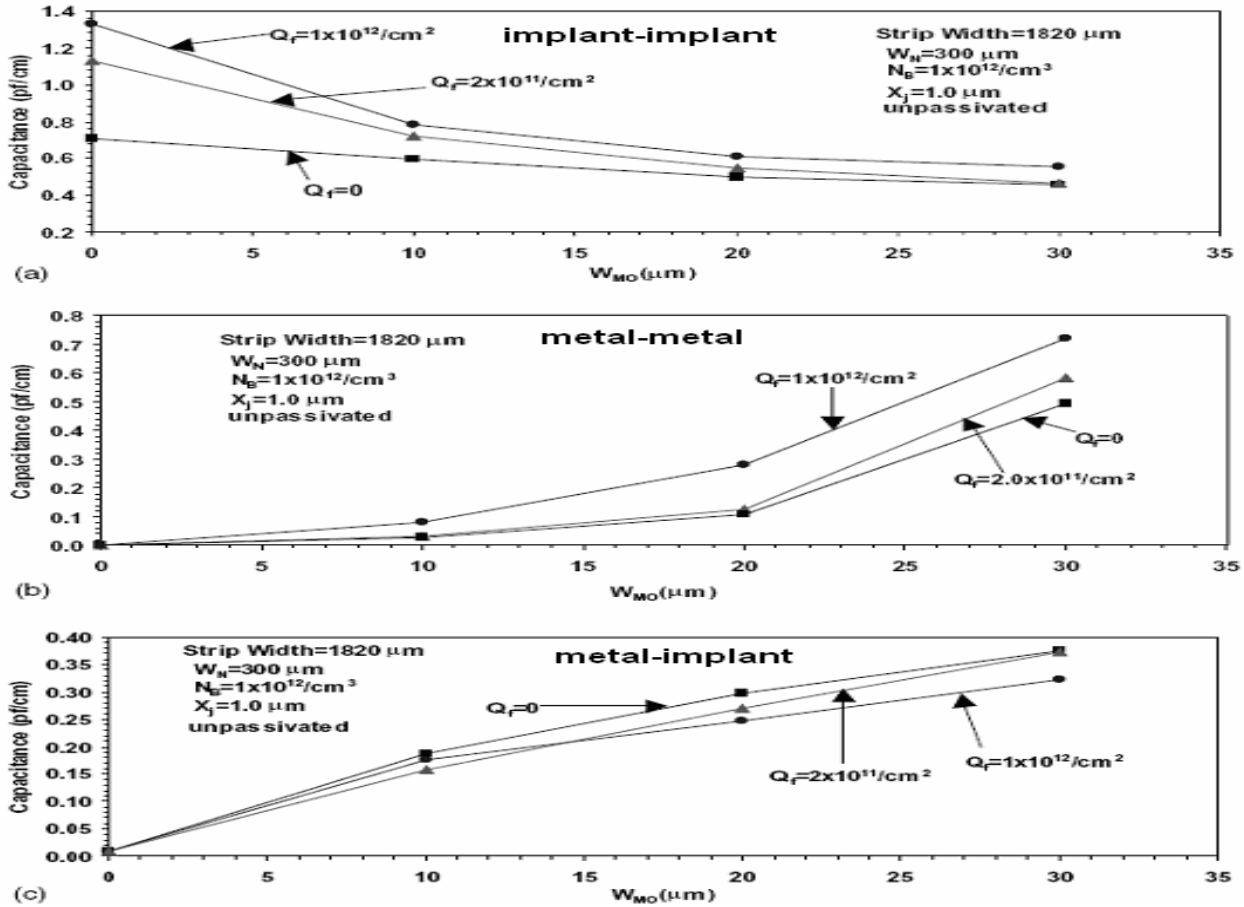

- When W_{MO} is increased from 0 to 10μm, there is a sharp decrease in $C_{Ii\text{-}Ij}$.
- The other two components remain unchanged as Q_f is increased from 0 to $2x10^{11}/cm^2$.

Sudeep Chatterji, University of Delhi, India

Noise measurement of Si sensors

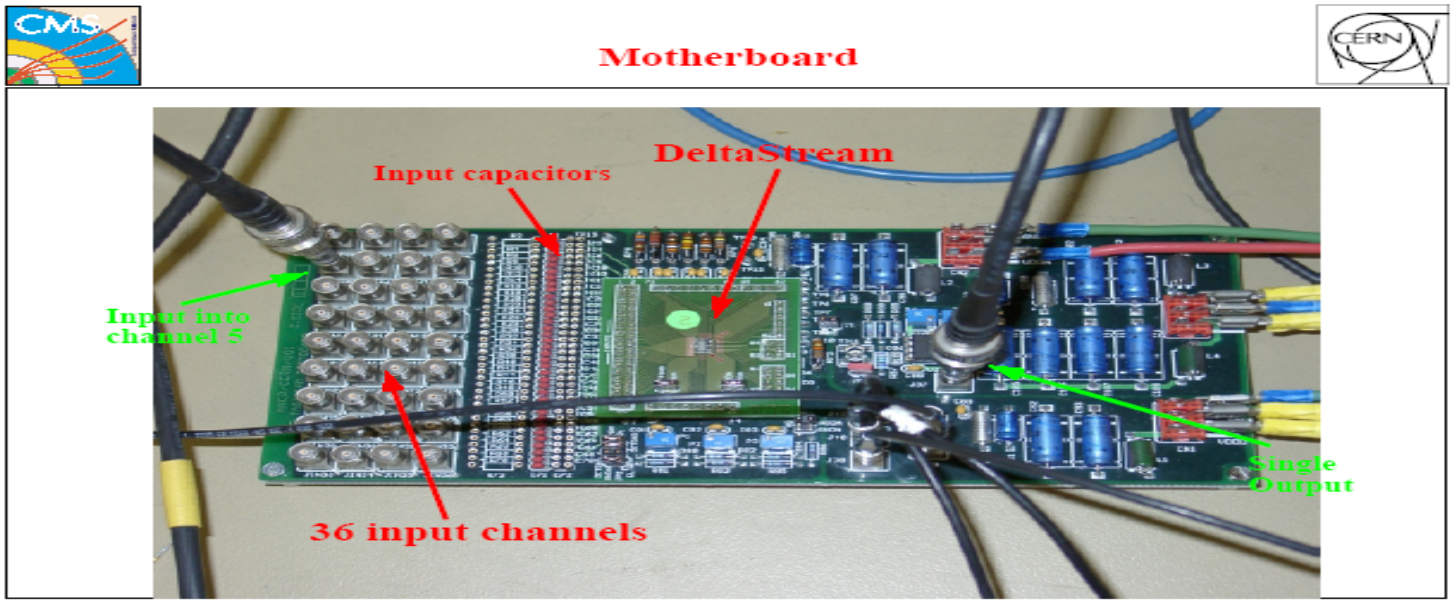

- The amount of charge produced by a single traversing MIP depends on the thickness of the depletion region
- A common benchmark is a mean of 25000 e (~4 fC of charge) for 300μm thick Si sensor
- Noise measurements on a set of 7 non-irradiated detectors were performed at CERN

Noise measurement of Si sensors

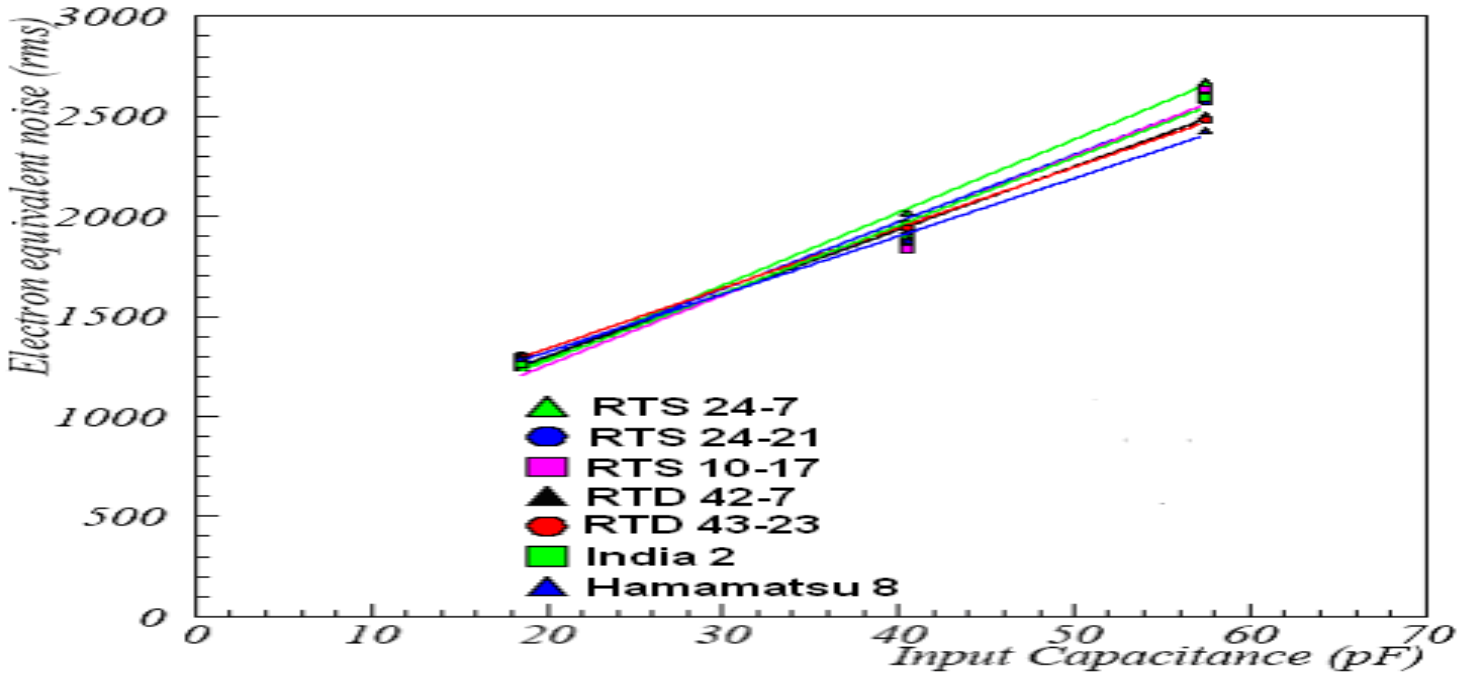

- All measurements have been made using test pulses to inject charge corresponding to 4 fC for each equivalent 1 MIP
- As is clear, in order to achieve a S/N >10 the total input capacitance should be < 56 pF

Conclusion #1

- Metal-overhang is beneficial in improving the V_{BD} even after SCSI.
- There is a shift in tox(opt) with irradiation.
- The value of W_N should be high enough to enhance the V_{BD} after SCSI.
- S-I passivation is beneficial in terms of its insensitivity to fluence, $t_{ox(opt)}$ and W_{MO}.
- Limited metal overhang can be beneficial for improving the noise performance of the device and at the same time eliminating the adverse effect of junction curvature.
- A very important advantage of device equipped with metal overhang is that the C_{int} is almost insensitive to the variation in Q_f.

γ + Jet

Direct Photons: Photons that originate directly from hard scattering….

$$pp \rightarrow \gamma + jet + X$$

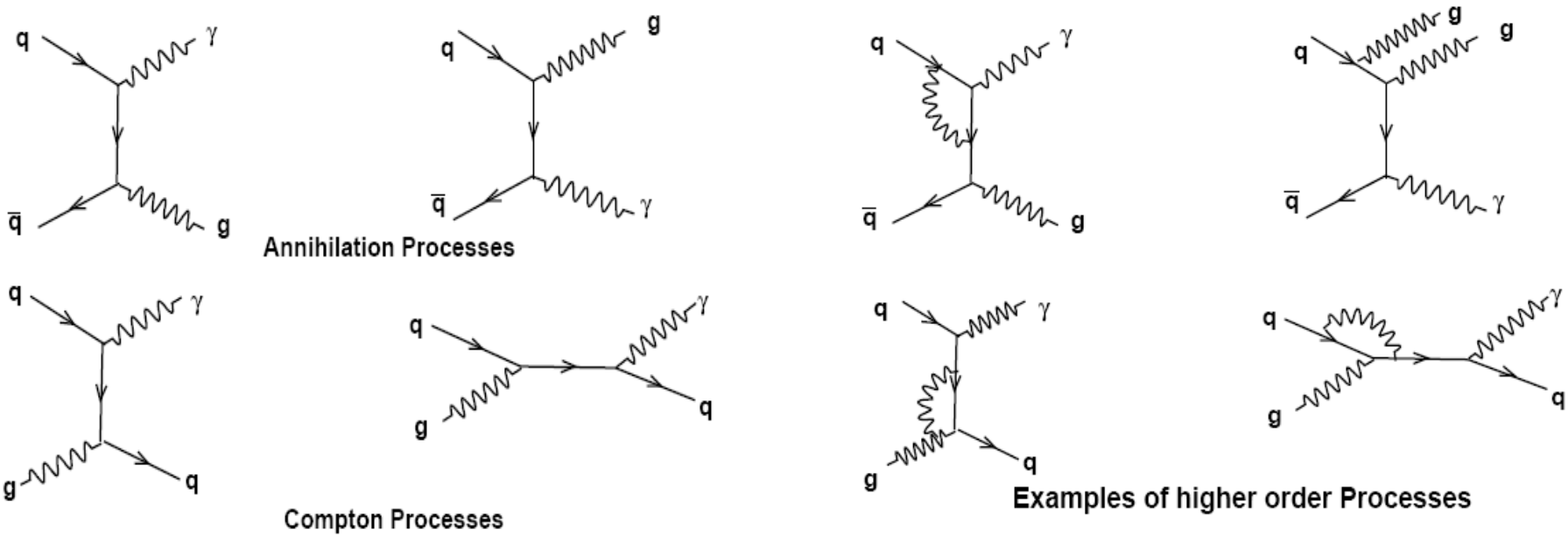

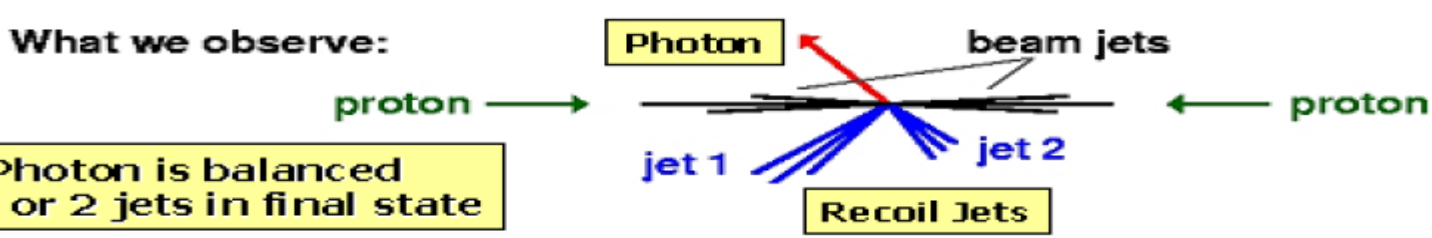

Background Processes

A fraction of jets (10^{-2} – 10^{-3}) fragments in a way such that a single particle carries most of the momentum of the parent parton. Several neutral mesons decay to produce two or more photons

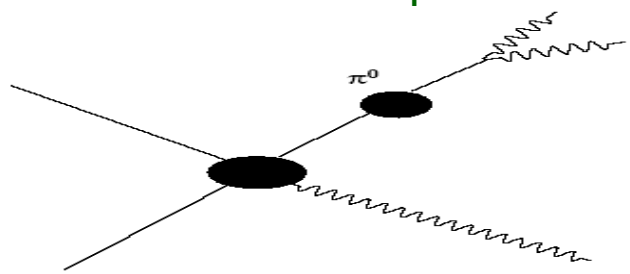

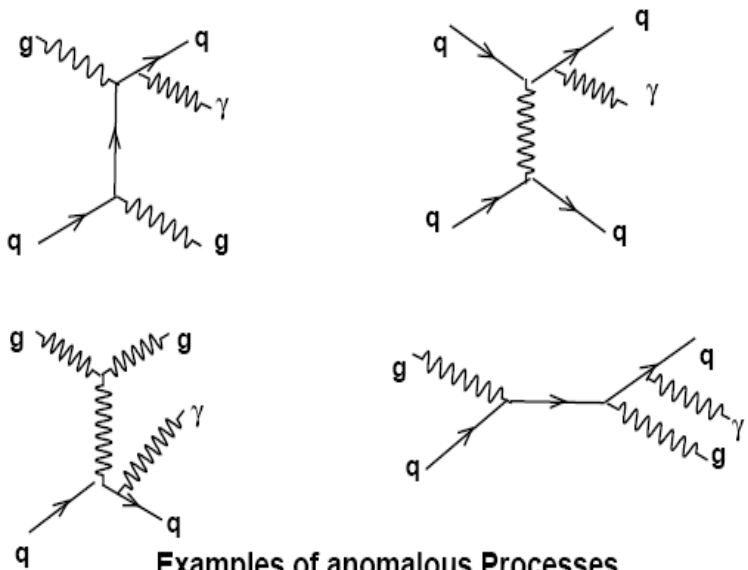

Examples of anomalous Processes

Particle	Mass (GeV/c^2)	Decay Products	Branching Ratio
π^0	0.135	$\gamma\gamma$	0.99
η	0.547	$\gamma\gamma$	0.39
η	0.547	$3\pi^0$	0.32
η	0.547	$\pi^0 \pi^+ \pi^-$	0.23
K_s^0	0.494	$2\pi^0$	0.31
ω	0.781	$\pi^0\gamma$	0.09

Background Processes

$gg \rightarrow gg$	$q\bar{q} \rightarrow gg$	$gq \rightarrow qg$
$qg \rightarrow qg$	$gg \rightarrow q\bar{q}$	$qq \rightarrow qq$
$qq' \rightarrow qq'$	$q\bar{q}' \rightarrow q\bar{q}'$	$q\bar{q} \rightarrow q\bar{q}$
$q\bar{q} \rightarrow q'\bar{q}'$		

CMS Software

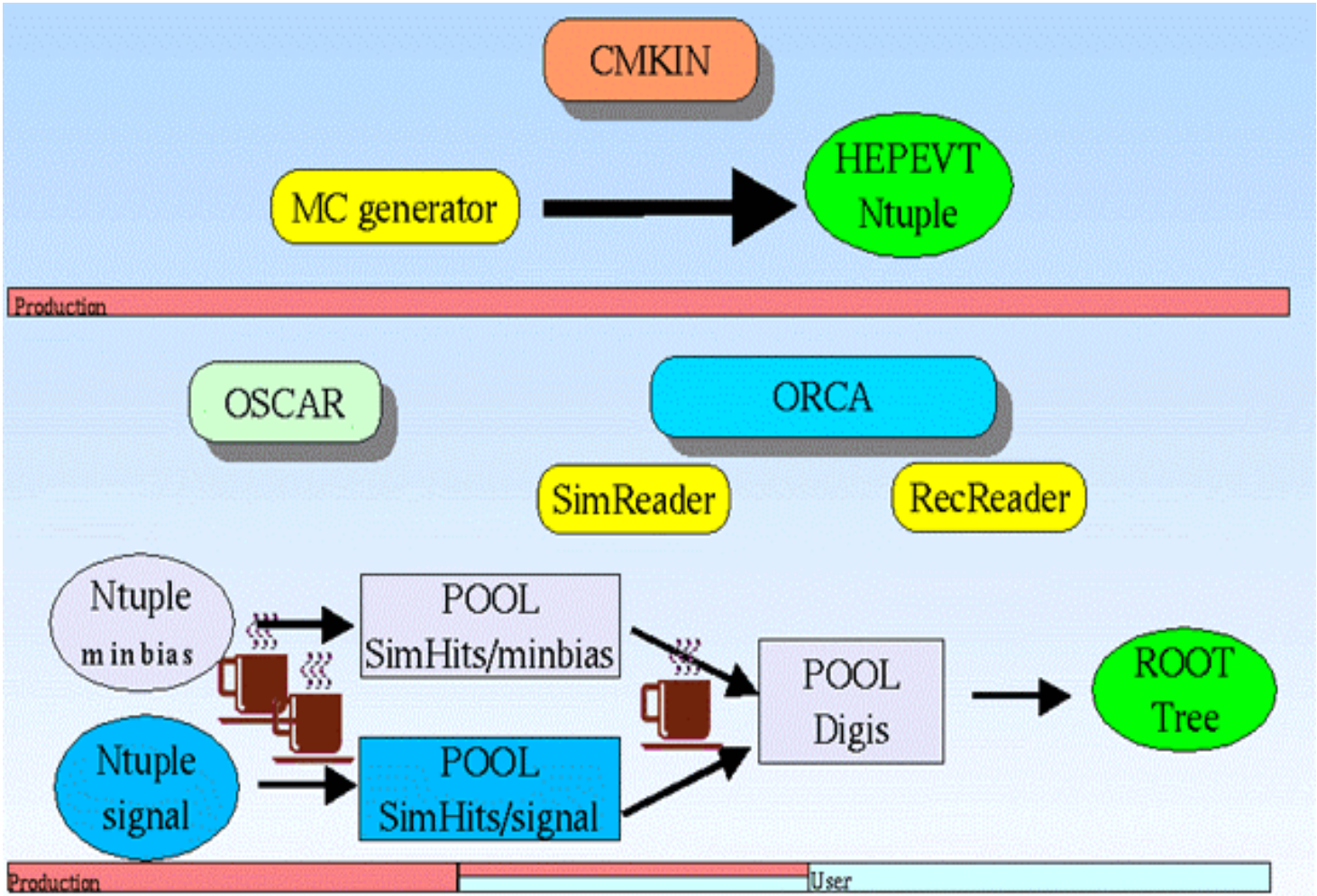

Generation Parameters

Generator used: PYTHIA (CMKIN_4_4_0)

Parameter	Direct Photon Signal
Process	MSUB = 14 (Gluon Compton Scattering) MSUB = 29 (Annihilation Process)
$\sqrt{s}$	14 TeV
PDF Used	CTEQ5L
P_T Range	>50 GeV (in different bins)

Pre-selection Used : Select only those events which have a direct photon with P_T >70 GeV & $|\eta^{\gamma}|$<2.8

Sudeep Chatterji, University of Delhi, India

Generation Parameters

Parameter	Background
Process	MSEL = 1 (QCD Jets)
$\sqrt{s}$	14 TeV
PDF Used	CTEQ5L
P_T Range	>50 GeV (in different bins)

Two DST Samples :

Data Sample Name	Pre-selection Used
eg03_jets_1e	Yes
jm03b_qcd	No

Preselection Used

- **Look for the seed particles of electromagnetic objects like photons, electrons and positrons which have P_T >5 GeV & $|\eta|$<2.7.**
- **Candidate electromagnetic calorimeter trigger tower energies are then estimated by adding energies of all electromagnetic particles found within $\Delta\eta$<0.09 and $\Delta\varphi$ < 0.09 from the seed.**
- **Trigger tower candidates that lie within $\Delta\eta$<0.2 and $\Delta\varphi$ < 0.2 from each other are suppressed and only those with the highest PT are retained.**
- **The Level-1 single photon electromagnetic trigger is simulated by requiring that one such candidate has transverse energy larger than 20 GeV.**

Sudeep Chatterji, University of Delhi, India

Data Samples

Data Samples	P_T (in GeV)	σ Generated (in pb)	σ Preselected (in pb)	Number of Simulated Events	Integrated Luminosity (in pb^{-1})
γ +jet	50-120	8.53E+03	1.82E+03	30000	16.5
γ +jet	120-170	2.77E+02	2.35E+02	12740	54.2
γ +jet	170-230	6.76E+01	6.19E+01	11918	192.5
γ +jet	230-300	1.90E+01	1.83E+01	11531	630.9
γ +jet	> 300	9.07E+00	8.98E+00	9887	1212.3
eg03_jets_1e_50170	50-170	2.43E+07	4.35E+06	2314853	0.53
eg03_jets_1e_170up	> 170	1.34E+05	1.07E+05	473668	4.4
jm03b_qcd_50_80	50-80	2.09E+07	2.09E+07	198993	0.009
jm03b_qcd_80_120	80-120	2.94E+06	2.94E+06	276986	0.094
jm03b_qcd_120_170	120-170	4.99E+05	4.99E+05	247002	0.5
jm03b_qcd_ 170_230	170-230	1.01E+05	1.01E+05	50000	0.5
jm03b_qcd_ 230_300	230-300	2.38E+04	2.38E+04	50000	2.09

Sudeep Chatterji, University of Delhi, India

Analysis

- **The histograms were made for all the standard isolation variables suggested for Level 3 single isolated photon trigger after applying the $P_T^{\gamma} > 80$ GeV and $|\eta^{\gamma}| < 2.6$ cuts.**
- **Tracker isolation: the number of tracks which have $P_T > P_T^{thres}$ (which has been taken as 1.0 GeV,1.5 GeV, 2.0 GeV) should be less than the threshold values.**
- **ECAL isolation : the sum of the transverse energy of all the basic clusters lying in the Cone size R around the photon candidate should be less than the threshold value.**
- **HCAL isolation: the sum of the transverse energy of all the particles depositing energies in the HCAL should be less than the threshold value.**
- **All the efficiency plots have been done by varying the threshold values for all the parameters.**

Sudeep Chatterji, University of Delhi, India

Plots of the Number of Tracks with P_T >1.5 GeV for various Cone Sizes

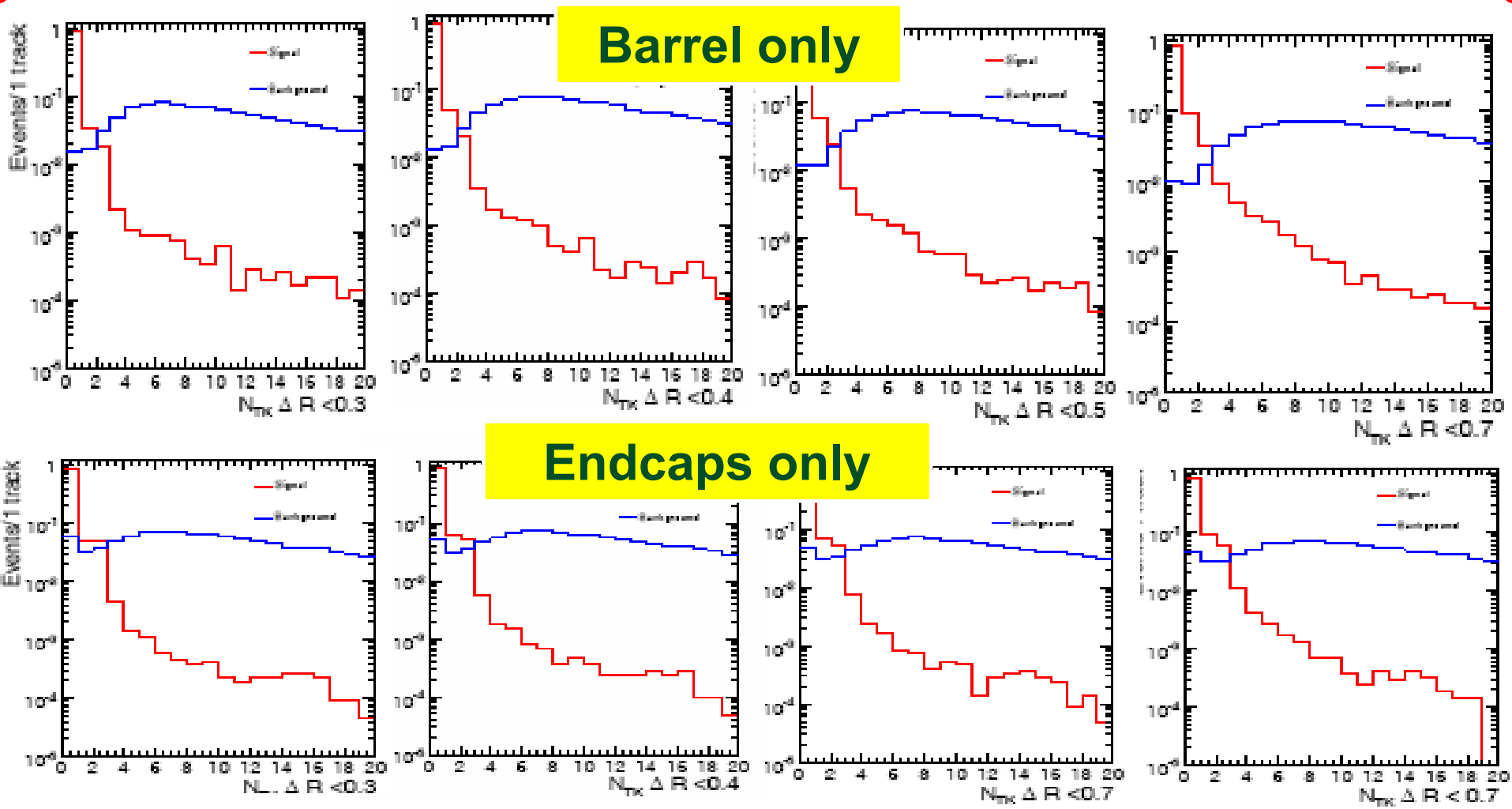

R= 0.3 **R= 0.4** **R= 0.5** **R= 0.7**

Sudeep Chatterji, University of Delhi, India

Signal Efficiency vs. Background Rate

No. of Tracks in Cone size R = 0.3 and 0.4

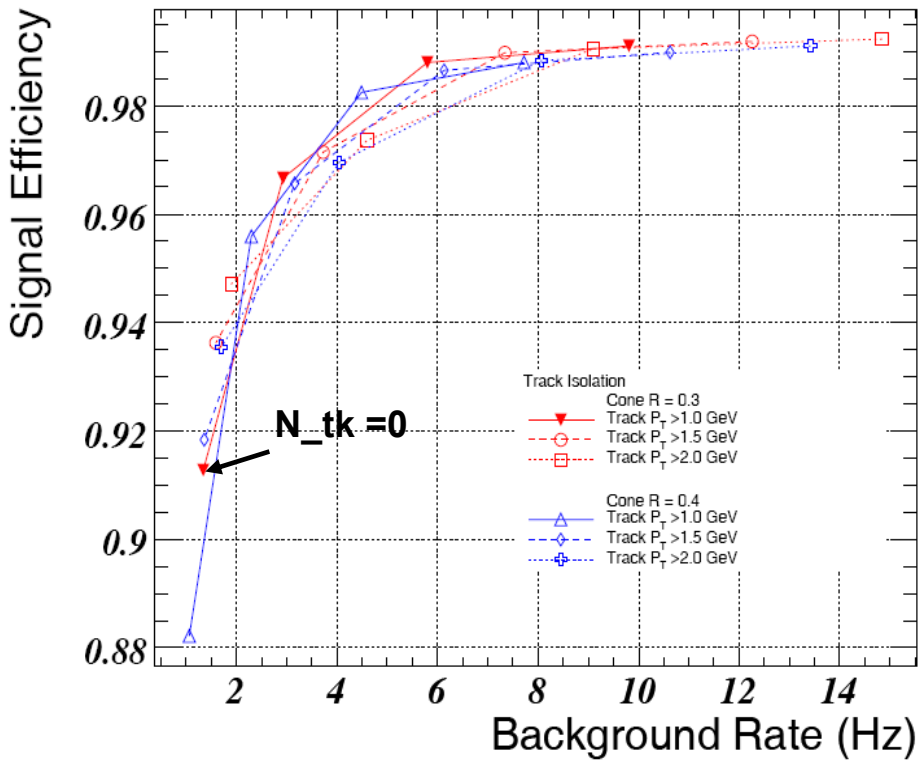

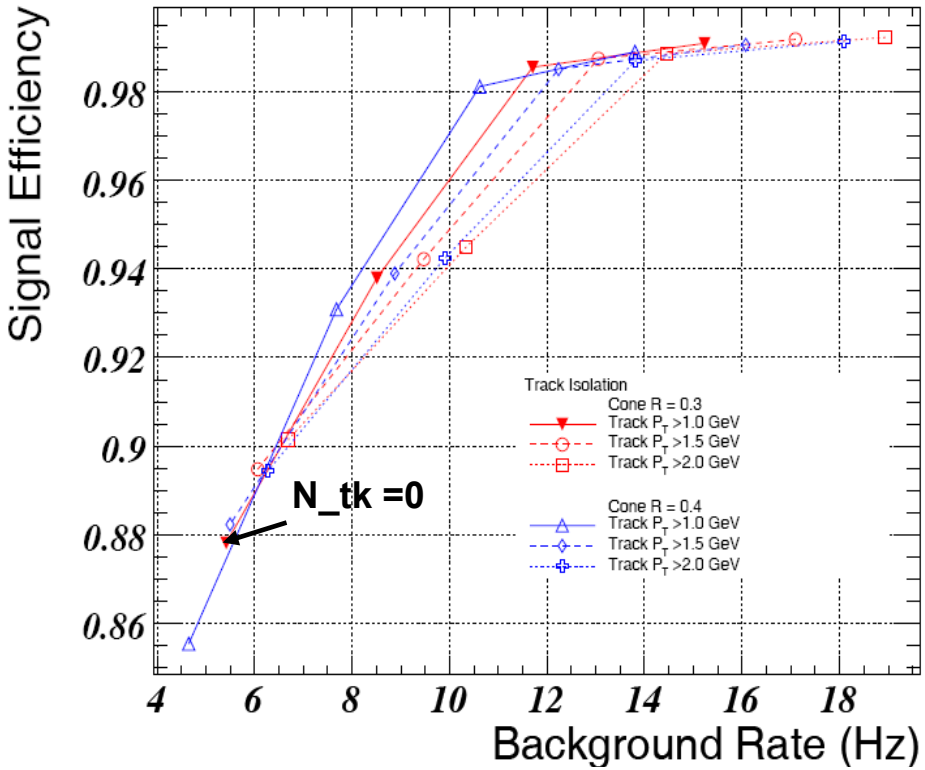

For each of the cone size R, the efficiency and rate are calculated by Varying the Number of tracks in the cone R which have Track P_T > 1.0 GeV, 1.5 GeV and 2.0 GeV for leading HLT Photon.

Sudeep Chatterji, University of Delhi, India

Plots of the ΣE_T in the ECAL for various Cone Sizes

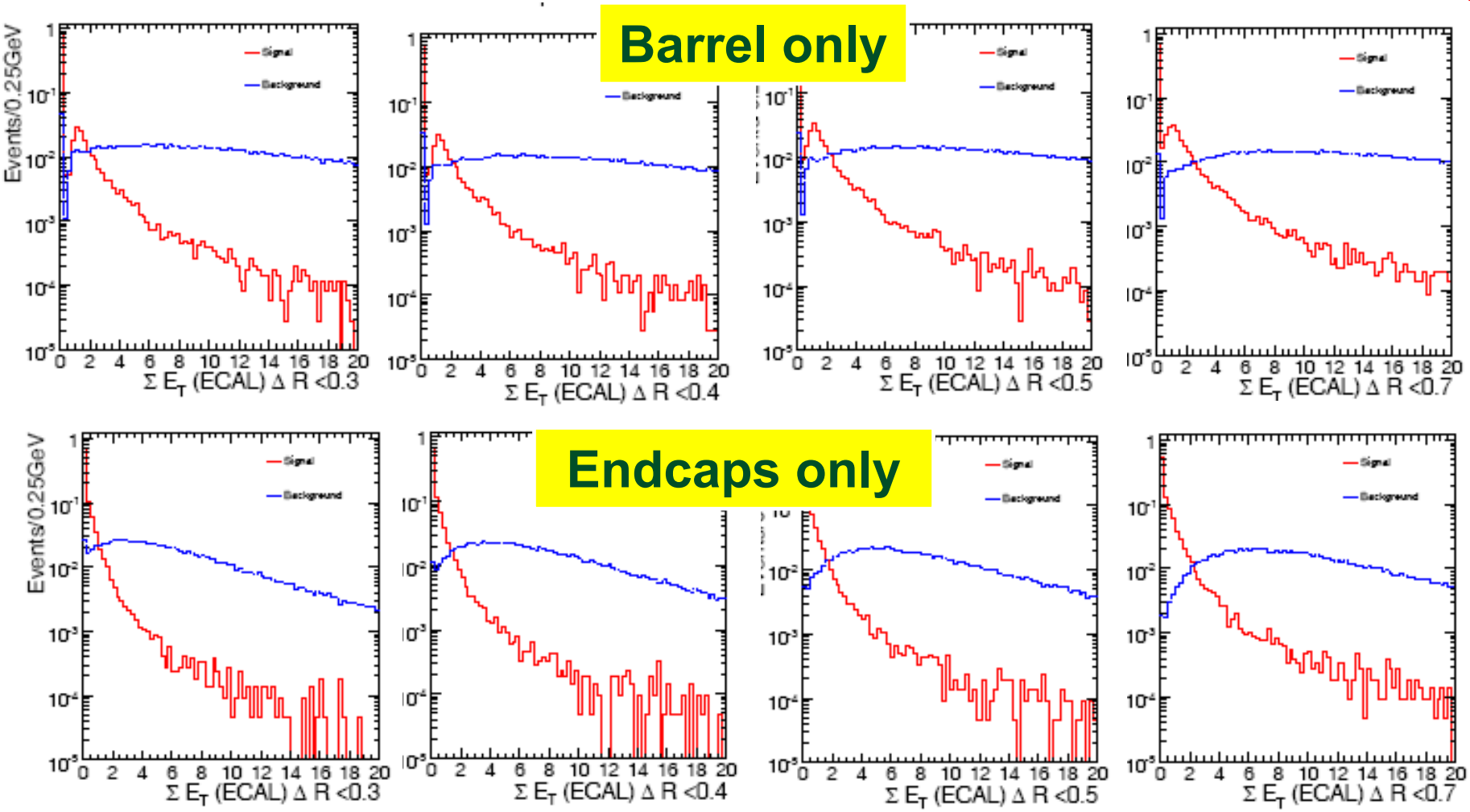

R= 0.3 **R= 0.4** **R= 0.5** **R= 0.7**

Sudeep Chatterji, University of Delhi, India

Signal Efficiency vs. Background Rate

ΣE_T in ECAL

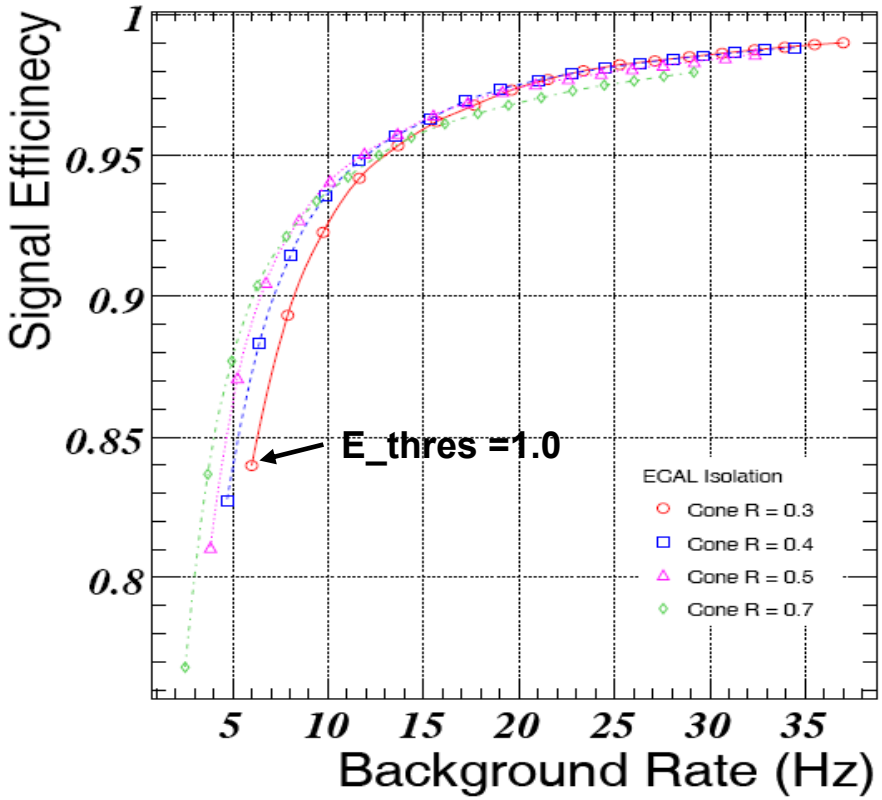

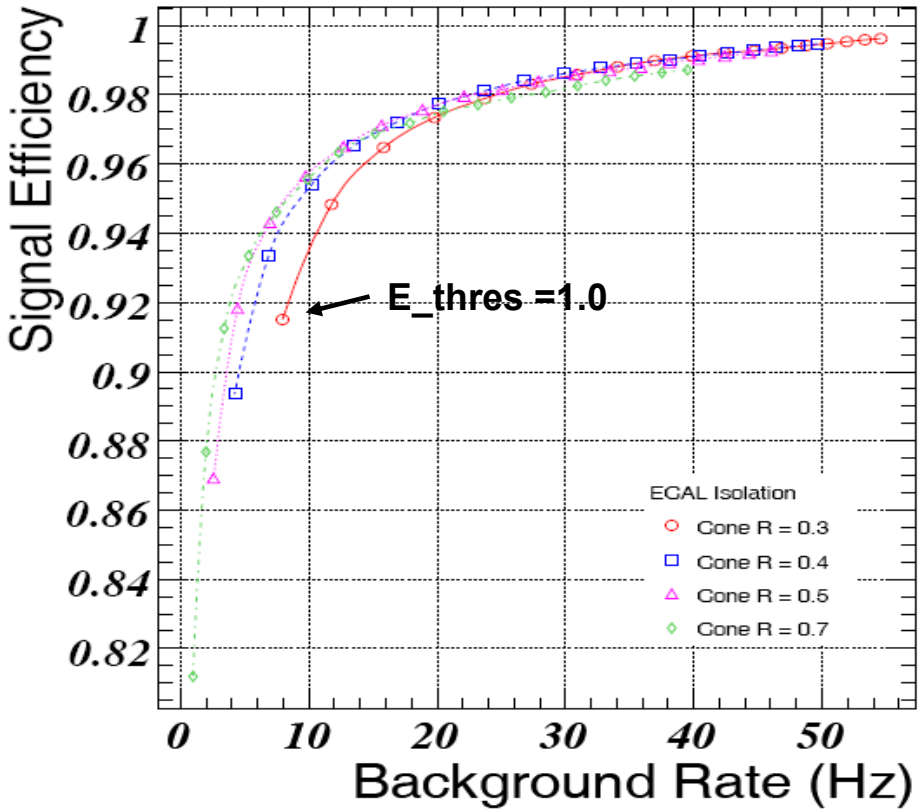

Barrel Only **Endcaps Only**

For a leading photon $P_T^{\gamma} > 80$ GeV and $|\eta^{\gamma}| < 2.6$

Sudeep Chatterji, University of Delhi, India

Plots of the ΣE_T in the HCAL for various Cone Sizes

Barrel only

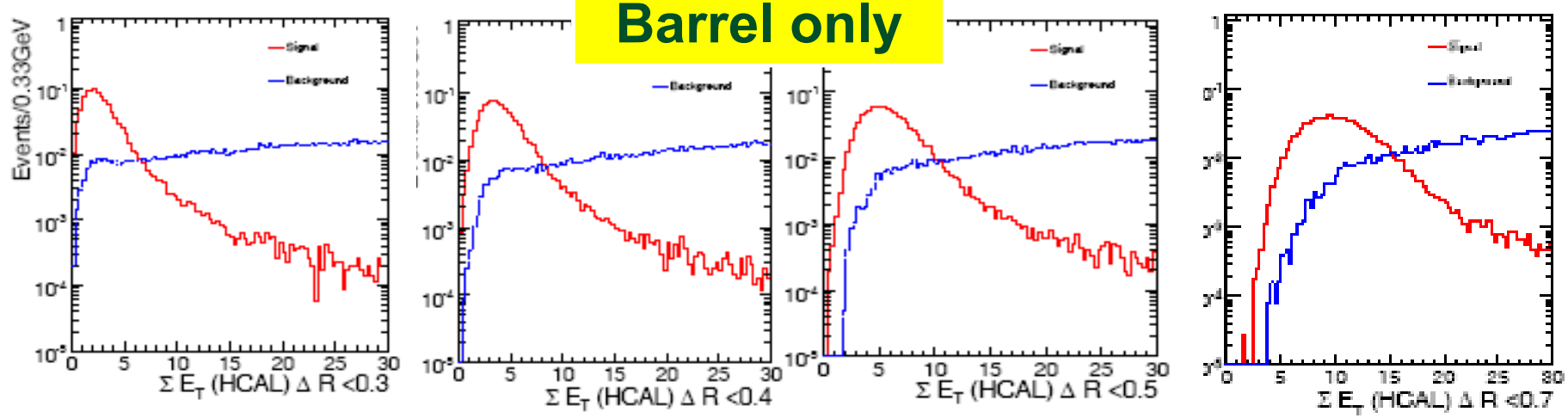

Endcaps only

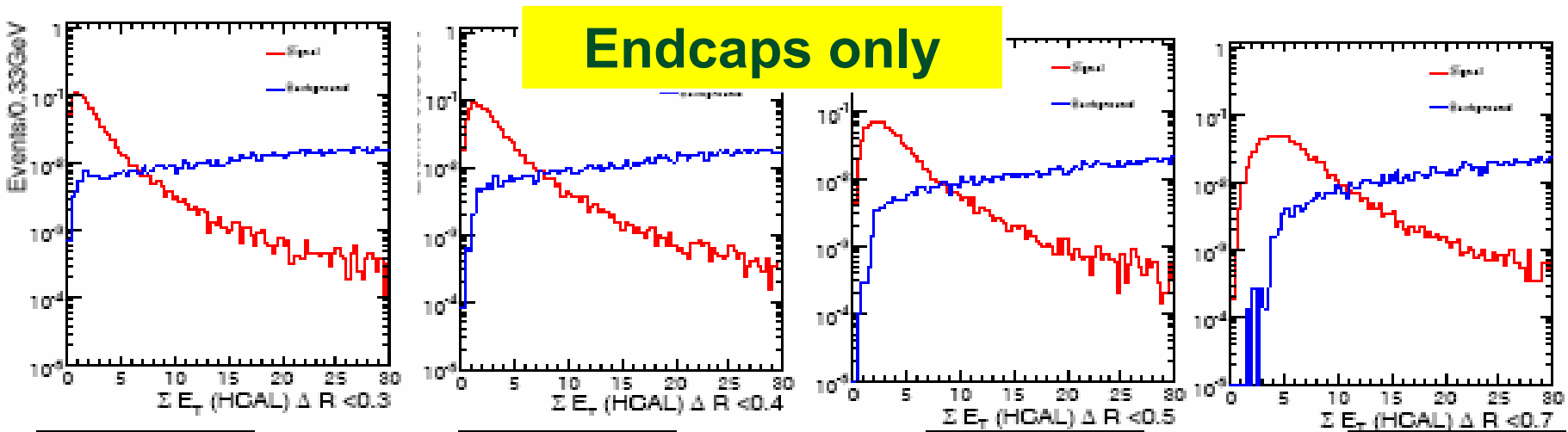

R= 0.3 **R= 0.4** **R= 0.5** **R= 0.7**

Sudeep Chatterji, University of Delhi, India

Signal Efficiency vs. Background Rate

ΣE_T in HCAL

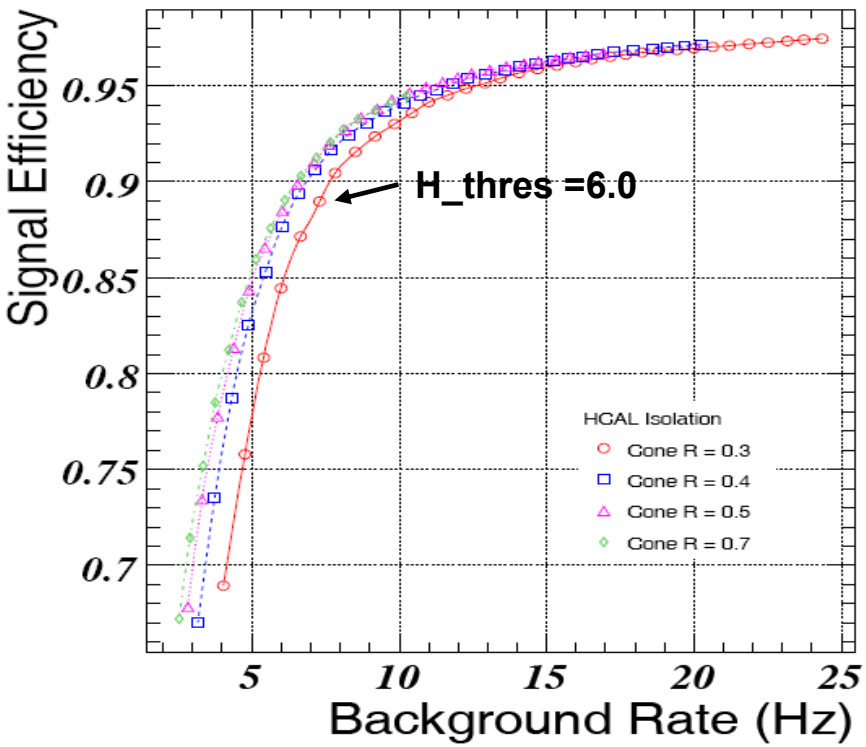

Barrel Only

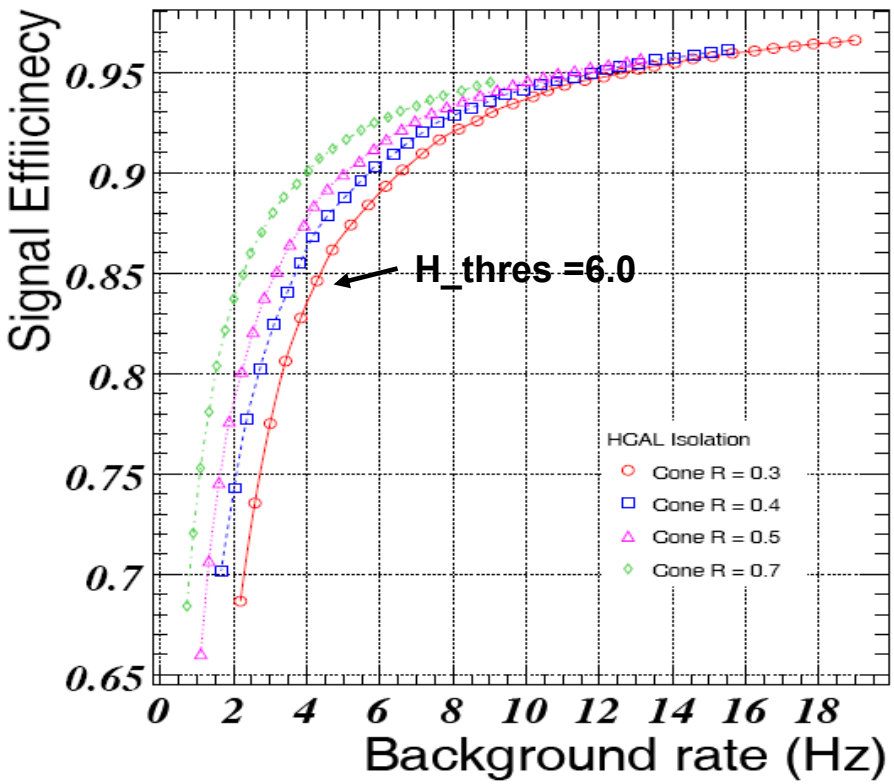

Endcaps Only

For a leading photon $P_T^{\gamma} > 80$ GeV and $|\eta^{\gamma}| < 2.6$

Sudeep Chatterji, University of Delhi, India

Next Step

- **The combination of detector parameters for Tracker, ECAL & HCAL has been studied.**
- **The points which have maximum rejection to background but have a high signal efficiency have been chosen.**
- **Tracker information provides a better rejection of the background.**
- **The HCAL information has been found to be partially redundant as most of the events where jet has faked as photon were already rejected by Tracker isolation or ECAL isolation.**
- **Based on the these isolation variables we have devised five schemes to get a better and improved S/B ratio.**

Sudeep Chatterji, University of Delhi, India

Selection Cuts

Cuts	Cone Size R	P_T^{γ} (GeV)	$\lvert\eta^{\gamma}\rvert$	ECAL Isolation (GeV)	HCAL Isolation (GeV)	No. of tracks	Threshold Track P_T (GeV)
A	0.3	80	<2.6	<1.5	<6 Barrel <4 Endcap	0	1.5
B	0.3	80	<2.6	<1.5	<6 Barrel <5 Endcap	0	1.0
C	0.4	80	<2.6	<2.0	<7 Barrel <5 Endcap	0	1.5
D	0.4	80	<2.6	<2.0	<6.5 Barrel <5 Endcap	0	1.5
E	0.5	80	<2.6	<2.5	<8Barrel <6 Endcap	0	1.5

Sudeep Chatterji, University of Delhi, India

Comparison of Rates

Selection Cuts	Signal Rate (Hz)	Background Rate (Hz)	S/B
A	2.12	1.40	1.52
B	2.09	1.26	1.66
C	2.09	1.09	1.92
D	2.07	1.06	1.94
E	1.99	0.84	2.37

Selection A : These analysis cuts were used for calculating the HLT rates for γ+jet and its backgrounds in Physics TDR -I.

The rates reported – Signal: 2.1 Hz & Background : 1.4 Hz

Sudeep Chatterji, University of Delhi, India

Selection Efficiency

Selection cut	γ + jet	jet-jet background
L1+HLT	61860 (81.31%)	208581 (7.48%)
$\lvert\eta^{\gamma}\rvert$ <2.6	58961 (95.31%)	197232 (94.56%)
Photon Isolation in R=0.4		
No track with P_T>1.5 GeV	53312 (90.42%)	6414 (3.25%)
ECAL Isolation E_iso<2.0	50279 (94.31%)	1420 (22.14%)
HCAL Isolation H_iso<7.0(Barrel) H_iso<5.0 (Endcaps)	42508 (84.54%)	507 (35.70%)
Jet P_T >40 GeV & $\lvert\eta^{jet}\rvert$ <5.0	42341(99.61%)	501 (98.82%)
Overall Efficiency	55.88%	0.02%

Sudeep Chatterji, University of Delhi, India

No. of Events/GeV

Before any Photon isolation requirement

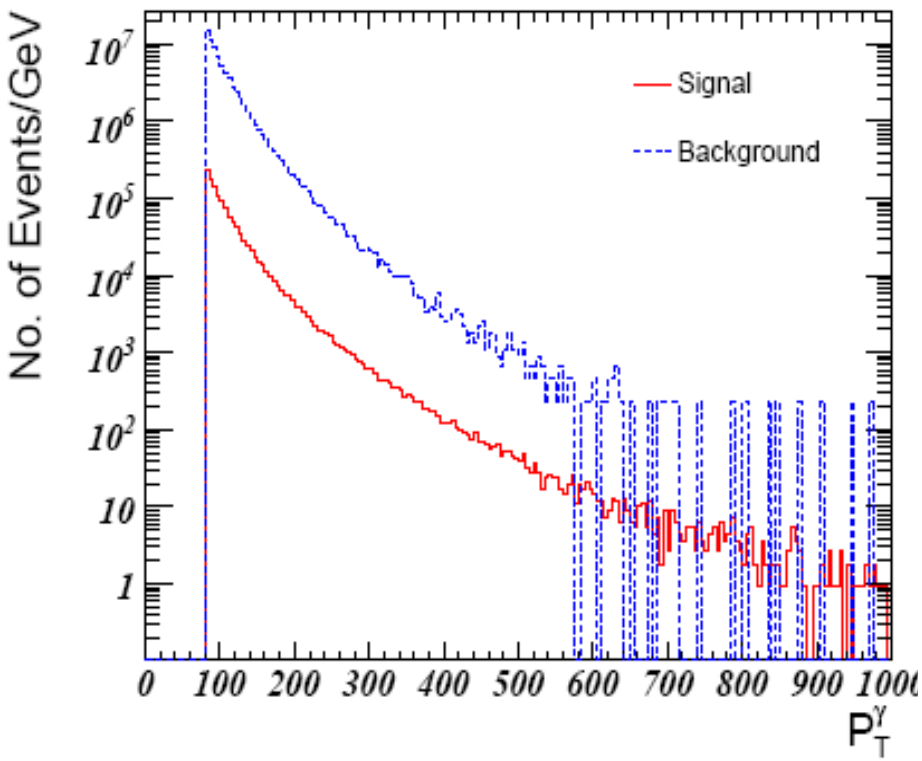

After Photon isolation requirements

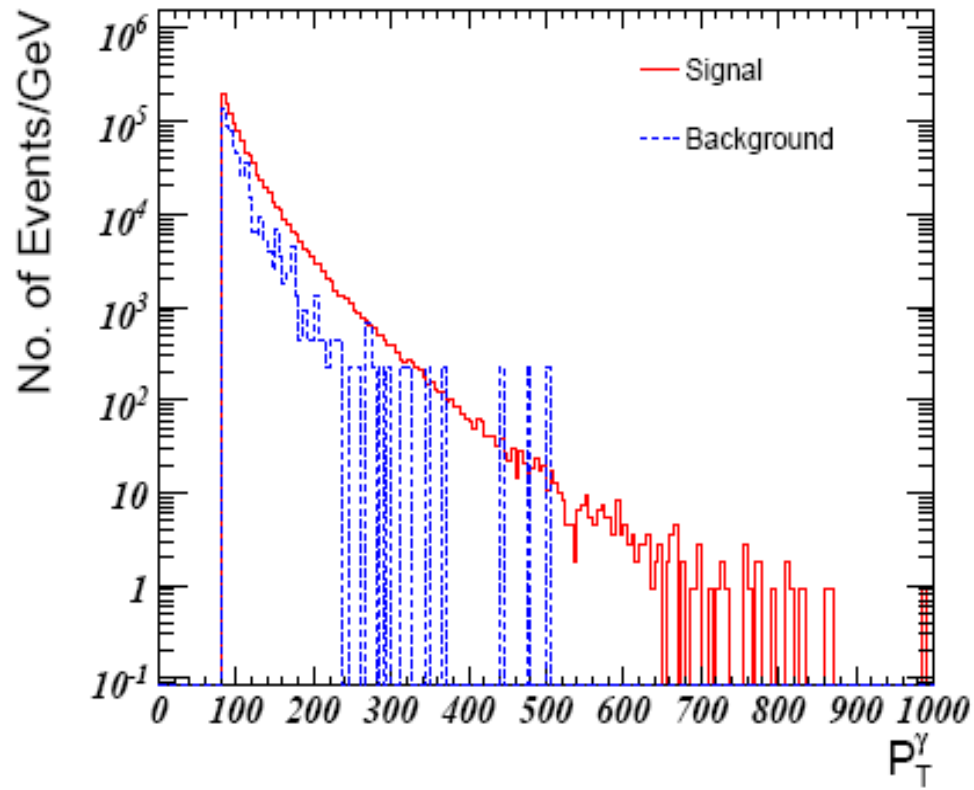

$\int L.dt = 1fb^{-1}$

Sudeep Chatterji, University of Delhi, India

Differential Cross Section

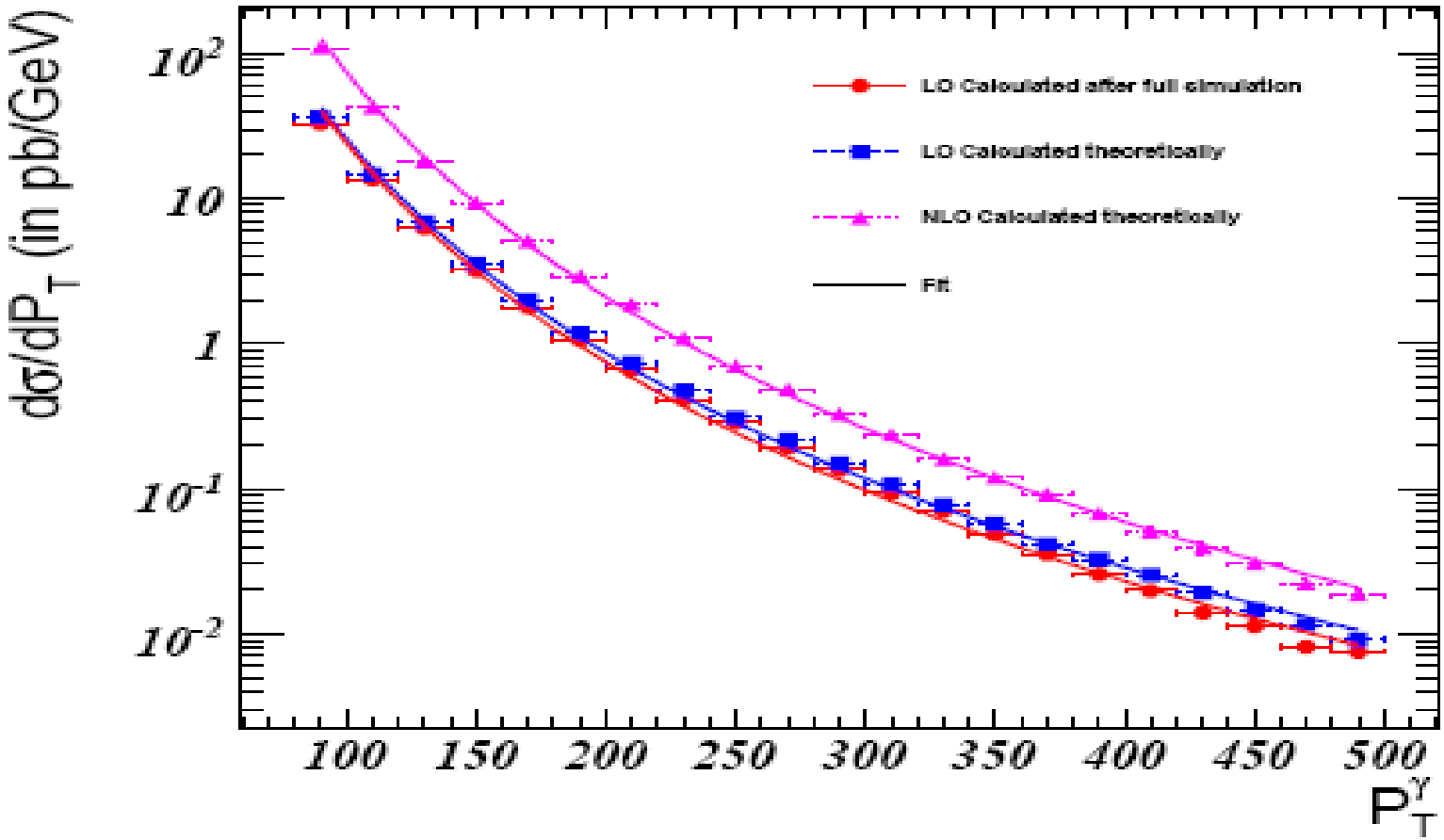

Theoretical calculations were provided by Jeff Owens.

Effect of Δφ cut

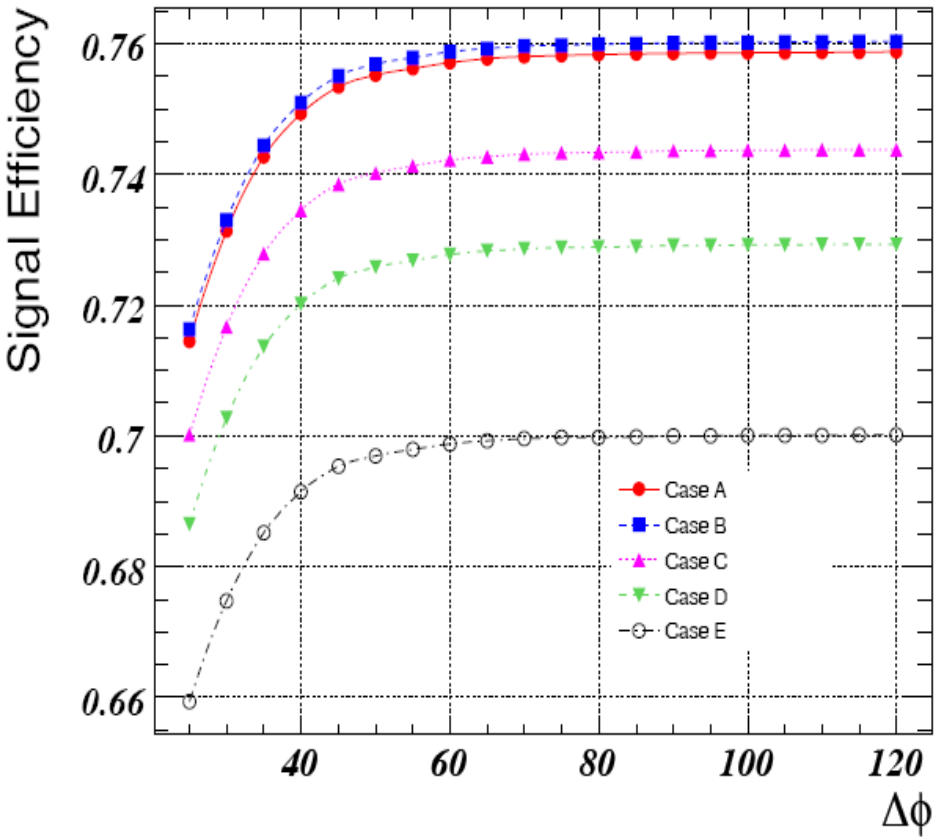

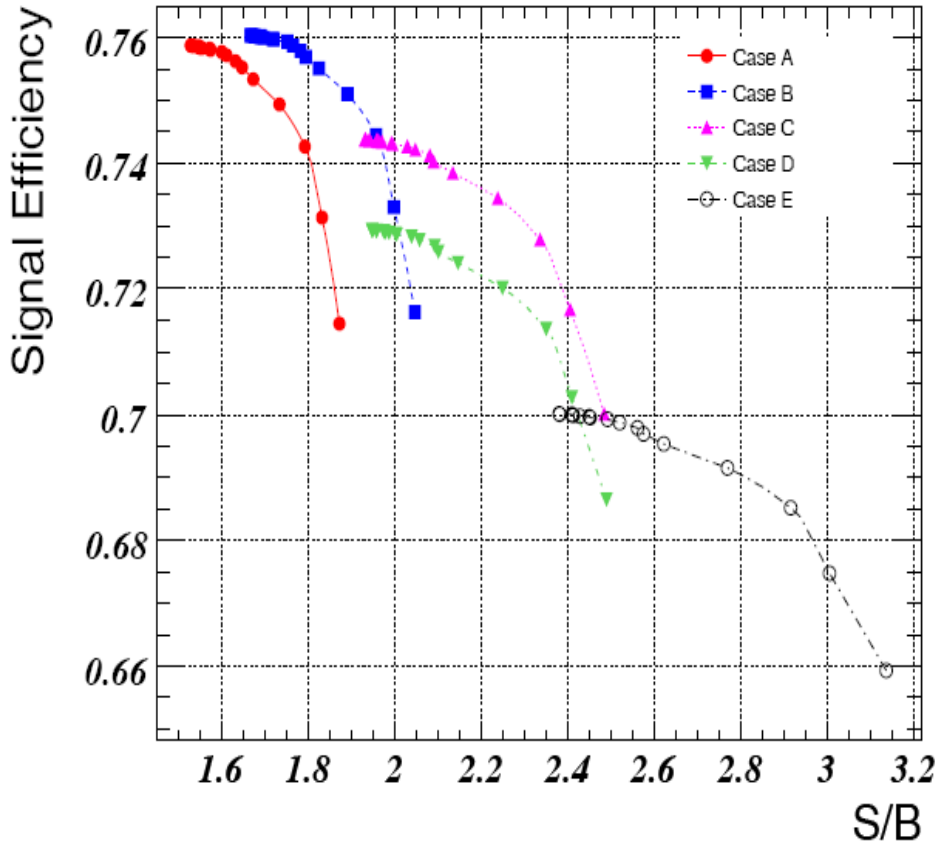

Where $\Phi(\gamma, \text{jet}) = 180^0 \pm \Delta\varphi$

Sudeep Chatterji, University of Delhi, India

Systematics

LHC Integrated Luminosity : ± 5%

L1/HLT Trigger Efficiency : ± 1%

Experimental:

Photon Energy Scale : ± 0.5% (Barrel) & ±1% (Endcaps)

Photon Energy Resolution : ± 1%

Jet Energy Scale : ± 5%

Jet Energy Resolution : ± 10%

❖γ + Jet channel has been used for Jet energy scale calibration

Sensitivity to Gluon distribution….Direct Photon

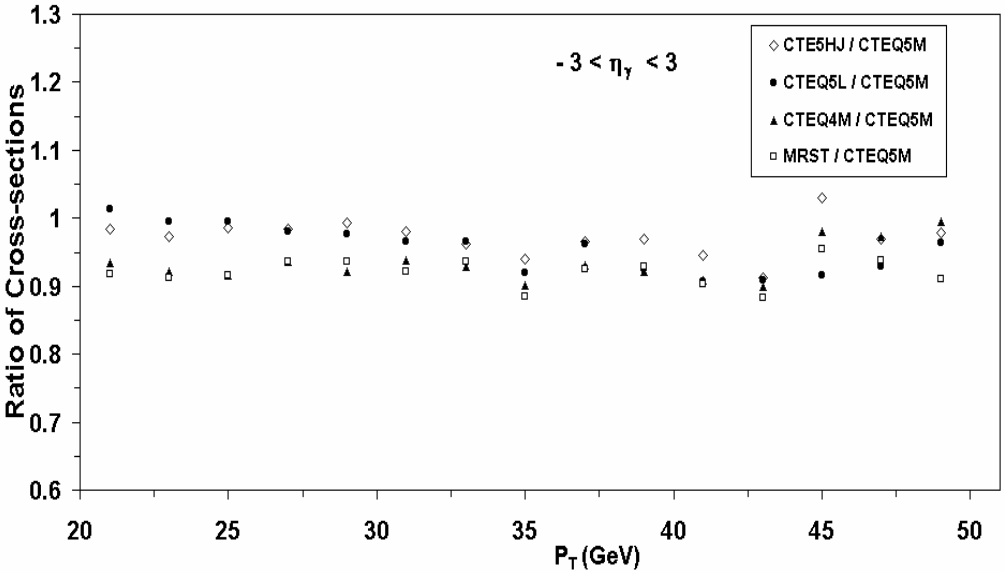

P_T Spectrum

- Variation of ~ 5-10%.
- Difficult to distinguish between different distributions.

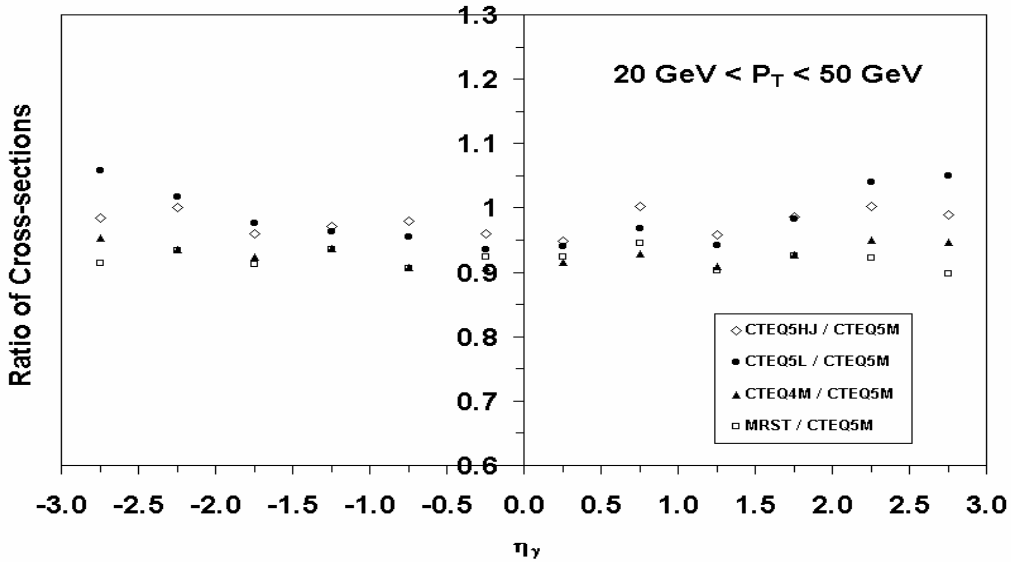

η_γ Spectrum

- More variation between different pdfs.
- Pronounced variation at high η_γ.

Sensitivity to Gluon distribution….Gamma+1Jet

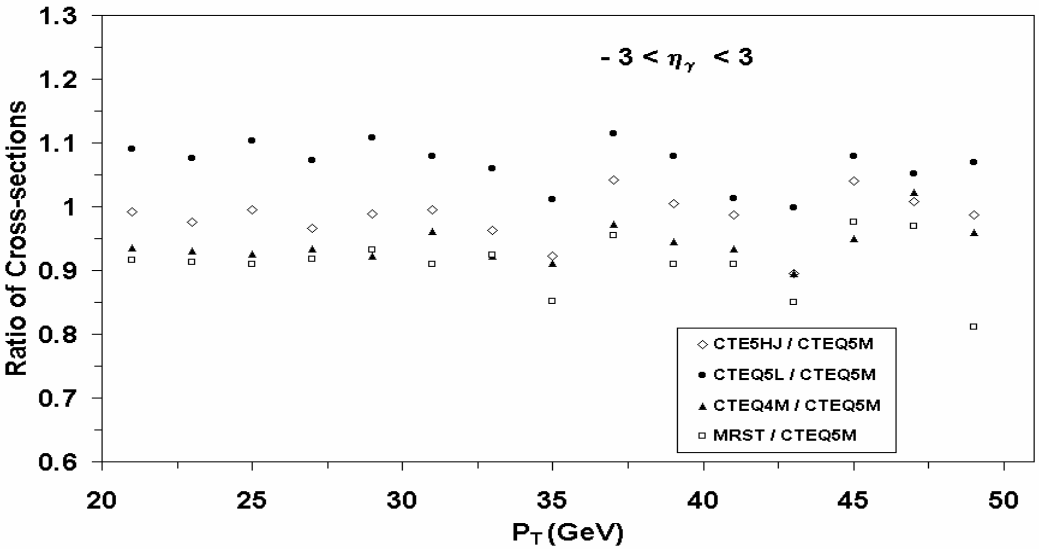

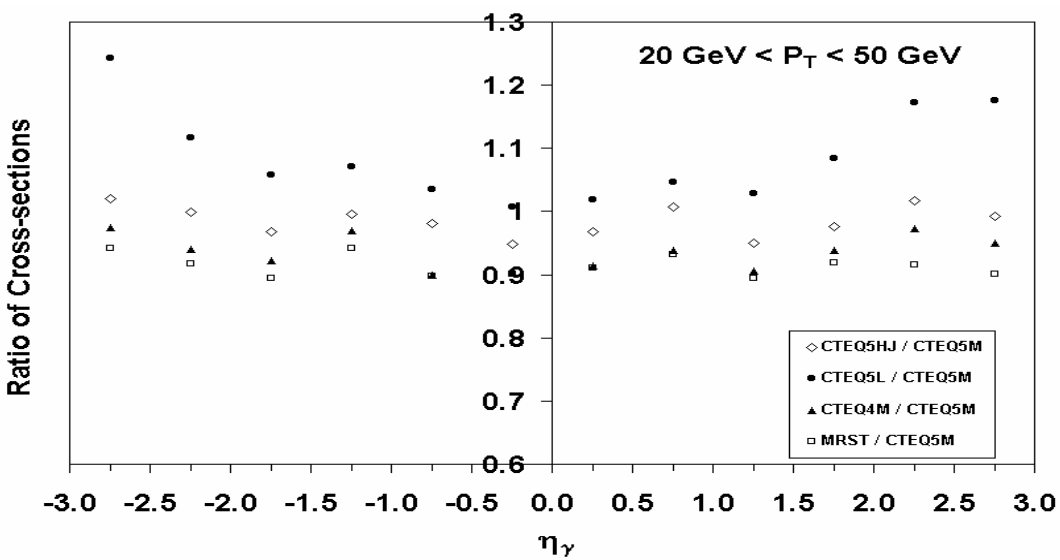

For Jet Finding in PYTHIA

- PYCELL: cluster finding algorithm
- Jet P_T > 10GeV; Jet $|\eta|$ < 5.0

P_T and η_γ spectrum

- Sensitivity is more pronounced both for P_T and η_γ .

- η_γ Spectrum is more useful.

Sensitivity to Gluon Distribution…Gamma+1Jet

Using event topology

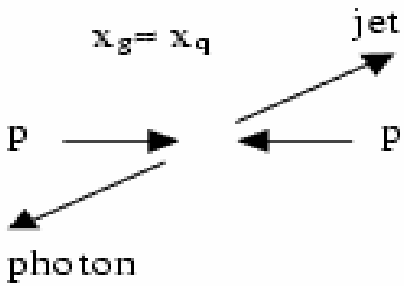

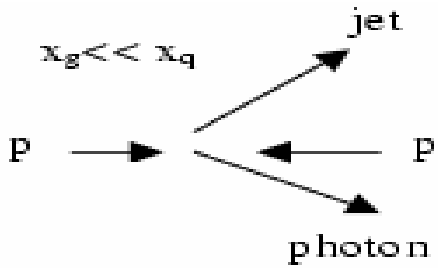

Interacting partons of equal momenta :

- γ-jet back to back in lab. frame

Partons of unequal momenta :

- γ-jet tend to be on the same side
- dominate in LHC (since $x_g << x_q$)

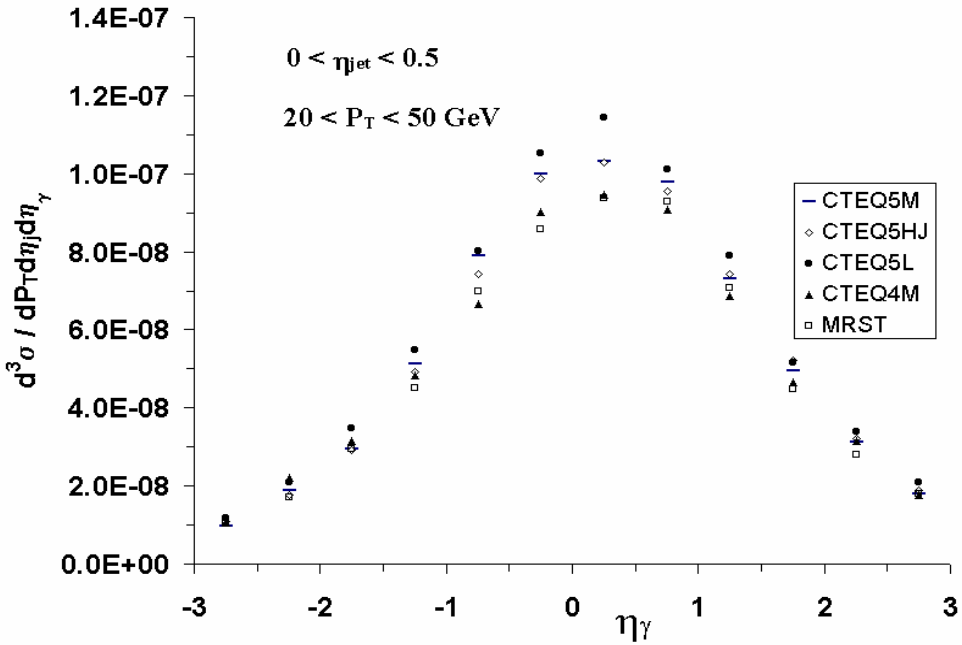

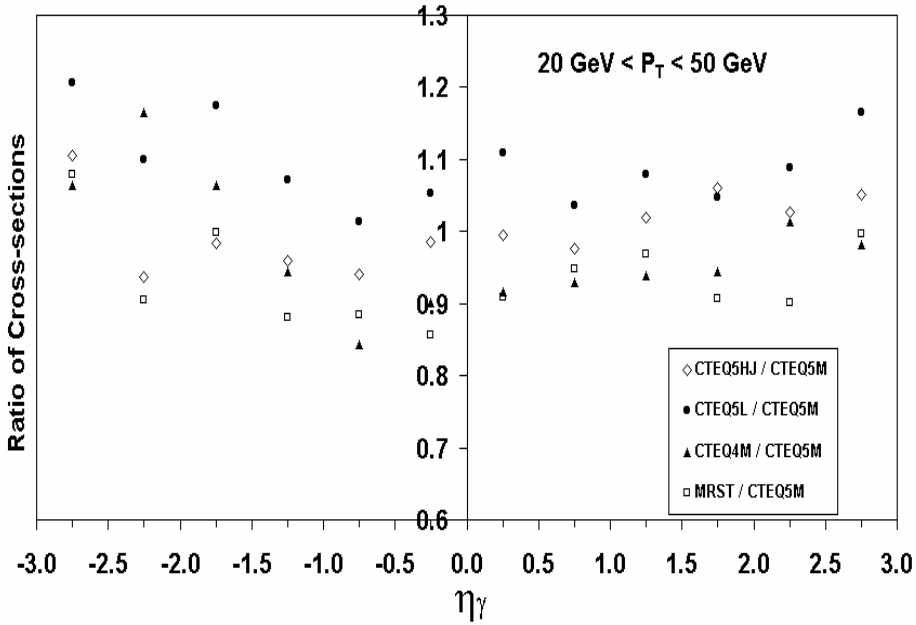

Sudeep Chatterji, University of Delhi, India

Sensitivity to Gluon Distribution…Gamma+1Jet

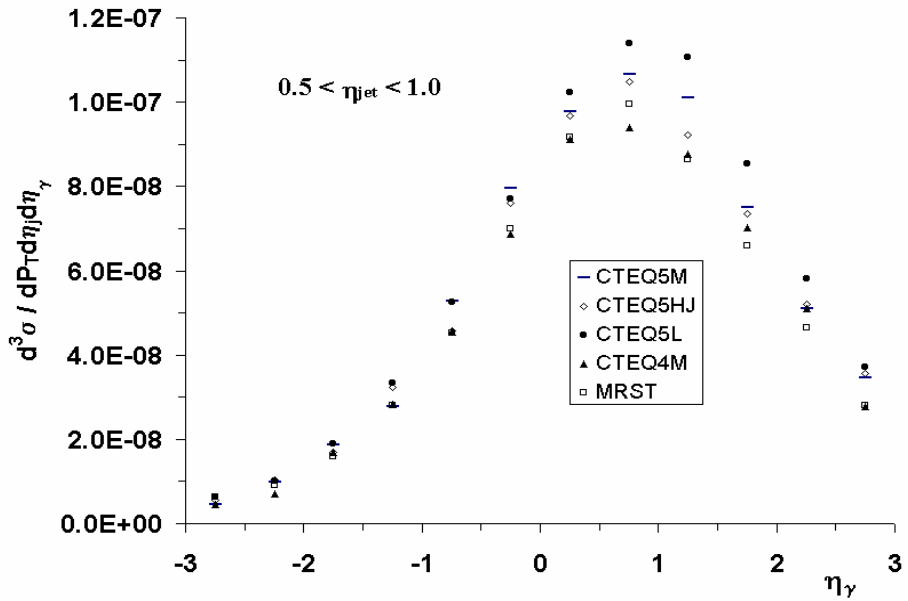

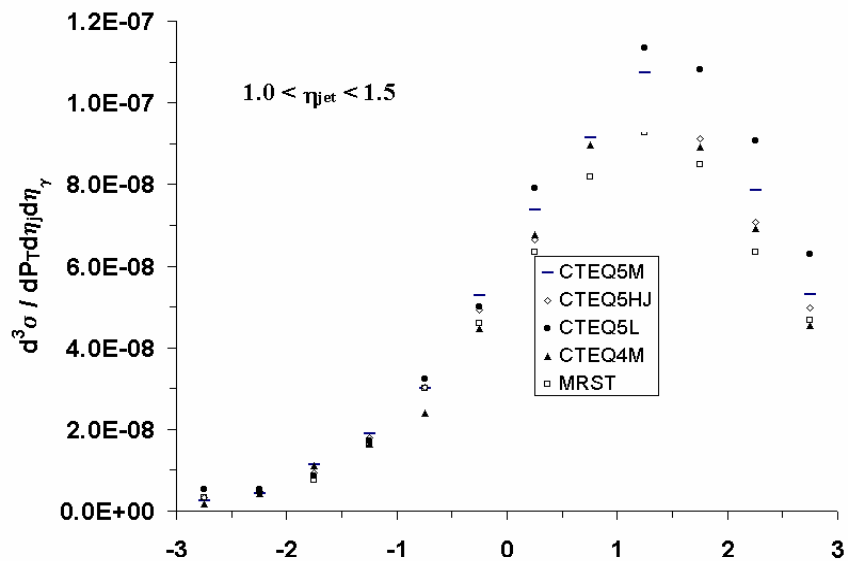

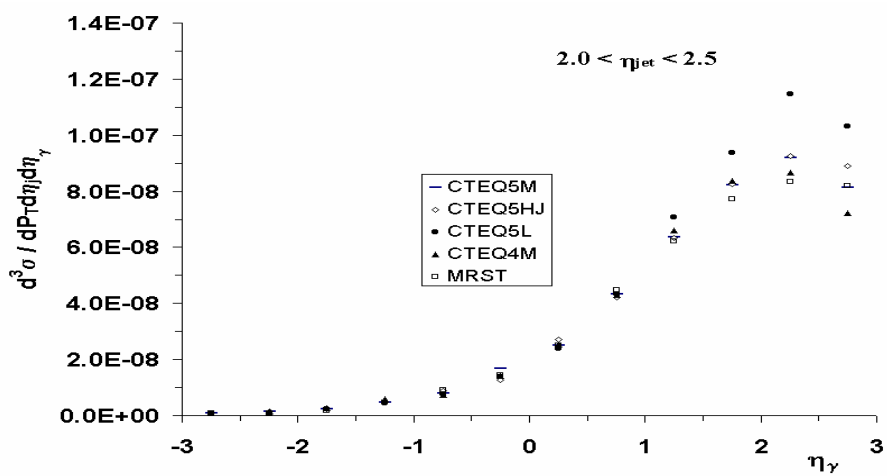

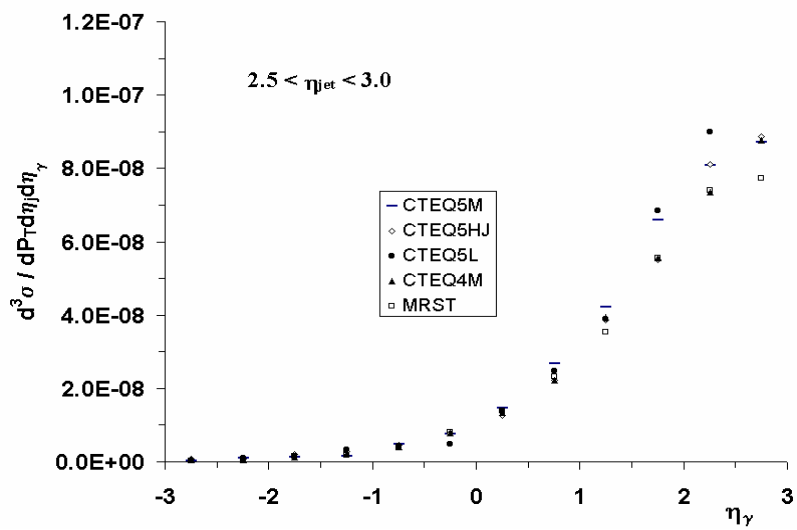

Sudeep Chatterji, University of Delhi, India

Sensitivity to Gluon Distribution…CDF Measurements

- **P-Pbar collisions at 1.8 TeV.** **(PRD 57(3), 1998, 1359-65)**
- **Data : 1992-1993 Tevatron run, 16pb^{-1}.**
- **Triple differential cross-section, integrated over $16 < P_T < 40$ GeV and $|\eta_\gamma| < 0.9$.**

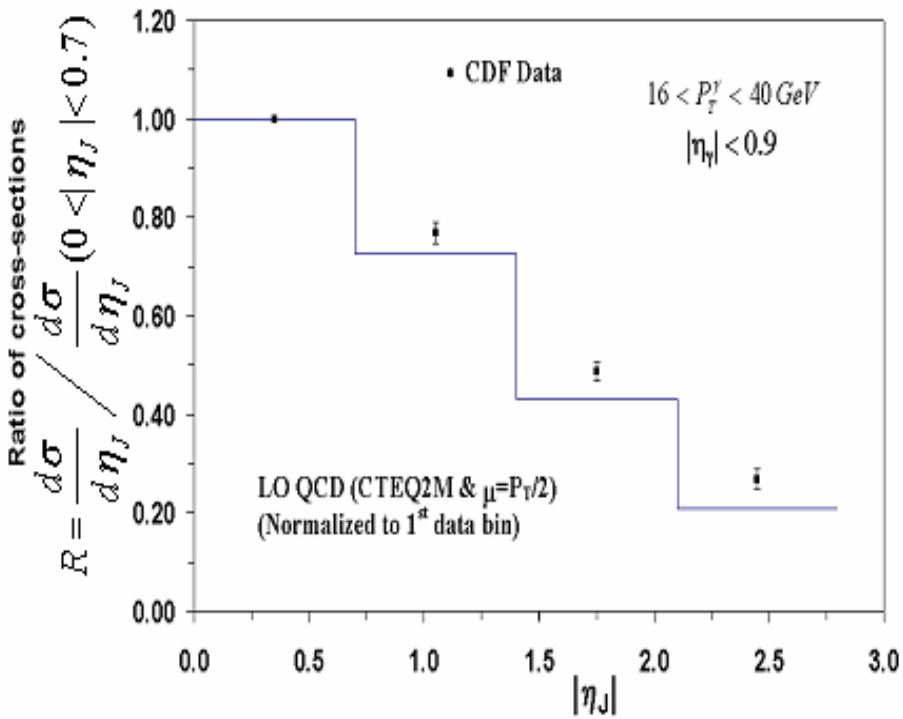

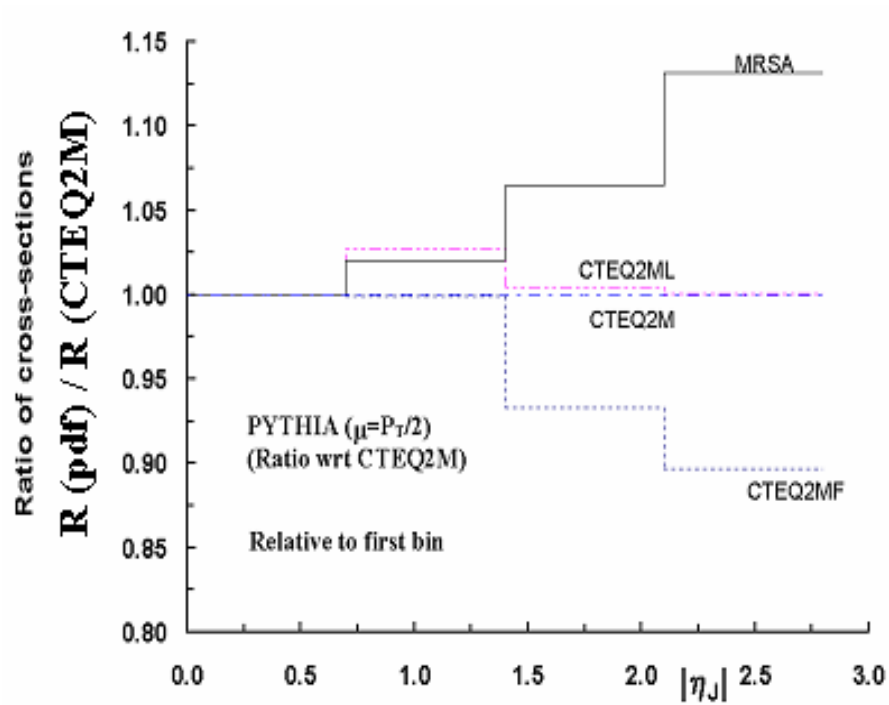

- **Photon+jet samples in 4 diff. η_j bins:**

  0 – 0.7; 0.7 – 1.4; 1.4 - 2.1; 2.1 - 2.8

- **LO predictions are slightly below the data**

- **Highest sensitivity at high η_j :**

  Provide important constraint on PDFs at high η_j

Sensitivity to Gluon Distribution…LHC Prospects

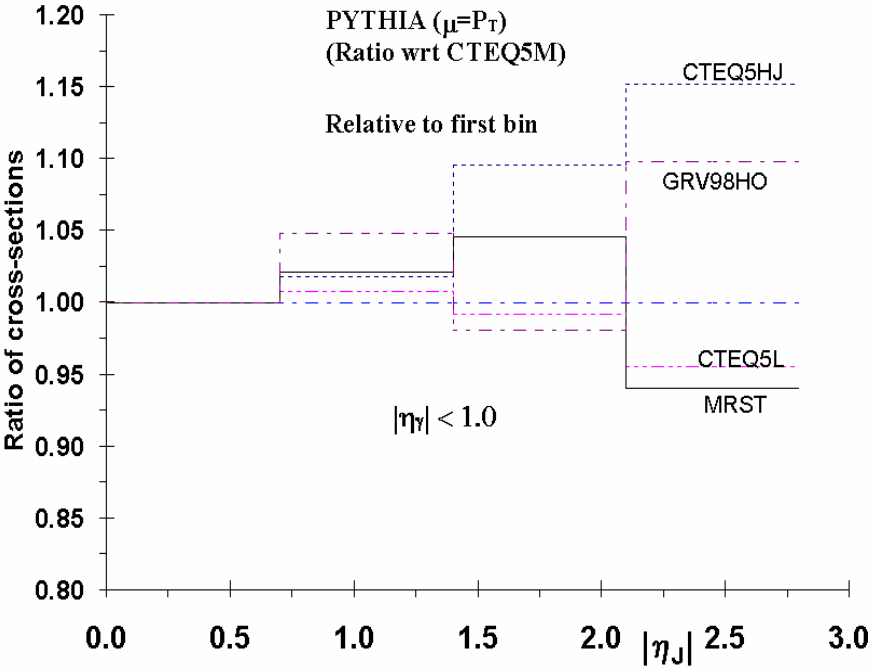

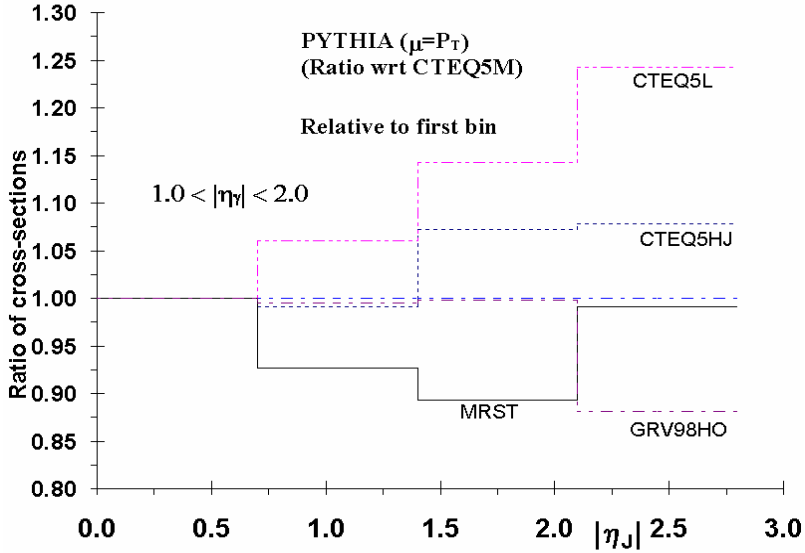

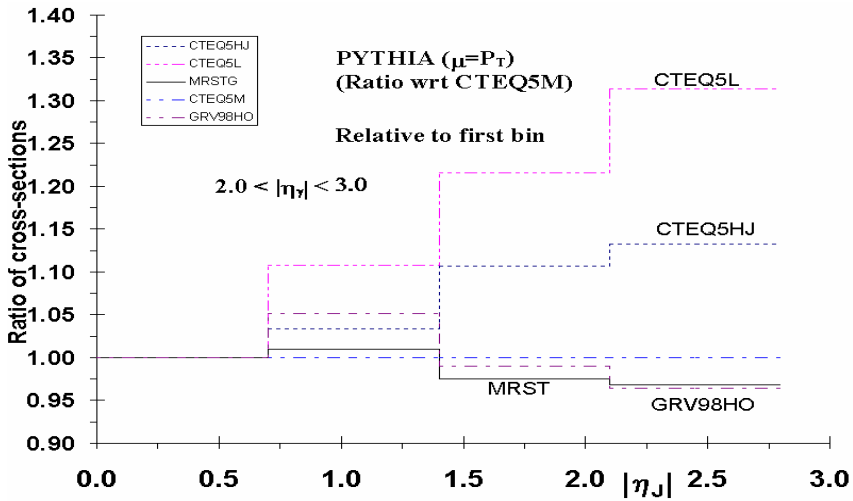

- Analysis similar to CDF may be useful to constraint PDFs
  - Large acceptance of CMS will prove useful.

Conclusion #2

- **The calculated rates match with the published rates in the Physics TDR Vol-I. We have further optimized the study and have improved the S/B by ~25% while barely losing 2% in signal efficiency.**
- **The isolation conditions reduce the background by three orders of magnitude while keeping the signal efficiency between 70-80% for the low luminosity phase of the LHC running.**
- **We have matched our differential cross-section for the direct photon+jet production results from Pythia based simulation with an independent theoretical calculation and they are found to be in good agreement.**
- **Inclusion of a very wide $\Delta\varphi$ cut at 40^0 in the analysis leads to a further increase of 15-17% in S/B with no significant loss in signal efficiency.**
- **Gamma+Jet channel can be used to constrain the Gluon PDF.**
- **LHC will open a new kinematical region of low x at high Q^2 where Gluon PDF can be constrained.**

Sudeep Chatterji, University of Delhi, India

BACKUP SLIDES

Sudeep Chatterji, University of Delhi, India

Electric Field distribution near the surface at breakdown

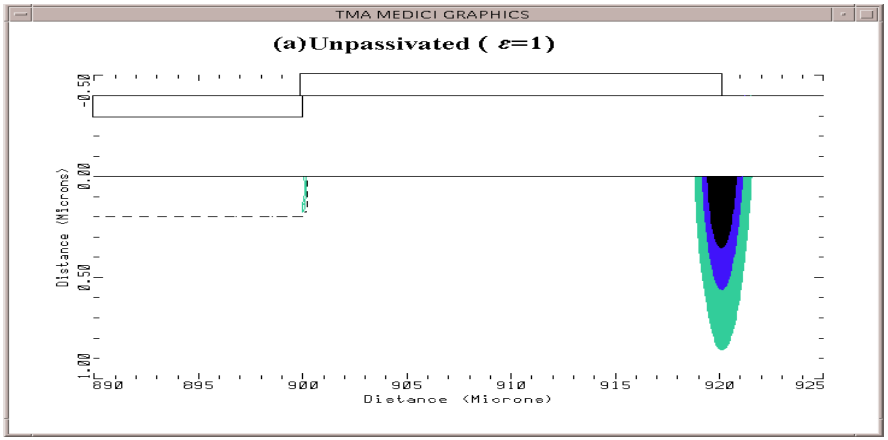

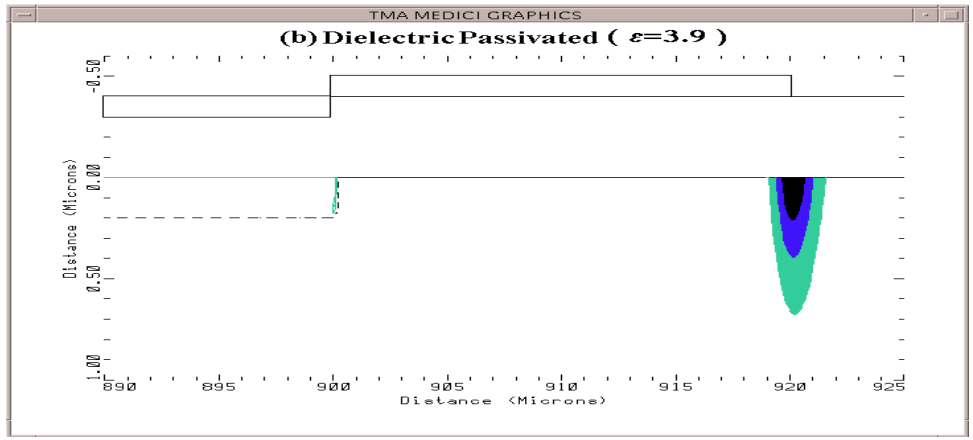

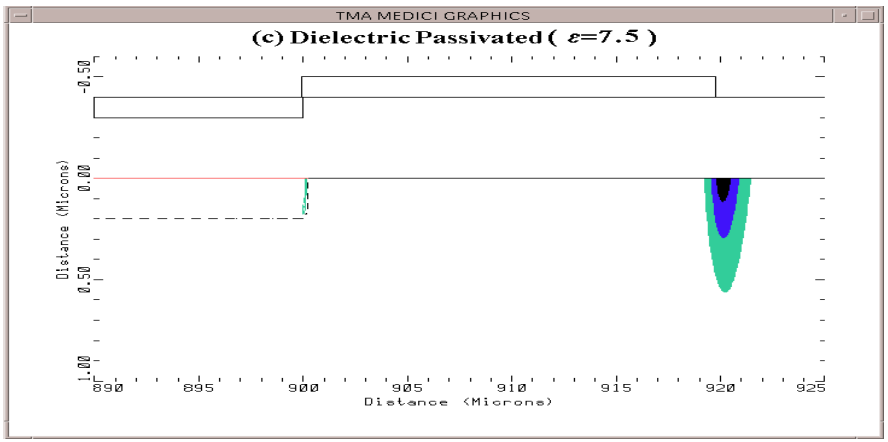

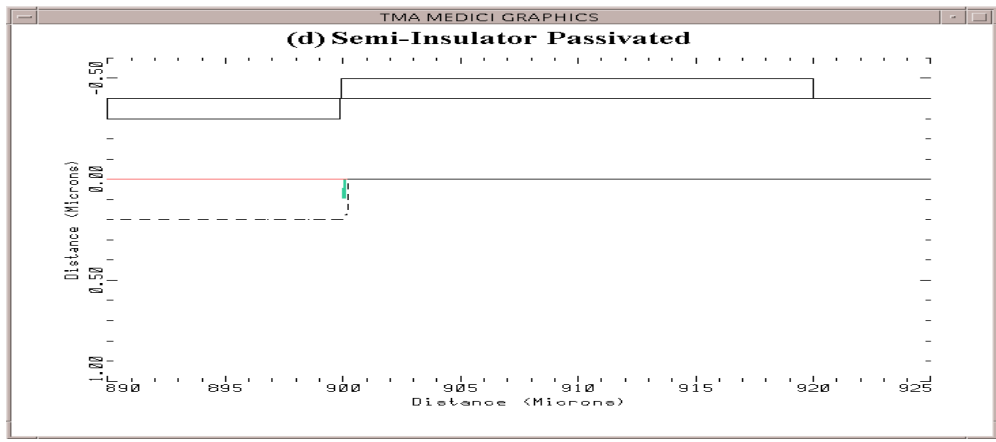

: 4.0E4 – 4.5E4 : 4.5E4 – 5.0E4

: 5.0E4 – 5.5E4

Capacitance plots

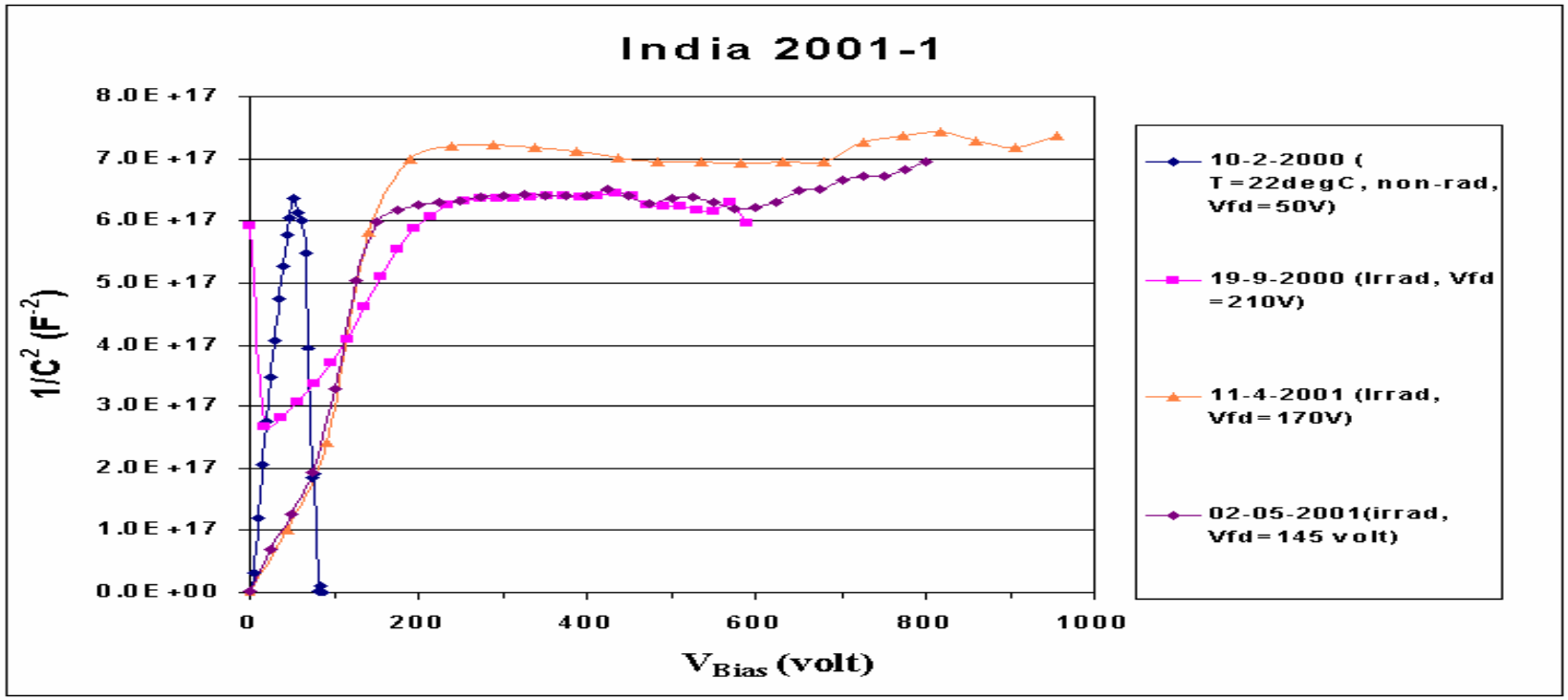

$$W(V) = \sqrt{\frac{2\varepsilon_{si} V}{q N_B}}$$

$$\frac{d(1/C^2)}{dV} = \frac{2}{q \varepsilon_{si} N_B}$$

$$C_j = \sqrt{\frac{q \varepsilon_{Si} N_B}{2}} \left(V_{bi} + V \frac{-2kT}{q}\right)^{-1/2} \quad for \;\; V < V_{FD}$$

$$= \frac{\varepsilon_{Si}}{d} \qquad for \;\; V > V_{FD}$$

Sudeep Chatterji, University of Delhi, India

Test Setups

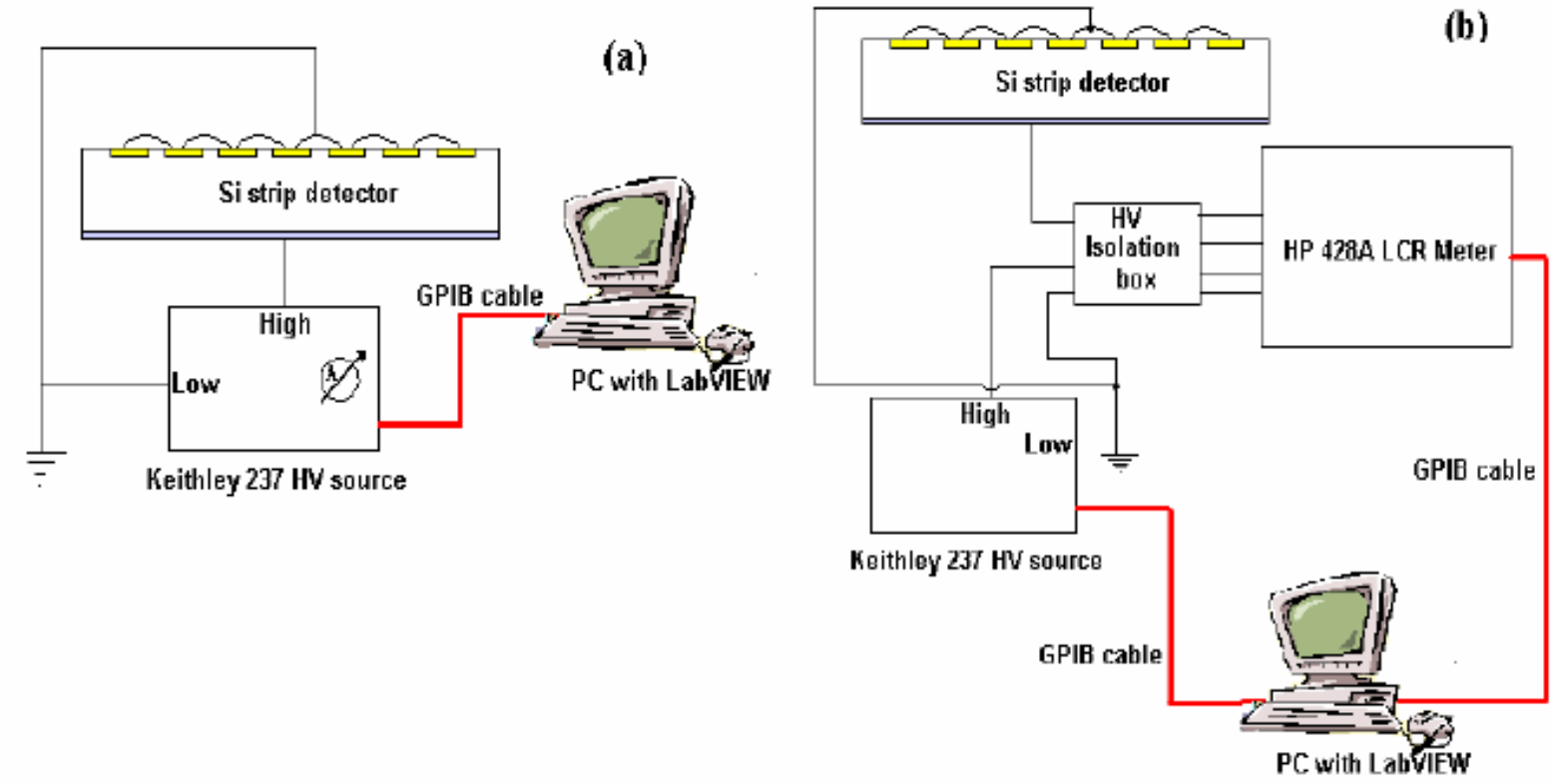

Test setup for measurement of Total current and Total capacitance

Sudeep Chatterji, University of Delhi, India

Delta Switched Gain Channel Design

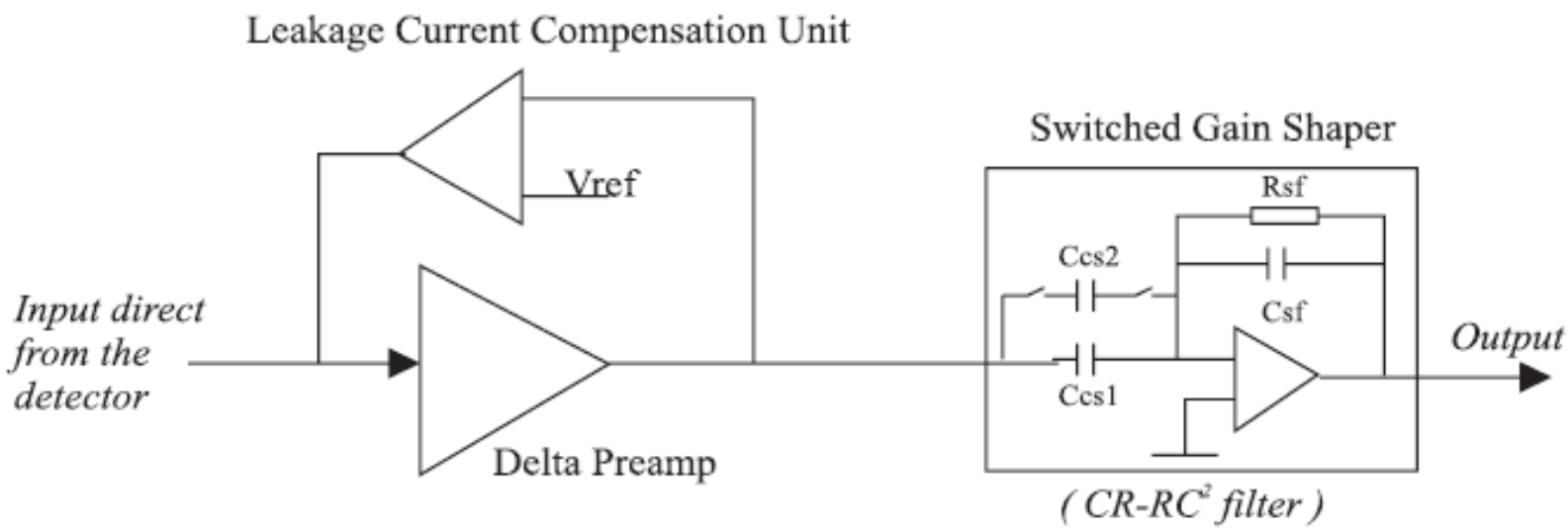

- For CMS Preshower, two modes of operation have been defined:
  - Run mode (low gain), full dynamic range (1-400 MIPs)
  - Calibration mode (high gain), reduced dynamic range (0.1-50 MIPs)

Sudeep Chatterji, University of Delhi, India

Noise Analysis

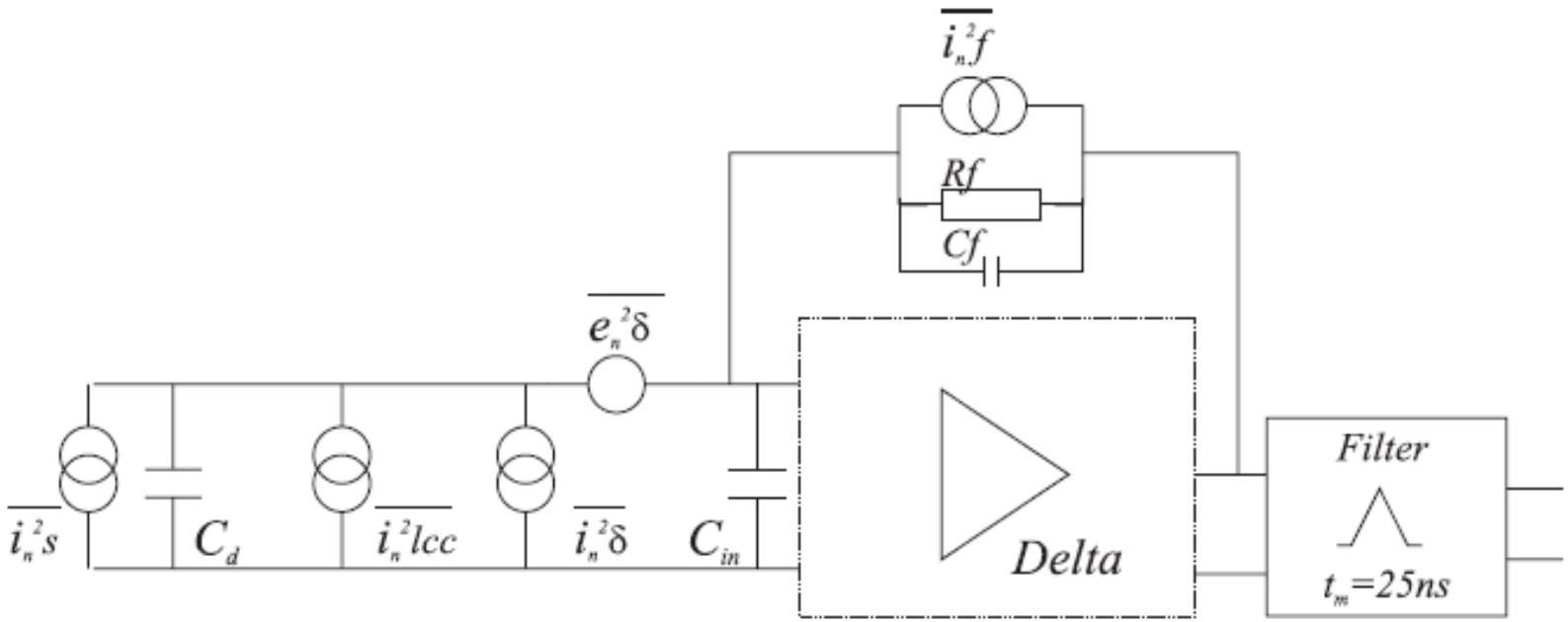

$$\overline{i_{n\delta}^2} = 2\,q\,i_b \;\; where \;\; i_b = \frac{i_c}{\beta}$$

$$\overline{e_{n\delta}^2} = 4\,k\,T\,R_{eq} \;\; where \;\; R_{eq} = r_{bb'} + \frac{1}{2\,g_m}$$

$$\overline{i_{nf}^2} = \frac{4\,k\,T}{R_f}$$

$$\overline{i_{ns}^2} = 2\,q\,i_s$$

$$\overline{ENC_p^2} = \frac{\sum \overline{i_n^2}}{2} I_2$$

$$\overline{ENC_s^2} = \frac{\overline{e_{n\delta}^2}\,(C_d + C_f + C_{in})}{2} I_1$$

$$\overline{ENC_t} = \sqrt{\overline{ENC_p^2} + \overline{ENC_s^2}}$$

Sudeep Chatterji, University of Delhi, India

Track Isolation

cone size R =	0.3	0.4	0.5	0.7
Barrel only				
Track $P_T^{Thres} > 1.0$ GeV				
Signal Efficiency	0.91	0.88	0.85	0.76
Bkg Rate (Hz)	1.3	1.0	0.9	0.7
Track $P_T^{Thres} > 1.5$ GeV				
Signal Efficiency	0.94	0.92	0.90	0.84
Bkg Rate (Hz)	1.6	1.4	1.2	1.0
Track $P_T^{Thres} > 2.0$ GeV				
Signal Efficiency	0.95	0.93	0.92	0.89
Bkg Rate (Hz)	1.9	1.7	1.5	1.3
Endcaps only				
Track $P_T^{Thres} > 1.0$ GeV				
Signal Efficiency	0.88	0.86	0.83	0.77
Bkg Rate (Hz)	5.4	4.6	4.0	3.0
Track $P_T^{Thres} > 1.5$ GeV				
Signal Efficiency	0.89	0.88	0.87	0.83
Bkg Rate (Hz)	6.1	5.5	5.1	4.3
Track $P_T^{Thres} > 2.0$ GeV				
Signal Efficiency	0.90	0.89	0.89	0.86
Bkg Rate (Hz)	6.7	6.3	5.9	5.4

Number of Tracks in Cone size R =0

ECAL Isolation

cone size R = 0.3, $\|\eta^{\gamma}\| < 1.5$				
$\Sigma E_{TEcal} >$	9.0 GeV	6.5 GeV	4.0 GeV	1.5GeV
Signal Efficiency	0.99	0.98	0.97	0.89
Bkg Rate (Hz)	34.5	27.1	17.6	7.9
cone size R = 0.3, $1.5 < \|\eta^{\gamma}\| < 2.6$				
$\Sigma E_{TEcal} >$	8.0 GeV	4.0 GeV	2.0 GeV	1.0 GeV
Signal Efficiency	0.99	0.98	0.96	0.89
Bkg Rate (Hz)	50.4	30.9	15.8	7.9
cone size R = 0.4, $\|\eta^{\gamma}\| < 1.5$				
$\Sigma E_{TEcal} >$	9.0 GeV	6.5 GeV	4.5 GeV	2.0GeV
Signal Efficiency	0.99	0.98	0.97	0.89
Bkg Rate (Hz)	32.8	24.5	17.2	8.0
cone size R = 0.4, $1.5 < \|\eta^{\gamma}\| < 2.6$				
$\Sigma E_{TEcal} >$	8.0 GeV	4.0 GeV	2.0 GeV	1.0 GeV
Signal Efficiency	0.99	0.98	0.95	0.89
Bkg Rate (Hz)	44.6	23.6	10.1	4.2
cone size R = 0.5, $\|\eta^{\gamma}\| < 1.5$				
$\Sigma E_{TEcal} >$	9.0 GeV	6.0 GeV	4.0 GeV	1.5GeV
Signal Efficiency	0.98	0.97	0.96	0.87
Bkg Rate (Hz)	30.8	20.8	13.6	5.2
cone size R = 0.5, $1.5 < \|\eta^{\gamma}\| < 2.6$				
$\Sigma E_{TEcal} >$	8.0 GeV	4.0 GeV	2.0 GeV	1.0 GeV
Signal Efficiency	0.99	0.97	0.94	0.87
Bkg Rate (Hz)	40.4	18.8	6.9	2.6
cone size R = 0.7, $\|\eta^{\gamma}\| < 1.5$				
$\Sigma E_{TEcal} >$	9.0 GeV	7.0 GeV	4.5 GeV	2.0GeV
Signal Efficiency	0.98	0.97	0.95	0.88
Bkg Rate (Hz)	27.5	21.1	12.6	4.9
cone size R = 0.7, $1.5 < \|\eta^{\gamma}\| < 2.6$				
$\Sigma E_{TEcal} >$	9.0 GeV	6.0 GeV	4.0 GeV	1.5 GeV
Signal Efficiency	0.99	0.98	0.96	0.88
Bkg Rate (Hz)	37.5	23.2	12.3	2.0

HCAL Isolation

cone size R = 0.3, $\lvert\eta^{\gamma}\rvert < 1.5$			
$\Sigma E_{THCAL} >$ Signal Efficiency Bkg Rate (Hz)	17.0 GeV 0.97 20.6	11.0 GeV 0.95 13.4	6.0 GeV 0.89 7.3
cone size R = 0.3, $1.5 < \lvert\eta^{\gamma}\rvert < 2.6$			
$\Sigma E_{THCAL} >$ Signal Efficiency Bkg Rate (Hz)	15.0 GeV 0.95 13.5	11.0 GeV 0.93 9.6	6.0 GeV 0.86 4.7
cone size R = 0.4, $\lvert\eta^{\gamma}\rvert < 1.5$			
$\Sigma E_{THCAL} >$ Signal Efficiency Bkg Rate (Hz)	17.0 GeV 0.97 16.7	11.0 GeV 0.94 10.1	7.0 GeV 0.85 5.5
cone size R = 0.4, $1.5 < \lvert\eta^{\gamma}\rvert < 2.6$			
$\Sigma E_{THCAL} >$ Signal Efficiency Bkg Rate (Hz)	15.0 GeV 0.94 10.8	11.0 GeV 0.92 7.17	6.0 GeV 0.82 3.1
cone size R = 0.5, $\lvert\eta^{\gamma}\rvert < 1.5$			
$\Sigma E_{THCAL} >$ Signal Efficiency Bkg Rate (Hz)	17.0 GeV 0.96 13.6	11.0 GeV 0.91 7.1	8.0 GeV 0.78 3.8
cone size R = 0.5, $1.5 < \lvert\eta^{\gamma}\rvert < 2.6$			
$\Sigma E_{THCAL} >$ Signal Efficiency Bkg Rate (Hz)	15.0 GeV 0.94 13.4	11.0 GeV 0.90 5.4	6.0 GeV 0.78 1.9
cone size R = 0.7, $\lvert\eta^{\gamma}\rvert < 1.5$			
$\Sigma E_{THCAL} >$ Signal Efficiency Bkg Rate (Hz)	17.0 GeV 0.91 7.2	14.0 GeV 0.81 4.2	12.0 GeV 0.67 2.5
cone size R = 0.7, $1.5 < \lvert\eta^{\gamma}\rvert < 2.6$			
$\Sigma E_{THCAL} >$ Signal Efficiency Bkg Rate (Hz)	15.0 GeV 0.91 5.1	11.0 GeV 0.86 2.5	8.0 GeV 0.75 1.1

Signal Efficiency vs. Background Rate

No. of tracks in cone size R =0.5 & 0.7

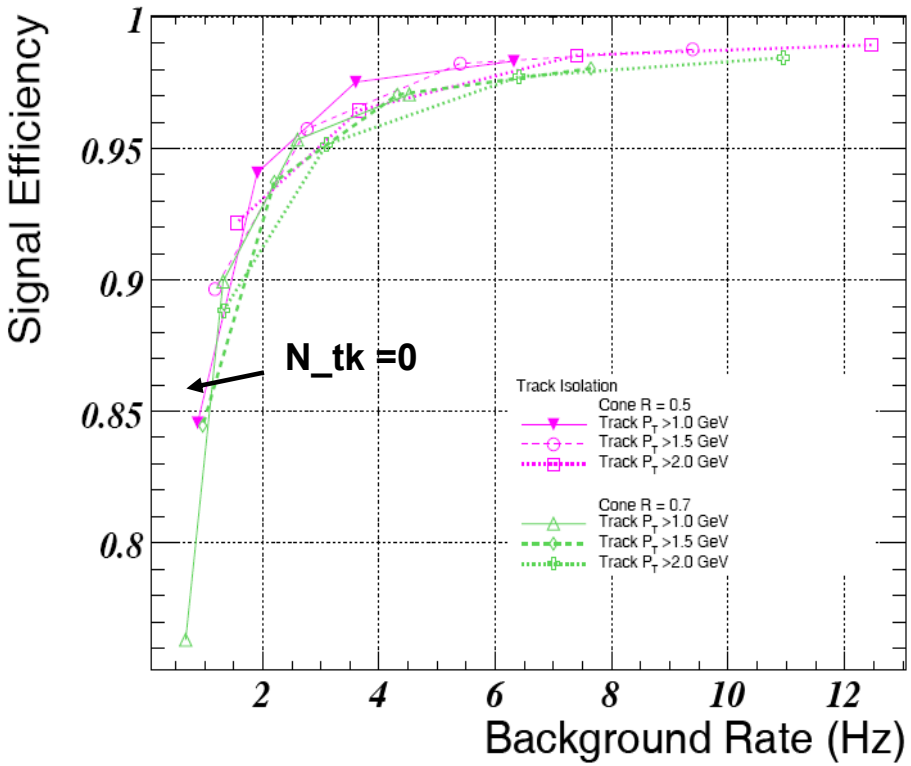

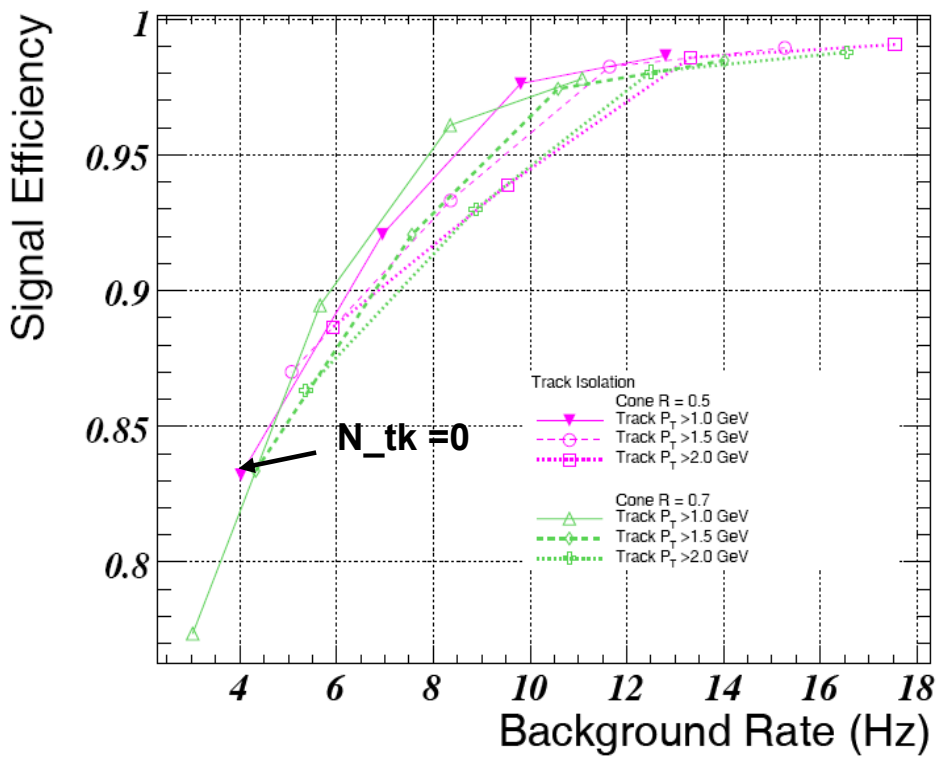

For each of the cone size R, the efficiency and rate are calculated by varying the number of tracks in cone R which have Track P_T >1.0 GeV, 1.5 GeV & 2 GeV for leading HLT photon

Sudeep Chatterji, University of Delhi, India